DISS. ETH NO. 22512

Microbial Transglutaminase as a Versatile Tool for Site-Specific Protein Modification

A thesis submitted to attain the degree of

DOCTOR OF SCIENCES of ETH ZURICH

(Dr. sc. ETH Zurich)

presented by

PATRICK DENNLER

MSc Medicinal and Industrial Pharmaceutical Sciences, ETH Zurich

born on 04.07.1986

citizen of Heiligenschwendi BE

accepted on the recommendation of

Prof. Dr. Roger Schibli, examiner

Prof. Dr. Dario Neri, co-examiner

Dr. Eliane Fischer, co-examiner

2015

You snooze, you lose

Acknowledgement

Science is never a one-man-show. Therefore, I would like to thank everyone who contributed to this work.

First and foremost, I want to express my gratitude to Prof. Roger Schibli for entrusting me with his project, Dr. Eliane Fischer for supervising me throughout the entire thesis and Prof. Dario Neri for being part of the committee.

I would like to thank Dr. Laura K. Bailey for scientific advice, fruitful discussions, proof-reading manuscripts and for being English. Furthermore, I thank all members of the Fischer group, all colleagues the at CRS and at Innate Pharma for an unforgettable time. I also thank Sabine Sonderegger for proof-reading the German part.

Finally, I would like to express my gratitude to my parents Caroline and Erich for their lifetime support which brought me to where I am today.

Summary

Classical chemical bioconjugation methods usually yield heterogeneous products because the site of conjugation and the number of substrates that are attached to the protein are random. In particular, therapeutic bioconjugates such as radioimmunoconjugates (RICs) and antibody-drug conjugates (ADCs) suffer serious consequences as a result of heterogeneity since species with different number of substrates attached at various sites exhibit different *in vivo* properties. But also protein conjugates that are used for *in vitro* applications could profit from novel conjugation methods. Being able to control the site of modification would enable us, for example, to anchor proteins on surfaces in an oriented manner. As a consequence, numerous site-specific protein modification strategies have been developed in the last few years to overcome these limitations including approaches that exploit novel chemical functionalities, enzymes or a combination of both.

Microbial transglutaminase (MTGase) is an enzyme that catalyzes the formation of an isopeptide bond between the γ-carboxyamide group of glutamine residues and primary amines. Our lab has previously demonstrated that MTGase can be exploited to site-specifically modify antibodies because the enzyme exclusively recognizes one glutamine in the constant region of the antibody heavy chain.

In the first part of the thesis MTGase was employed to produce homogeneous ADCs comprising monomethyl auristatin E (MMAE) as the toxic entity. Two different strategies were therefore evaluated: (i) An enzymatic approach where the drug was directly attached to the antibody by MTGase and (ii) an indirect chemo-enzymatic approach where a small linker was attached to the antibody by MTGase to introduce a bioorthogonal functionality, thiol or azide, which could then be selectively targeted to chemically attach the drug. The enzymatic approach required a 40 molar equivalent excess of drug and yielded heterogeneous ADCs with a drug-to-antibody ratio (DAR)

of between 1.0 to 1.6. On the contrary, the chemo-enzymatic approach required a minimal drug excess of 1.25 molar equivalents and yielded homogeneous ADCs with a DAR of exactly two. Once established, the protocol was successfully used to endow trastuzumab, a well-characterized therapeutic anti-HER2/neu antibody, with MMAE. We could demonstrate that the immunoreactivity of the antibody was retained and the ADC proved its biological *in vitro* activity by killing HER2/neu-positive cells. In a different study, we aimed to investigate the impact of ADC homogeneity on its *in vivo* properties. Our novel conjugation strategy was therefore exploited to generate homogeneous ADCs that consist of the same antibody (brentuximab) and toxin (MMAE) as Adcetris®, a chemically conjugated approved ADC, and the *in vivo* characteristics of both conjugates were subsequently evaluated and compared. Ultimately, we could demonstrate that the homogeneous ADCs exhibited a more favourable pharmacokinetic profile associated with a three-fold higher maximal tolerated dose (MTD) in comparison to Adcetris®.

In parallel, we expanded the applicability of MTGase-mediated site-specific protein modification by establishing a generic bioconjugation platform that targets the c-myc-tag (EQKLISEEDL) as glutamine donor. In order to prove the feasibility of our strategy, three c-myc-tagged targeted proteins *i.e.,* a Fab-fragment, a nanobody and an affibody were enzymatically modified with biotin. Mass spectrometric analysis and peptide mapping of the three conjugates revealed that all proteins were site-specifically modified with exactly one substrate on the c-myc-tag. We selected the Fab-fragment as a model protein and enzymatically modified it with a selection of eight different functionalities including fluorescent dyes, chelating systems for radiolabeling and different bioorthogonal chemical handles. The different conjugates were then successfully used for applications such as fluorescence-activated cell sorting, immunofluorescence microscopy, nuclear imaging, protein oligomerization and protein immobilization, clearly demonstrating the versatility of our novel protein modification platform. This versatile technology enables us to site-specifically modify virtually any given c-myc-tagged protein with functionalities that are suitable for various downstream applications.

Besides bioconjugation approaches that covalently attach ligands to antibodies, non-covalent antibody conjugates display a useful alternative. Small antibody Fc binding domains (FcBD) are used as adaptor molecules that can bind to any

antibody of the same subtype and thus, direct modification of the antibody is not required. Furthermore, the domains are very robust and so can be modified under harsher conditions compared to antibodies. FcBDs have been extensively used for *in vitro* applications but only a few *in vivo* experiments have been reported where, no stability data was documented. In a third project, we expressed two different FcBDs, a monomeric Z-domain (ZD) and a dimeric ZZ-domain (ZZD), and aimed to investigate their *in vitro* and *in vivo* characteristics by means of radiolabeling. In order to avoid impairment of the antibody-ZD interaction a c-myc-tag was genetically engineered at the terminus of the proteins and our MTG-based bioconjugation strategy was employed to site-specifically attach a chelator to the ZD and ZZD. Both domains could be easily expressed, purified and modified and exhibited excellent thermal stability *i.e.,* they refolded properly after heating to 90 °C for 30 min. While the ZD formed defined conjugates with IgGs, the ZZD promoted antibody crosslinking that resulted in the formation of high molecular weight protein species and hence was not used for further experiments. Radiolabeling of the ZD with the SPECT-nuclide indium-111 and subsequent incubation with an antibody yielded non-covalent conjugates of which the *in vitro* and *in vivo* stability was tested. While the conjugate was stable in human plasma, we observed degradation in mouse and rat plasma, which was also confirmed by the *in vivo* SPECT/CT data. The majority of the injected activity was located in the kidneys one hour post-injection, indicating that the complex was no longer intact. Consequently, neither domain could be used on their own as adaptor molecules for non-covalent antibody conjugates for studies in mice.

The results of this thesis demonstrate the versatility and potential of MTGase as tool for site-specific protein modification. The conjugation strategy can be applied to develop homogeneous antibody conjugates and enables us to readily attach a broad variety of functionalities to virtually any c-myc-tagged protein. Hence, MTGase-mediated bioconjugation is a valuable technology for both therapeutic and research purposes.

Additionally, it is important to furtherinvestigate and evolve the methodologies behind ZD and other FcBDs in order to discover novel domains that exhibit, as a complex with an antibody, improved *in vivo* stability. This could then be, in combination with

our MTG-based protein modification platform, an inexhaustible and flexible source of antibody conjugates for any conceivable application.

Zusammenfassung

Klassische chemische Biokonjugationsmethoden bringen normalerweise heterogene Produkte hervor, da die Konjugationsstelle und die Anzahl an Substraten, mit welchen das Protein modifiziert wird, willkürlich sind. Von dieser Heterogenität speziell betroffen sind therapeutische Biokonjugate wie Antikörper-Wirkstoff-Konjugate (AWK) oder Radioimmunkonjugate (RIK), da Spezies mit unterschiedlicher Anzahl an Substraten, die sich zusätzlich an verschiedene Stellen des Proteins befinden, unterschiedliche *in vivo* Eigenschaften aufweisen. Aber auch Proteinkonjugate, welche für *in vitro* Anwendungen verwendet werden, könnten von neuen Konjugationsmethoden profitieren. Wenn wir imstande sind, zu kontrollieren, an welcher Stelle ein Protein modifiziert wird, könnten zum Beispiel Proteine in einer bestimmten Ausrichtung auf Oberflächen verankert werden. Aufgrund dessen wurden in den letzten Jahren unzählige ortsspezifische Protein-Konjugationsmethoden entwickelt, welche diese Limitierungen überwinden, darunter Ansäze, welche neue chemische Funktionalitäten, Enzyme oder eine Kombination von Beidem nutzen.

Die mikrobielle Transglutaminase (MTGase) ist ein Enzym, welches die Bildung einer Isopeptidbindung zwischen der γ-Carboxyamid-Gruppe von Glutaminresten und primären Aminen katalysiert. Unser Labor hat aufgezeigt, dass die MTGase genutzt werden kann, um Antikörper ortsspezifisch zu modifizieren, weil das Enzym nur ein einziges Glutamin in der konstanten Region der schweren Kette von Antikörpern erkennt.

Der erste Teil der Dissertation behandelt die Anwendung der MTGase, um homogene AWK zu produzieren, wobei Monomethylauristatin E (MMAE) als Wirkstoff verwendet wurde. Zwei verschiedene Strategien wurden evaluiert: (i) ein enzymatischer Ansatz, bei welchem der Wirkstoff mit Hilfe der MTGase direkt an den Antikörper angebracht wurde; (ii) ein indirekter chemo-enzymatischer Ansatz, bei welchem

ein kleiner Linker mit Hilfe der MTGase am Antikörper angebracht wurde, um eine bioorthogonale Funktionalität, Thiol oder Azid, einzuführen. Diese Funktionalität konnte dann selektiv genutzt werden, um den Wirkstoff chemisch anzuhängen. Der enzymatische Ansatz erforderte einen 40-fachen molaren Überschuss an Wirkstoff und ergab heterogene AWK mit einem Wirkstoff-zu-Antikörper-Verhältnis (WAV) zwischen 1.0 und 1.6. Im Gegensatz dazu erforderte der chemo-enzymatische Ansatz nur einen minimalen molaren Wirkstoffüberschuss des 1.25-Fachen und ergab dabei homogene AWK mit einem WAV von genau 2.0. Das entwickelte Protokoll wurde nun erfolgreich angewendet, um Trastuzumab, einen gut charakterisierten therapeutischen anti-HER2/neu-Antikörper, mit MMAE auszustatten. Wir konnten dann zeigen, dass die Immunreaktivität des Antikörpers erhalten werden konnte und das AWK bewies durch das Abtöten von HER2/neu-positiven Zellen seine biologische *in vitro* Aktivität. Eine weitere Studie hatte zum Ziel, die Auswirkung der Homogenität von AWK auf deren *in vivo* Eigenschaften zu untersuchen. Unsere neue Konjugationsstrategie wurde genutzt, um homogene AWK herzustellen, welche aus demselben Antikörper (Brentuximab) und Wirkstoff (MMAE) wie Adcetris®, einem chemisch konjugierten zugelassenen AWK, bestehen. Anschliessend wurden die *in vivo* Eigenschaften der beiden Konjugate evaluiert und untereinander verglichen. Letztlich konnten wir demonstrieren, dass die homogenen AWK ein vorteilhafteres pharmakokinetisches Profil aufwiesen, was in direktem Zusammenhang mit einer im Vergleich zu Adcetris® dreifach höheren maximal tolerierbaren Dosis steht.

Parallel dazu haben wir den Anwendungsbereich der ortsspezifischen Proteinmodifizierung mittels MTGase erweitert, indem wir eine generische Biokonjugationsplattform entwickelt haben, welche den c-myc-Tag (EQKLISEEDL) als Glutamin-Donor nutzt. Um die Machbarkeit unserer Strategie zu beweisen, wurden drei zielfindende Proteine, die jeweils einen c-myc-Tag enthielten, d.h. ein Fab-Fragment, ein Nanobody und ein Affibody, enzymatisch mit Biotin modifiziert. Die massenspektrometrische Analyse sowie das Peptid-Mapping der drei Konjugate haben gezeigt, dass alle Proteine ortsspezifisch mit genau einem Biotinmolekül am c-myc-Tag modifiziert worden sind. Wir haben das Fab-Fragment als Modellprotein definiert und es mit einer Auswahl von acht verschiedenen Funktionalitäten enzymatisch modifiziert. Unter anderem haben wir Fluoreszenzfarbstoffe, chelatbildende Verbindungen für die Radiomarkierung und verschiedene bioorthogonale chemische Funktionen

verwendet. Durch die erfolgreiche Verwendung der Konjugate für verschiedene Anwendungen wie etwa die Durchflusszytometrie, Immunofluoreszenz-Mikroskopie, radioaktive Bildgebung, Oligomerisierung von Proteinen und Immobilisierung von Proteinen konnte die Vielseitigkeit unserer neuen Proteinmodifikationsplattform demonstriert werden. Diese flexible Technologie erlaubt es uns, praktisch jedes Protein, das einen c-myc-Tag enthält, ortsspezifisch mit Funktionalitäten zu modifizieren, die für die unterschiedlichsten Anwendungen geeignet sind.

Nicht-kovalente Antikörperkonjugate stellen eine nützliche Alternative zu Biokonjugationsmethoden dar, welche Liganden kovalent an Antikörper anbringen. Kleine Fc-bindende Domänen (FcBD) werden als Adaptermoleküle verwendet. Da sie an jeden Antikörper vom selben Subtyp binden können, ist die direkte Modifikation des Antikörpers nicht mehr nötig. Zudem sind die Domänen sehr robust und können deshalb im Vergleich zu Antikörpern unter härteren Reaktionsbedingungen modifiziert werden. FcBDs wurden zwar ausgiebig für *in vitro* Anwendungen benutzt, *in vivo* Experimente wurden bisher jedoch nur vereinzelt beschrieben und enthielten zudem keine Stabilitätsdaten. In einem dritten Projekt haben wir zwei verschiedene FcBDs, eine monomere Z-Domäne (ZD) und das entsprechende Dimer (ZZD), mit dem Ziel exprimiert, deren *in vitro* und *in vivo* Eigenschaften mit Hilfe von Radiomarkierung zu untersuchen. Um eine Beeinträchtigung der Interaktion zwischen der Domäne und dem Antikörper zu verhindern, haben wir ein c-myc-Tag am Ende der Proteine eingeführt und unsere auf MTGase basierende Biokonjugationsstrategie verwendet, um ortsspezifisch das chelatbildende Molekül an die Domäne anzubringen. Beide Domänen konnten mühelos exprimiert, aufgereinigt und modifiziert werden und zeigten eine exzellente Temperaturstabilität, d. h. sie haben sich wieder richtig gefaltet, nachdem sie für 30 Minuten auf 90 °C erhitzt wurden. Während die ZD definierte Konjugate mit IgG bildete, förderte die ZZD die Vernetzung der Antikörper, was zur Bildung von Proteinspezies mit hohem molekularem Gewicht führte. Deshalb wurde die ZZD nicht für weitere Experimente benutzt. Die Radiomarkierung der ZD mit dem SPECT-Nuklid Indium-111 und die anschliessende Inkubation mit einem Antikörper brachten nicht-kovalente Konjugate hervor, deren *in vitro* und *in vivo* Stabilität getestet wurde. Während das Konjugat in humanem Plasma stabil war, beobachteten wir in Maus- und Rattenplasma eine Degradation, welche sich auch in den *in vivo* SPECT/CT-Daten bestätigte. Der grösste Teil der injizierten

Aktivität konnte schon nach einer Stunde in den Nieren nachgewiesen werden, was darauf hinweist, dass der Komplex nicht mehr intakt war. Somit kann keine der beiden Domänen alleine als Adaptermolekül zur Herstellung nicht-kovalenter Antikörperkonjugate für Mausstudien verwendet werden.

Die Resultate dieser Dissertation demonstrieren die Vielseitigkeit und das Potential der MTGase als Instrument für ortsspezifische Proteinmodifikationen. Die Konjugationsstrategie kann nicht nur zur Entwicklung homogener Antikörperkonjugate verwendet werden, sondern erlaubt es uns auch, praktisch jedes Protein, welches einen c-myc-Tag enthält, in einfacher Art und Weise mit einer Vielzahl von Funktionalitäten zu versehen. Deshalb ist die auf MTGase basierende Biokonjugation eine sehr nützliche Technologie, sowohl für therapeutische als auch für Forschungszwecke.

Zusätzlich ist es aber auch wichtig, die ZD oder andere FcBDs weiter zu untersuchen und zu entwickeln, um neue Domänen zu entdecken, die, im Komplex mit einem Antikörper, eine verbesserte *in vivo* Stabilität aufweisen. Daraus könnte sich dann, in Kombination mit der auf MTGase basierenden Proteinmodifikationsplattform, eine unerschöpfliche und flexible Quelle von Antikörperkonjugaten für jede erdenkliche Anwendung ergeben.

Contents

Abbreviations

AA	Amino acids
ACN	Acetonitrile
ADC	Antibody-drug conjugate
Amp	Ampicillin
AU	Arbitrary unit
AzK	Azido-lysine
BNC	Bionanocapsules
Boc	*tert*-Butyloxycarbonyl
Bq	Becquerel
BSA	Bovine serum albumin
C2-GalNAz	2-azido-galactose
C2-keto-Gal	2-keto-galactose
CD	Circular dichroism
CDR	Complementarity determining region
CH domain	Constant heavy domain
CHO	Chinese hamster ovarian
CT	X-ray computed tomography
CTC	C-terminal cysteine
Da	Dalton
DNA	Deoxyribonucleic acid
DAR	Drug-to-antibody ratio
DBCO	Dibenzylcyclooctyne

DIPEA	*N*-Ethyldiisopropylamin
DMF	Dimethylformamide
DMSO	Dimethyl sulfoxide
DOTA	1,4,7,10-tetraazacyclododecane-1,4,7,10-tetraacetic acid
DTNB	5,5'-dithiobis(2-nitrobenzoic acid)
DTPA	Diethylene triamine pentaacetic acid
DTT	Dithiothreitol
E.coli	*Escherichia coli*
EDTA	Ethylenediaminetetraacetic acid
EGFP	Enhanced green fluorescence protein
EGFR	Epidermal growth factor receptor
ELISA	Enzyme-linked immunosorbent assay
ESI	Electrospray Ionization
Fab	Fragment antigen-binding
FACS	Fluorescence-activated cell sorting (FACS)
FAP	Fibroblast activation protein
Fc	Fragment crystallizable
FcBD	Fc-binding domain
FCS	Fetal calf serum
FGE	Formylglycine generating enzyme
FITC	Fluorescein isothiocyanate
fXIII	Fibrin-stabilizing factor
Gal T	β1,4-galactosyltransferase
GH	Growth hormone
GST	Glutathione S-transferase
Guan	Guanidine
HEPES	2-(4-(2-hydroxyethyl)piperazin-1-yl)ethanesulfonic acid
HPLC	High-performance liquid chromatography

i.v.	Intravenously
IAM	Iodoacetamide
IC_{50}	Half maximal inhibitory concentration
IgG	Immunoglobulin G
IPTG	Isopropyl β-D-1-thiogalactopyranoside
K_d	Dissociation constant
L1CAM	Cell adhesion molecule L1
LB	Luria-Bertani medium
LC	Immunoglobulin light chain or liquid chromatography
m/z	Mass per charge
mAb	Monoclonal antibody
MALDI	Matrix-assisted laser desorption/ionization
MALS	Multi angle light scattering
MMAE/F	Monomethyl auristatin E/F
MOPS	3-morpholinopropane-1-sulfonic acid
mRNA	Messenger RNA
MS	Mass spectrometry
MTGase	Microbial transglutaminase
MTT	3-(4,5-dimethylthiazol-2-yl)-2,5-diphenyltetrazolium bromide
MW	Molecular weight
MWCO	Molecular weight cutoff
NCAA	Non-canonical amino acids
NHS	*N*-hydroxysuccinimide
NMR	Nuclear magnetic resonance
NTPs	Nucleoside triphosphates
OCFS	Open cell-free synthesis
OD	Optical density

p.i.	Post injection
PAB	*p*-Aminobenzyl
pAcF	*p*-Acetylphenylalanine
PAGE	Polyacrylamide gel electrophoresis
pAMF	*p*-Azidomethyl-L-phenylalanine
PBS	Phosphate buffered saline
PCR	Polymerase chain reaction
PE38	*Pseudomonas* exotoxin A
PEG	Polyethylene glycol
PES	Polyethersulfone
PET	Positron emission tomography
PNGase F	N-Glycosidase F
PTAD	4-phenyl-3H-1,2,4-triazole-3,5(4H)-dione
QCM-D	Quartz crystal microbalance with dissipation monitoring
RIC	Radioimmunoconjugate
rpm	Revolutions per minute
RT	Room temperature
scFv	Single chain variable fragment
SDS	Sodium dodecyl sulfate
SEC	Size-exlusion chromatography
Sial T	α2,6-sialyltransferase
SLB	Supported lipid bilayers
SMWP	Small molecular weight payload
SPAAC	Strain-promoted azide-alkyne cycloaddition
SPECT	Single photon emission computed tomography
SrtA	Sortase A
TAMRA	Tetramethylrhodaminyl
TBS	Tris-buffered saline
TCEP	Tris(2-carboxyethyl) phosphine

TFA	Trifluoroacetic acid
TGase	Transglutaminase
TLC	Thin layer chromatography
TOF	Time-of-flight
t_R	Retention time
tRNA	Transfer RNA
TYE	Tryptone-yeast extract
U	Units
UV	Ultraviolet
vc	Valine-citrulline
z	Charge
ZD	Z-domain
ZZD	ZZ-domain

1

Introduction: Antibody Conjugates - From Heterogeneous Populations to Defined Reagents

Adapted from

Patrick Dennler *et al.*. "Antibody Conjugates - From Heterogeneous Populations to Defined Reagents". Will be submitted as review to *MAbs*

Authors contribution

Patrick Dennler wrote the manuscript and designed the figures, Eliane Fischer reviewed the manuscript

1.1 Abstract

Monoclonal antibodies (mAbs) and their derivatives are currently the fastest growing class of therapeutics. But even if naked antibodies have proven their value as successful biopharmaceuticals they suffer from some limitations. To overcome suboptimal therapeutic efficacy, immunoglobulins are conjugated with drugs and chelating systems bearing therapeutic radioisotopes. Immunoconjugates, including antibody drug conjugates (ADCs) and radioimmunconjugates (RICs), are continuously emerging in anticancer therapy. Besides today's most significant application as therapeutics, antibody conjugates are also extensively used for *in vitro* applications. The decision as to which conjugation method to use strongly depends on the final purpose of the antibody conjugate. Chemical coupling *via* amino acid residues is still the most common method to produce antibody conjugates and is suitable for most *in vitro* applications. Nevertheless, more site-specific ligation techniques based on chemoenzymatic or enzymatic conjugation are emerging technologies that are needed, especially in the field of ADCs. Here, we review different strategies to generate antibody conjugates.

1.2 Introduction

The introduction of the 'magic bullet' principle by Paul Ehrlich at the very beginning of the 20th century and the following work of Köhler and Milstein on the production of the first mouse monoclonal antibodies in 1975 gave rise to the development of a novel class of therapeutics [1]. Today, monoclonal antibodies cover the majority of recombinant therapeutic proteins used in the clinic and many more are in clinical trials [2–6]. However, therapeutic effects of unmodified antibodies are often not curative, especially in cancer therapy. Thus, researchers started to focus on methods to arm antibodies with cytotoxic entities which gave rise to antibody drug conjugates (ADCs) [7–9] and radioimmunconjugates (RICs) [10]. In contrast to ADCs that carry a cytotoxic drug, RICs are armed with suitable therapeutic radionuclides. To date, only a few therapeutic antibody conjugates have made it onto the market, namely Adcetris®, Kadcyla® (ADCs) and Zevalin® (RIC) (Table 1.1). Nevertheless, there are several promising candidates in clinical phases [4, 11–14]. At the same time, monoclonal as well as polyclonal antibody conjugates are important tools for a

variety of *in vitro* assays that are indispensable for research, including Western Blot analysis or immunofluorescence.

Tab. 1.1.: Clinically relevant antibody conjguates: their target and conjugation chemistry that has been employed to attach the corresponding payload.

Antibody conjugate	Target	Payload	Conjugation chemistry
Ibritumomab tiuxetan Zevalin®	CD20	Tiuxetan (DTPA-derivative, chelator)	Isothiocyanate (targeting Lys)
Trastuzumab emtansine Kadcyla®	HER2/neu	Mertansine (DM1, maytansine-derivative)	*N*-hydroxysuccinimide (NHS) (targeting Lys)
Brentuximab vedotin Adcetris®	CD30	Monomethylauristatin E (MMAE, dolastatin-derivative)	Maleimide (targeting Cys)

It is of high importance to select the most appropriate conjugation technique according to the final purpose of an antibody conjugate [15]. Chemical conjugation is often sufficient for antibodies that are used for *in vitro* assays where it is only important to maintain the binding affinity towards the antigen but not to control the payload. Conversely, antibody conjugates that are used for medical applications have different requirements. In addition to an unaltered binding affinity, the ligand-to-antibody ratio, for example, needs to be controllable.

Different sites within the structure of an antibody can be targeted to generate antibody conjugates (Figure 1.1). As proteins are based on an amino acid backbone, conjugation *via* reactive natural or engineered residues is the most obvious method. The difficulty, however, is to control the stoichiometry of chemical reactions with lysines or cysteines, which are the two most commonly targeted amino acids for bioconjugation. The reaction outcome is usually a mixture of conjugate species with different antibody-to-ligand ratios which can have different pharmacokinetics and thus influence the conjugates biodistribution, efficiency and safety profile [16–18]. Additionally, heterogeneity is not only created by different antibody-to-ligand ratios but also by different sites of conjugation. Depending on the purpose, certain antibody conjugates require a clearly defined uniform population to help to reduce batch-to-batch variability and possible impairment of antibody conjugates' characteristics [16, 17]. Hence, a lot of effort has been made to find and establish antibody conjugation strategies which enable us to better control stoichiometry and

site-specificity. Some of the approaches require site-directed mutagenesis, whereas others are more complicated as they include multiple enzymes or combine protein expression machineries from different hosts. These techniques are in general more time consuming compared to a classical chemical conjugation approach since the genetic code of the antibody has to be altered or additional proteins have to be expressed.

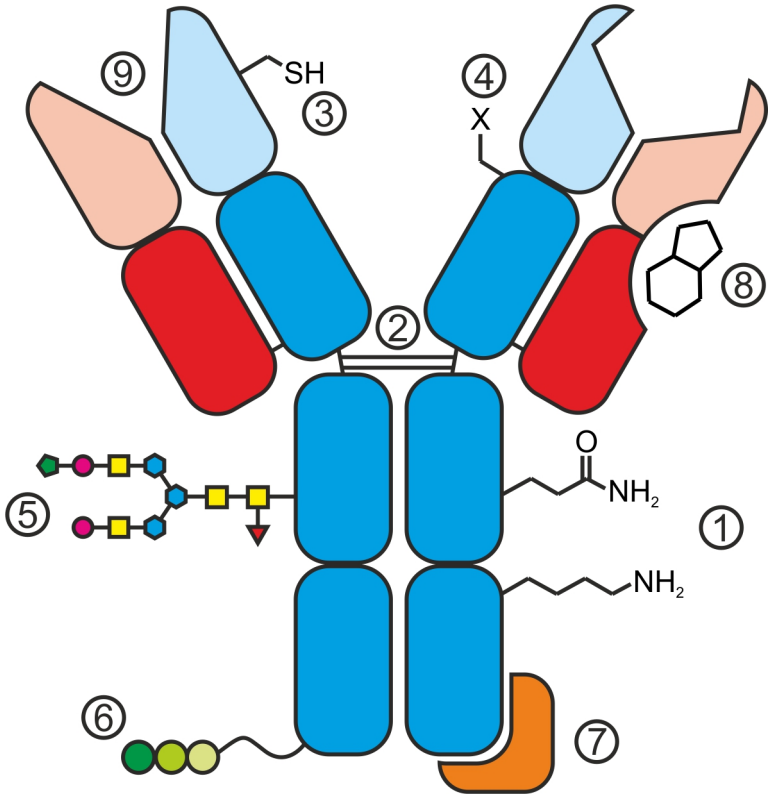

Fig. 1.1.: Antibody conjugates can be generated by targeting natural canonical amino acids (1) including interchain disulfides (2), engineered cysteines (3), non-natural amino acids (4), the carbohydrate moiety (5) or engineered tags (6). Strong protein-protein interaction *i.e.,* Fc-binding domains (FcBD) can be used to form non-covalent antibody conjugates (7). Additionally, the nucleotide binding site is a valuable antibody modification site for photoaffinity labeling (8) and antibodies with catalytic activity (9) can be exploited to form bioconjugates where the coupled pharmacophore *e.g.,* a peptide assumes the targeting function and the antibody acts as a cargo molecule.

This review summarizes the currently available conjugation methods with a focus on newly emerged technologies that allow better control over stoichiometry and site-specificity.

1.3 Conjugation *via* natural amino acid residues

In theory, bioconjugation is possible *via* most amino acids [19–24]. Nevertheless, the nucleophilic primary amines of lysine and reactive thiols of cysteine are the most commonly used amino acids in bioconjugation of antibodies and are still the current method of choice. Additionally, tyrosine and selenocysteine have also been exploited as reactive sites for antibody modification (Figure 1.2).

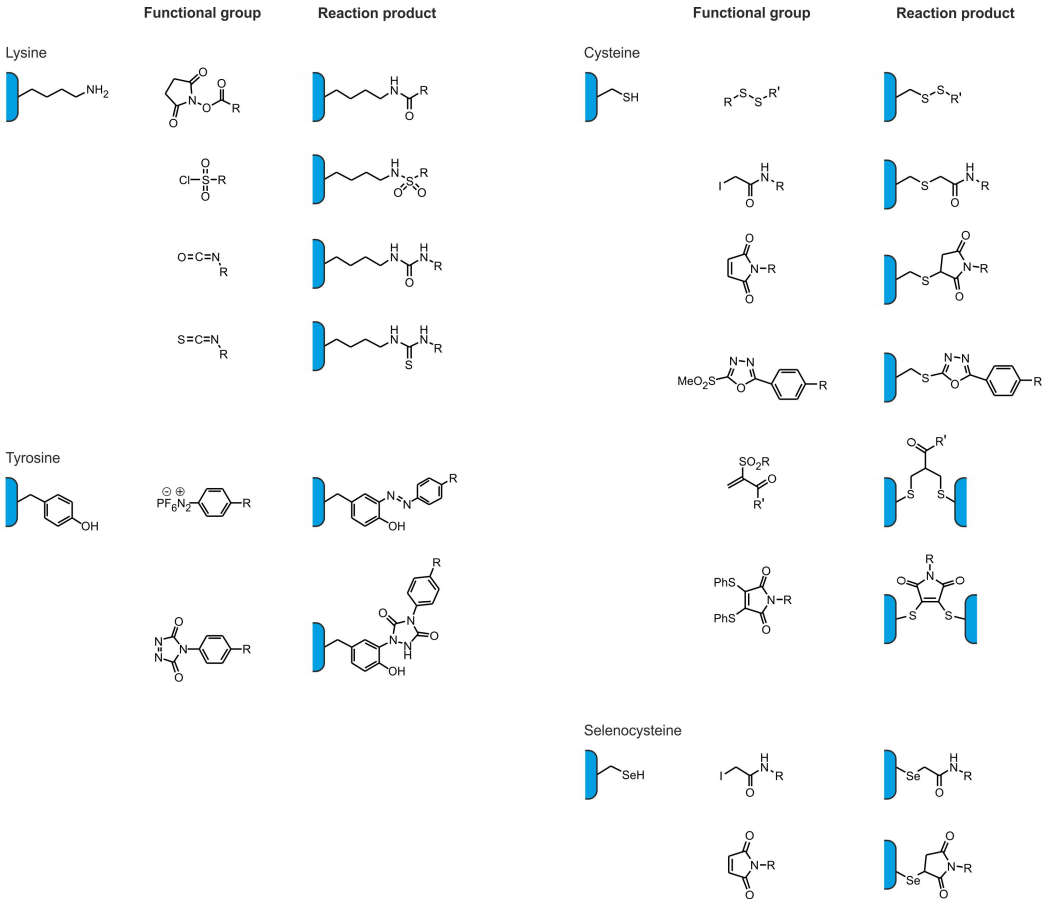

Fig. 1.2.: Overview on functional groups and their reaction product with the corresponding amino acid residue.

1.3.1 Lysines

Lysine is one of the most commonly used amino acid residues for linking substrates to antibodies because they are usually exposed on the surface of the antibody and are thereby easily accessible. Alkylation and acylation are the most important reactions with the nucleophilic ϵ-amine [21]. Antibodies generally contain up to 80 lysine residues that are widely distributed throughout their backbone [25] and as a

consequence, conjugation *via* lysines inevitably leads to a twofold heterogeneity: (i) Different number of substrate per antibody and (ii) antibodies with the same number of substrates have them attached at different sites [26, 27]. Furthermore, modified lysines in proximity to the antibody binding site may influence the performance of the IgG. However, the heterogeneity can be controlled to a certain extent by adapting the molar ratio of ligand and antibody used in the reaction [28–30].

Lysines are typically modified with *N*-hydroxysuccinimide (NHS) esters, sulfonyl chlorides, isocyanates and isothiocyanates, among which the former and latter are by far the mostly used functionalities. Among a countless number of lysine-coupled antibody conjugates, for both *in vitro* and *in vivo* applications, there are two that are clinically relevant the antibody-drug conjugate (ADC) trastuzumab emtansine (Kadcyla®) and the radioimmunoconjugate (RIC) ^{90}Y-ibritumomab tiuxetan (Zevalin®) (Table 1.1). Whereas the drug was attached to the antibody *via* a heterobifunctional crosslinker [31], an isothiocyanate-functionalized chelator was used to accomplish an antibody conjugate that can be labeled with the therapeutic radioisotope ^{90}Y [32].

Although NHS esters are widely applied, it should be taken into account that they can also react with other amino acids such as threonine, tyrosine, serine and cysteine or even with the N-terminus of a protein [33, 34]. In contrast to the stable amide bond between NHS esters and lysine residues, bonds that are formed with those amino acids can be labile and susceptible to hydrolysis. As a result, the premature release of free drug from ADCs can lead to unwanted side-effects [35].

1.3.2 Cysteines

Native cysteines

In contrast to lysines, the number of cysteines within the sequence of IgGs is much lower. There are only four interchain disulfide bonds that can be targeted as potential conjugation sites and thus, the heterogeneity of immunoconjugates can be dramatically reduced. Moreover, these cysteines exclusively form covalent disulfide bonds to stabilize the tertiary structure of the antibody and are therefore, under non-reducing conditions, not reactive [36–39]. Sun *et al.* took advantage of the fact that the susceptibility of different disulfide bonds in an antibody towards reduction varies [40]. They developed two strategies that enabled tighter control of the site

of conjugation. While partial reduction with either dithiothreitol (DTT) or tris(2-carboxyethyl) phosphine (TCEP) predominantly yielded conjugates where ligands were attached to heavy-light chain disulfides, partial reoxidation with 5,5'-dithiobis(2-nitrobenzoic acid) (DTNB) yielded conjugates where ligands were mainly attached to heavy-heavy chain disulfides [41]. McDonagh *et al.* developed a different approach to control the site modification by replacing four or six of the interchain cysteines with serine, thereby reducing the number of accessible cysteines to either four or two. Accordingly, stoichiometric homogenous antibody conjugates with clearly defined sites of ligand attachment could be generated [42].

Classically, cysteine residues are modified through disulfide exchange, iodoacetamide as alkylation reagent or maleimides [21, 22, 24]. Alkylation of thiols with iodoacetamide is predominantly used in order to prevent the formation of disulfide bonds (possible crosslinking) after reduction of an antibody and is therefore often required for analytical purposes. Probably the most frequently used cysteine-based conjugation strategy uses maleimide-functionalized reagents or linkers. While the number of conjugates for both *in vitro* and *in vivo* applications is, as for lysine-based approaches, unlimited, only one antibody conjugate is currently used in the clinics. The ADC brentuximab vendotin (Adcetris®) was generated by the conjugation of the maleimide-functionalized drug to reduced interchain cysteines (Table 1.1) [43].

Engineered cysteines

The incorporation of additional unpaired cysteine residues into the backbone of an antibody is a valuable strategy towards improved homogeneity of antibody conjugates. Stimmel *et al.* used this approach and replaced a serine in the CH3 domain with a cysteine. Controlled reduction conditions enabled them to generate RICs by site-specifically attach a chelating system exclusively to the two additional cysteines while all other cysteines in the antibody backbone remain unaffected [44]. A similar approach was exploited by Junutula and co-workers to develop homogeneous ADCs. The resulting defined drug-to-antibody ratio (DAR) of approximately 2 led to an improved therapeutic index compared to the corresponding ADC that was produced by conjugation *via* interchain disulfides [45, 46]. The homogeneity *i.e.,* the absence of ADCs with a high DAR, is most likely the reason for these encouraging results. Additionally, the site of conjugation influences the stability of the bond between the toxin and the cysteine [47]. Sites where the cysteine

is only partially accessible and surrounded by positively charged amino acids promoted succinimide ring hydrolysis resulting in better stability of the conjugate. In contrast, solvent exposed and easily accessible cysteines were prone to a maleimide exchange process with albumin, cysteine and glutathione both *in vitro* and *in vivo* [47].

Although cysteine-based bioconjugation represents a valuable tool for site-specific and stoichiometric uniform antibody modification, some aspects have to be considered: (i) Elimination of interchain disulfide bonds as described by McDonagh *et al.* can affect the quarternary structure of the antibody and therefore influence *in vivo* characteristics *e.g.,* antibody effector functions [48, 49], (ii) the introduction of novel solvent-exposed cysteine residues can influence the aggregation behaviour of the expressed antibodies as the reactive thiols can form disulfide bonds between immunoglobulins [50, 51] and (iii) the formed succinimide thioether bond (between maleimide and cysteine) undergoes exchange and retro-addition processes in the presence of other thiols *e.g.,* albumin or glutathione that can influence the *in vitro* but more importantly the *in vivo* performance of the antibody conjugate [47, 52, 53]. To circumvent this issue Patterson *et al.* developed a sulfone-based linker which exhibited, when conjugated to an antibody, superior stability compared to the corresponding maleimide-based linker [54]. Godwin *et al.* presented an alternative thiol conjugation approach where bis-sulfone-functionalized reagents are used to form a stable three carbon bridge with disulfides. In addition, the structure of the antibody remains intact and the ligand-to-antibody ratio can be tightly controlled [55]. A similar bridging approach was also described by Schumacher and co-workers. In contrast to Godwin, they developed a novel class of maleimides, designated as next generation maleimides, and successfully generated ADCs with all the aforementioned advantages [56]. Lyon and co-workers developed novel maleimide-derivatives that undergo rapid thiosuccinimide ring hydrolysis and are then no longer prone to maleimide elimination processes [57, 58].

1.3.3 Selenocysteines

Hofer *et al.* cotranslationally inserted selenocysteine, a cysteine analogue, into the C-terminus of IgG1 Fc fragments. The nucleophilic selenol group (pK_a 5.2) equips selenocysteine with unique chemical properties, enabling specific reaction with

electrophilic moieties - maleimide, maleimide-like or iodoacetamide - in the presence of other amino acids, including cysteine (pK_a 8.3) [59]. Moreover, reduction of the antibody is no longer required and hence, interchain disulfides will remain unaffected. By generating stoichiometrically uniform antibody conjugates with biotin, fluorescein and polyethylene glycol as a proof of concept, they demonstrated the impact of their technology for the development of novel antibody conjugates [60–62].

1.3.4 Tyrosines

Surface accessible tyrosines are rare and therefore an attractive target for bioconjugation. By using cyclic diazodicarboxamide derivatives, such as 4-phenyl-3H-1,2,4-triazole-3,5(4H)-dione (PTAD), Ban *et al.* established an efficient click-like tyrosine ligation and successfully conjugated PTAD-functionalized substrates to trastuzumab [63, 64]. Recently, they described a novel approach to conjugate *via* tyrosine residues, where diazonium hexafluorophosphate reagents are used to selectively modify trastuzumab. However, experiments with *N*-acyl methylamides of histidine, serine, cysteine, tryptophan and lysine revealed reactivity the latter two towards cyclic diazodicarboxamid. In addition histidine, tryptophan and unoxidized cysteine exhibited reactivity towards a diazonium hexafluorophosphate derivative [65, 66]. Even if both reagents exhibit a high chemoselectivity for tyrosine, side reactions with other amino acids are inevitable.

1.4 Conjugation *via* non-canonical amino acid residues

As an alternative to natural amino acids, non-canonical amino acids (NCAA) are valuable handles for site-selective protein labeling since they display a chemical functionality that is orthogonal to the functionalities found on natural amino acids [67]. Technologies to incorporate NCAAs require rearrangement of the antibody sequence and thus the exact localization and number of NCAA in the expressed protein can easily be controlled and changed. Schultz and co-workers are pioneers of cell-based approaches to incorporate NCAA into proteins, including antibodies [68, 69]. Their technology relies on the introduction of an orthogonal tRNA/aminoacyl-tRNA synthetase pair, which, in combination with *p*-acetylphenylalanine (*p*AcF),

was exploited to express NCAA displaying antibodies (Figure 1.3). In a second step, oxime ligation with alkoxy-amine derivatized auristatin yielded homogeneous ADCs with defined sites of drug attachment [18, 70]. Recently, they presented an extension of their technology whereby they incorporated two distinct NCAA into the same antibody, *p*AcF and azido-lysine (AzK). The two functionalities enabled them to then site-specifically conjugate a toxin and a fluorescent dye [71]. This approach could be an attractive basis for endowing antibodies with toxins that exhibit different cell-killing mechanisms, thereby increasing the potency of ADCs. Although quantitative yields could be accomplished, the reaction conditions of the oxime ligation are rather harsh for antibodies and could potentially lead to aggregation [72–74].

Open cell-free synthesis (OCFS) is a novel technology to incorporate NCAA into antibodies which, in contrary to the cell-based approach, does not use intact living cells [75–77]. The protein is synthesized by mixing cell extract (providing essential organelles) with chemical substrates (nucleoside triphosphates, amino acids, salts and co-factors), an energy regeneration system and the corresponding DNA template (Figure 1.3) [78]. Zimmerman *et al.* exploited OCFS to express *p*-azidomethyl-L-phenylalanine (*p*AMF)-displaying antibodies which could then be site-specifically modified with a drug to generate homogeneous ADCs [79].

1.5 Conjugation *via* the carbohydrate moiety

The carbohydrate moiety of antibodies represents a suitable modification site because its localization is distant from the Fab region's immunoreactive site. Therefore, the chances to impair the antibody binding affinity, a potential pitfall of chemical conjugation *via* lysines [20], are minimal. Various strategies to target the glycan for bioconjugation have been developed among which three different methodologies can be distinguished.

1.5.1 Chemical oxidation

Numerous approaches used sodium periodate as an oxidation reagent to introduce a bioorthogonal aldehyde functionality on the carbohydrate moiety of antibodies. The aldehydes were then used to react with hydrazide- or primary amine-functionalized

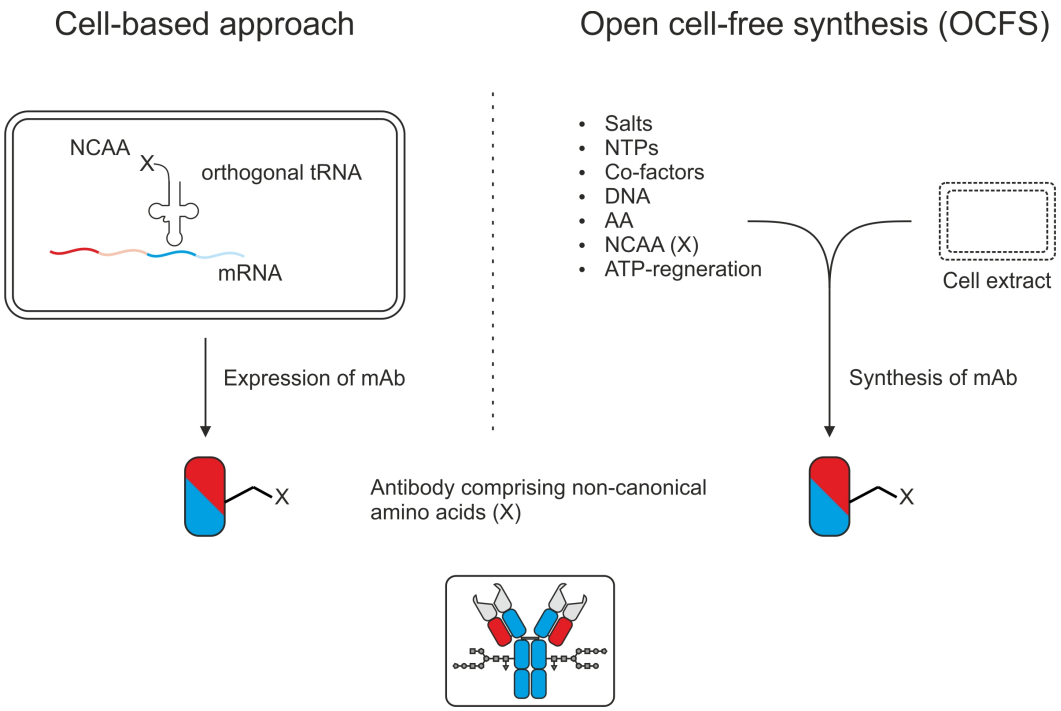

Fig. 1.3.: Two different approaches can be employed to incorporate non-canonical amino acids (NCAA) into an antibody. The cell-based approach uses an orthogonal tRNA/aminoacyl-tRNA synthetase pair to generate a tRNA that carries a NCAA (X) and hence an orthogonal functionality is integrated into the antibody. On the contrary, the open cell-free synthesis (OCFS) is used to synthesize, rather than to express, the protein in a living cell free environment. It requires cell extract (provides essential organelles), salts, nucleoside triphosphates (NTPs), co-factors, the corresponding DNA, amino acids (AA), NCAA and an energy regeneration system.

molecules such as biotin [80], toxins [81–84], chelating systems for radiolabeling [85, 86] or spacers to link proteins to antibodies [87–90]. The resulting antibody conjugates often lack homogeneity since (i) sodium periodate can cleave any *cis*-glycol group (Figure 1.4A) and (ii) the glycosylation pattern of antibodies is heterogeneous (Figure 1.4B) [91–93]. It has been shown that the rate of oxidation, and as a result the number of available aldehydes, can be controlled to a certain extent by adjusting *e.g.,* the concentration of the oxidation reagent, reaction temperature or pH [94–96]. Hence, selective oxidation is possible [84]. However, heterogeneity of the glycosylation pattern remains unchanged and additionally, chemical treatment of the antibody may also affect amino acid residues such as serine, threonine, proline and methionine which could ultimately perturb the immunoreactivity of the antibody.

1.5.2 Enzymatic or chemoenzymatic approaches

To overcome the problems of chemical oxidation various enzymatic and chemoenzymatic approaches have been established (Figure 1.4C). Solomon *et al.* treated the carbohydrate moiety concomitantly with neuraminidase and galactose oxidase to generate aldehydes and subsequently compared their enzymatic to the classical periodate-approach with respect to site-specificity. The enzymatic oxidation was, as expected, more specific than the chemical oxidation because it is restricted to galactose [97]. As with the chemical oxidation, this approach does not address the fact that each carbohydrate can bear zero (G0), one (G1) or two terminal galactose (G2) units and thus, accomplishing homogeneous antibody conjugates is impossible. Zhou *et al.* solved this problem by using a β1,4-galactosyltransferase to generate homogeneous G2 glycosylation and a α2,6-sialyltransferase to sialylate the antibody on the galactose units. Selective oxidation of sialic acid yielded aldehyde functionalities which were subsequently reacted with an aminooxy-functionalized toxin to produce homogeneous ADCs [98]. A slightly different approach consists of an enzymatic two-step procedure to incorporate non-natural glycan moieties. In a first step, terminal galactose units are removed by β1,4-galactosidase to yield homogeneous G0 species which are then reglycosylated to a uniform G2 species by a mutant β1,4-galactosyltransferase-mediated attachment of C-2 modified galactoses *e.g.,* 2-keto-galactose (C2-keto-Gal) or 2-azido-galactose (C2-GalNAz). While Boeggeman *et al.* applied this technology to develop biotinylated and fluorescently-labeled antibody conjugates [99, 100] other groups employed the protocol to generate radioactive antibodies as *in vivo* imaging agents [101, 102] or ADCs [101–103].

1.5.3 Metabolic engineering of the carbohydrate moiety

Instead of modifying the carbohydrate moiety of the purified antibody, Okeley *et al.* envisaged the introduction of unnatural fucose-derivatives at an earlier stage of the antibody production. Their antibody modification strategy is based on the metabolic incorporation of thio-fucose during the post-translational modification of the antibody by feeding the cells with the non-natural sugar (Figure 1.4D). The thiol-functionality could then be used as a bioorthogonal handle to attach a toxin by employing standard thiol-maleimide chemistry [104]. Nevertheless, the incorporation rate

varies significantly among different fucose derivatives which limits the extension of this technology to introduce various bioorthogonal functionalities.

Although it has been demonstrated that the carbohydrate moiety is an attractive multivalent target for bioconjugation, most of the described approaches still suffer from product heterogeneity either caused by non-homogeneous glycan patterns or non-quantitative bioconjugation yields. Moreover, it must be considered that antibodies can also be N-glycosylated in their variable region [93, 105]. These Fab carbohydrates can be involved into immunomodulation and their composition differs from the Fc glycans [106, 107]. Bioconjugation procedures, as described in this section, will inevitably affect these Fab glycans and as a consequence may influence the antibodies properties.

1.6 Conjugation *via* tags

Enzymes that recognize a specific amino acid tag, usually ranging from four up to 15 residues can be exploited for site-specific antibody conjugation [108, 109]. The uniqueness of the tag prevents random modification and allows the site of modification to be exactly determined in a similar manner as the incorporation of additional cysteines or NCAA (see section 1.3.2 and 1.4).

Formylglycine generating enzyme (FGE) recognizes a tag that comprises a 6-residue LCxPxR motif and oxidizes the cysteine to formylglycine (Figure 1.5A) [110, 111]. The bioorthogonal aldehyde functionality can then be reacted specifically with hydrazines and alkoxyamines to form hydrazones and oxime-coupled products, respectively (see also section 1.5). Hudak *et al.* employed this approach to join an antibody to a second protein. The tagged antibody and the tagged protein were first reacted with a cyclooctynes-aminooxy linker and an azido-aminooxy linker respectively and then covalently linked together *via* a copper-free azide-alkyne cycloaddition reaction that yielded heterobifunctional antibody conjugates [112]. A common problem of hydrazones and oximes is their susceptibility to hydrolysis. As a consequence, Agarwal *et al.* recently developed a novel aldehyde tag-compatible functionality that is based on an indol framework and reacts with the aldehyde to form an oxacarboline linkage. This bond is more stable towards hydrolysis and compatible with their FGE-based antibody bioconjugation approach [113]. As

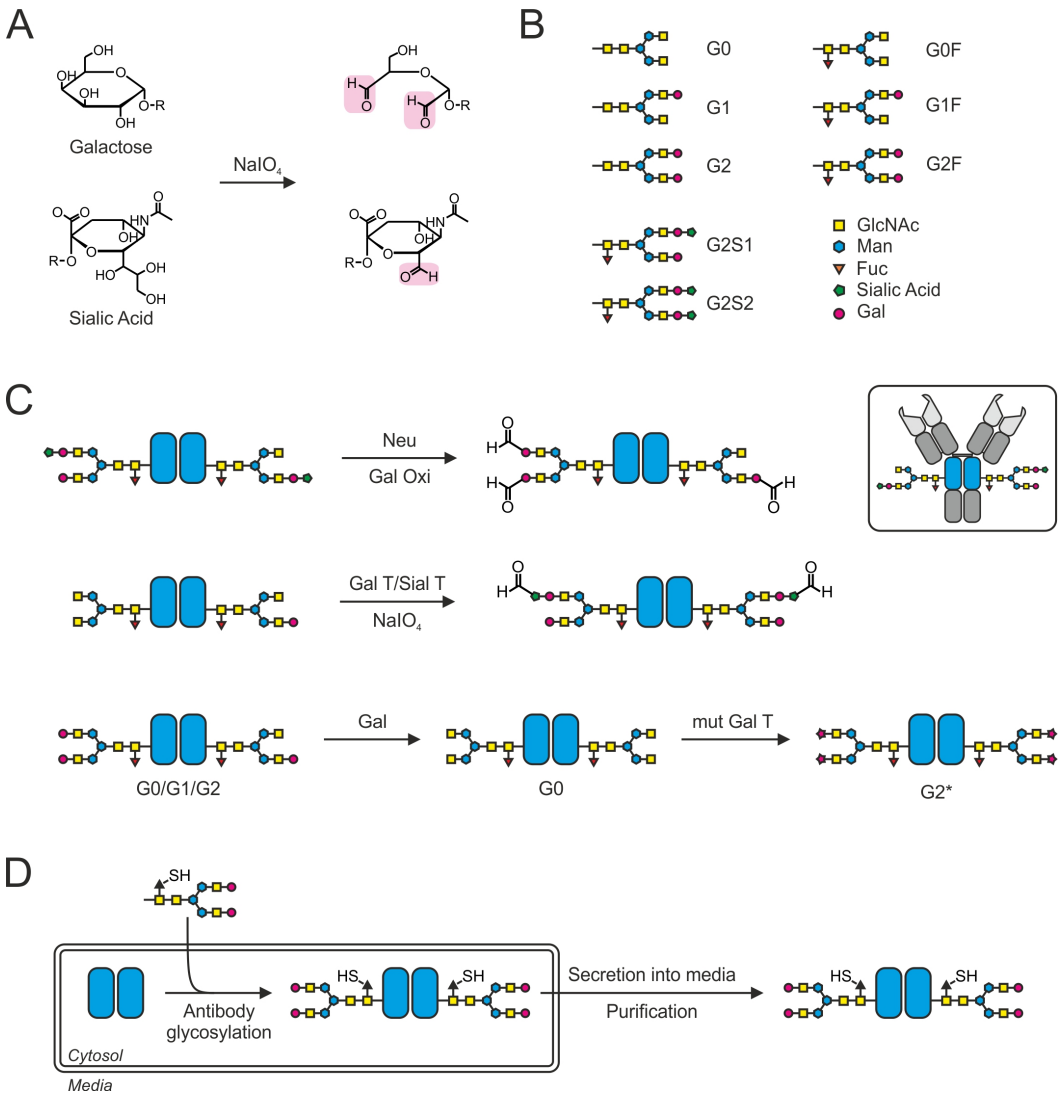

Fig. 1.4.: Different strategies to introduce bioorthogonal functionalities on the carbohydrate moiety for site selective conjugation. A) Classical chemical approaches use sodium periodate ($NaIO_4$) to oxidize *cis*-glycol groups of *e.g.,* galactose or sialic acid which results in the formation of an aldehyde functionality (red square). B) Schematic representation of a selection of different glycoforms that can be found on IgGs (G0 represents the conserved glycan core), to illustrate the heterogeneity of antibody glycosylation patterns. C) Novel enzymatic methods treat the sugar residue with neuraminidase (Neu, cleaves terminal sialic acids) and galactose oxidase (Gal oxi, oxidizes galactose residues) which results in the formation of bioorthogonal aldehyde functionalities (not homogeneous). Sequential treatment of the antibody with β1,4-galactosyltransferase (Gal T, generates homogeneous G2 species) α2,6-sialyltransferase (Sial T, attaches sialic acids) yields homogeneously sialylated antibodies that can be selectively oxidized to the corresponding aldehyde functionality (homogeneous). A more recent method does not generate aldehyde functionalities but introduces non-natural galactose derivatives. Therefore, the antibody is treated with β-galactosidase (Gal, removes all natural galactose resiudes) and a mutant Gal T (accepts bioorthogonal azide- or keto-galactoses) to yield homogeneous G2 glycan patterns comprising non-natural functionalities (G2*). D) Non-canonical thio-fucose derivatives were incorporated into the glycan of antibodies by feeding the cells with the bioorthogonal sugar resulting in expressed antibodies that display thiol functionalities (not homogeneous).

discussed above, the presence of unmodified cysteines on the tag could interfere with other free cysteines or with the folding of the protein. Furthermore, hydration of the formylglycine in aqueous systems makes it impossible to yield homogeneous antibody conjugates [114].

A second tag-based approach for antibody bioconjugation is sortagging, which relies on the ability of sortase A (SrtA), a bacterial transpeptidase from *Staphylococcus aureus*, to catalyze the ligation between an LPXTG and a polyglycine motif (Figure1.5B) [115–117]. Different groups have demonstrated the versatility of this this technology by fusing proteins including albumin, a Fab-fragment, an antibody, gelonin and green fluorescent protein (polyglycine tagged) and peptides to a LPETG-tagged antibody [118, 119]. At the same time, it is also possible to tag small molecules with one of the two motifs and use them to produce antibody conjugates. Wagner *et al.* modified LPETG-tagged antibodies with triglycine-functionalized chemical entities that are suitable for copper-free azide-alkyne cycloaddition and subsequently linked two different antibodies to yield bispecific antibody conjugates [120]. Recently, Bellucci *et al.* described a non-canonical function of SrtA where they replaced the polyglycine with a $WX_3VXVYPKH$ motif. The introduction of this sequence into the backbone of an antibody enabled them to site-specifically conjugate LPETG-functionalized biotin to the immunoglobulin [121]. This novel approach overcomes the limitations of classical SrtA mediated bioconjugation that is restricted to the terminal modification of proteins with only one molecule because it is conceivable to incorporate multiple copies of the sequence into the protein at virtually any location.

1.7 Miscellaneous conjugation methods

1.7.1 Fc binding domains (FcBD)

All previously described bioconjugation methods include the formation of a covalent bond between a specific functionality and an amino acid or carbohydrate moiety. Small domains that bind with high affinity to a conserved sequence in the Fc-domain of antibodies are used to form non-covalent antibody conjugates with a defined site of conjugation and stoichiometry. This approach does not require any modification of

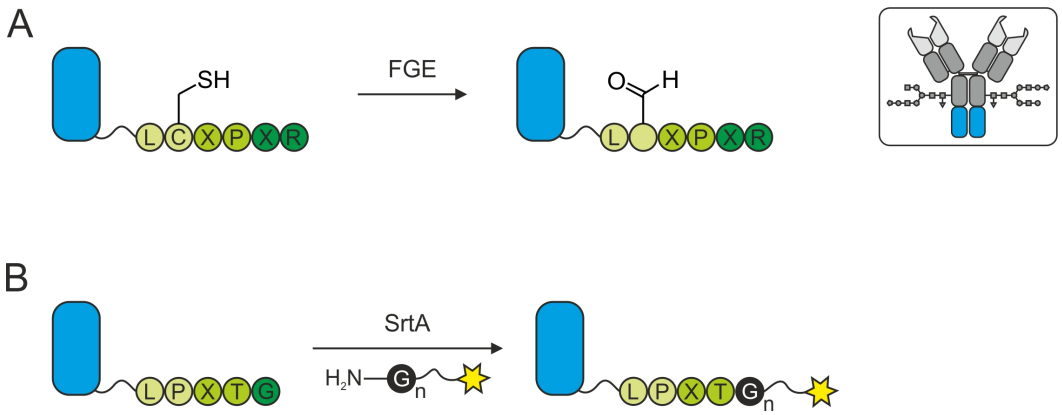

Fig. 1.5.: General concepts of antibody conjugation *via* tags. A) The formylglycine generating enzyme (FGE) converts the cysteine of a LCXPXR tag into formylglycine, thereby creating an bioorthogonal aldehyde handle for site-specific chemical antibody conjugation. B) Sortase A (SrtA) mediates that conjugation of an LPXTG motif with a polyglycine-functionalized ligand of interest (yellow star).

the antibody itself and the same domain can be used to readily form bioconjugates with virtually every immunoglobulin of the same isotype/subtype.

ZZ-Domain

Among numerous FcBDs the ZZ-domain, a dimer of the modified immunoglobulin binding site of protein A of *Staphylococcus aureus*, is the most widely used [122]. Its high-affinity interaction with the Fc part of antibodies has been exploited to generate antibody displaying nanocapsules that were employed for *in vitro* targeted delivery of proteins, for simultaneous detection of multiple antigens in immunological assays (Western blot analysis, immunocytochemistry, flow cytometric analysis, and immunohistochemistry), for immunosensor chips or for the establishment of drug-delivery systems (Figure 1.6A) [123–129]. Benhar and co-workers developed FcBD-based ADCs by genetically fusing the ZZ-domain to *Pseudomonas* exotoxin A (ZZ-PE38) (Figure 1.6B) [130]. Incubation with a corresponding antibody yielded highly toxic non-covalently coupled ADCs that have proven their potential by efficiently killing tumor cells *in vivo* [131–133]. By combining the SrtA mediated protein-protein conjugation technology with the ZZ-domain, Sakamoto *et al.* demonstrated the utility of FcBDs as versatile adapter molecules for the generation of antibody-protein conjugates [134].

Photoactivable FcBDs

Although the binding affinity of the ZZ-domain towards an antibody is high, it still remains a reversible interaction and hence may not be stable enough for applications

where conditions such as pH vary. A possible strategy to covalently link an FcBD to an antibody is to equip the domain with a photoactivable probe *e.g.,* benzophenone which, upon irradiation, is activated and forms a covalent bond to a closely located amino acid on the immunoglobulin surface (Figure 1.6C). This methodology has been successfully applied by using various FcBDs including different variants of the monomeric Z-domain and a minimal domain of protein G [135–139].

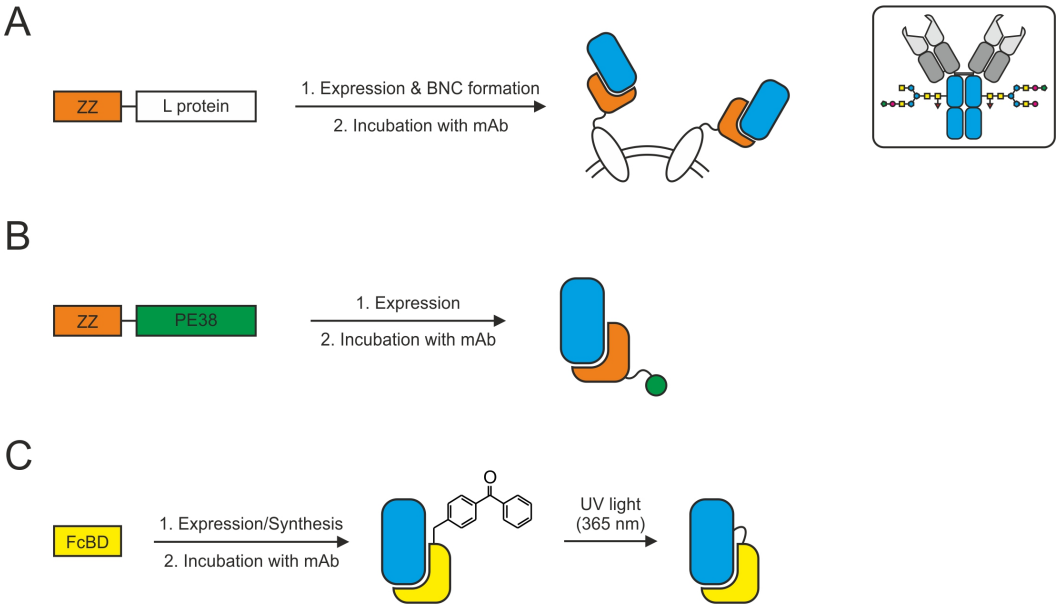

Fig. 1.6.: Fc binding domains (FcBD) were exploited as a tool to produce both non-covalent and covalent antibody conjugates. A) The ZZ-domain (ZZ) is expressed as a fusion with the L protein from hepatitis B virus to generate FcBD-bionanocapsules (BNC) that can be decorated with antibodies suitable various *in vitro* applications. B) When expressed as a fusion protein with *Pseudomonas* exotoxin A (PE38), the ZZ-domain can be used to generate ADCs. C) If FcBDs are endowed with photoactivable chemical groups *e.g.,* benzophenone it is possible to form covalent antibody conjugates by exposing the non-covalent conjugate to UV light.

1.7.2 Bioconjugation *via* the nucleotide binding site

Besides the canonical antigen binding sites of an IgG (CDRs), a rather unknown and unconventional nucleotide binding site can be found in the variable region of immunoglobulins [140]. Pavlinkova *et al.* were the first to recognize the potential of this binding pocket for site-specific antibody modification. They developed biotin-functionalized nucleotide derivatives that, upon binding, were photoactivated to form a covalent bond to the antibody (Figure 1.7A) [141, 142]. Alves *et al.* followed-up with the strategy and used various indole-functionalized ligands comprising biotin, a fluorescent dye, a cyclic peptide and paclitaxel to generate antibody conjugates

[143, 144]. Even though the conjugation site is not very distant from the antigen binding site, the immunoreactivity of the antibody is not impaired.

1.7.3 Catalytic antibodies

Catalytic antibodies are immunoglobulins that mechanistically mimic natural enzymes. Barbas *et al.* screened for such antibodies *via* reactive immunization and could identify antibody catalysts that mimic class I aldolase ezymes [145–148]. In contrast to any conjugation technology previously described, the antibody acts here solely as a cargo molecule and has no targeting properties. By fusing a small molecular weight payload (SMWP) *e.g.,* a peptide with a catalytic antibody, Barbas and co-workers created antibody conjugates (CovX-Bodies™ [149]) that combine the highly specific targeting properties of the SMWP and the pharmacokinetic characteristics of an antibody. The conjugation is based on the derivatization of the pharmacophore with a functional group that forms a covalent bond in the active site of the catalytic antibody (Figure 1.7B). This technology has been used extensively to develop a variety of novel therapeutics for cancer treatment, pain or growth hormone (GH) deficiency [150–155].

As mentioned before, it is no longer the targeting properties of the antibody that are desired but their pharmacokinetic characteristics and hence, these are no longer antibody conjugates in the classical sense.

1.8 Transglutaminases

Transglutaminase-based antibody conjugation methods target both endogenous glutamines and glutamine-containing tags on antibodies and are therefore addressed separately.

Transglutaminases (TGases, EC 2.3.2.13) are a family of enzymes that catalyze the acyl transfer reaction between the γ-carboxyamide group of glutamine residues and various primary amines including lysine (transamidation) under the loss of ammonia. Water and alcohols may compete with this reaction since they can act as a nucleophile leading to hydrolysis (deamidation) or esterification, respectively (Figure 1.8) [156–158]. TGases are involved in various biological, usually protein crosslinking-dependent, processes including blood coagulation, skin barrier formation and tissue

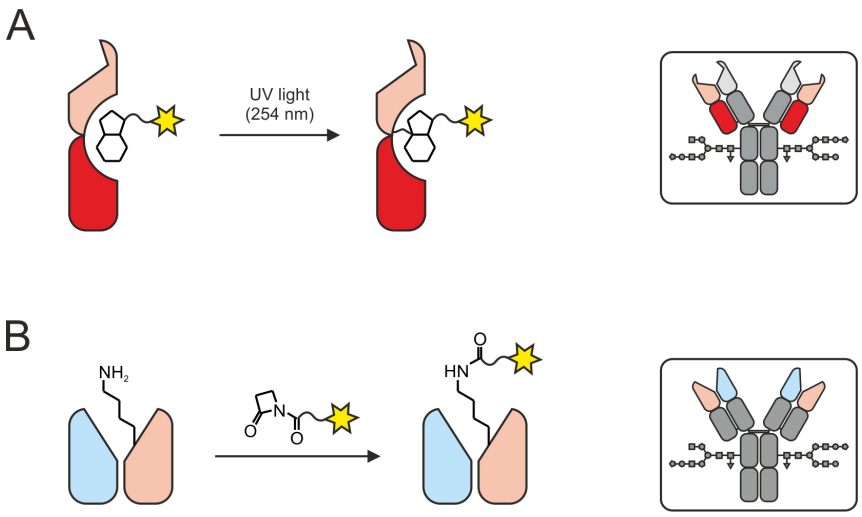

Fig. 1.7.: A) General procedure for photoaffinity labeling of antibodies. A ligand of interest (yellow, star) is functionalized with a nucleotide based chemical entity. Once bound to the nucleotide binding site, irradiation with UV light will activate the nucleotide which results in the formation of a covalent bond. B) The enzymatic activity of catalytic antibodies results in the formation of a covalent bond between a lysine of the catalytic site and azetidinone-functionalized small molecular weight payload *e.g.,* peptide (yellow star).

remodeling but also in cancer, neurodegenerative diseases and celiac disease [157, 159–163]. At the same time, recombinant TGases are extensively used in the area of food processing, leather and textile industry, development of novel biomaterials or protein modification [164–168].

Among the eight mammalian TGases, which differ in size, tissue distribution localization and function, fibrin-stabilizing factor (fXIII) is the most prominent since it is one of the key players in the terminal phase of blood coagulation [157, 169, 170]. Nevertheless, lower organisms such as algae, fungi and bacteria as well as plants express TGases and novel sources are still being discovered [158, 171].

1.8.1 Microbial Transglutaminase (MTGase) from *Streptomyces mobaraensis*

First expressed, purified and characterized by Ando *et al.* MTGase has become an indispensable and versatile tool, particularly for biotechnological technologies including protein conjugation [172–174]. MTGase is a Ca^{2+}- and GTP-independent, robust enzyme with a disc-like shape, low substrate specificity but high reaction rate and an active site that forms a deep cleft harboring a Cys-His-Asp catalytic triad at the bottom (Figure 1.9A and B) [168, 175–177]. The active site is surrounded

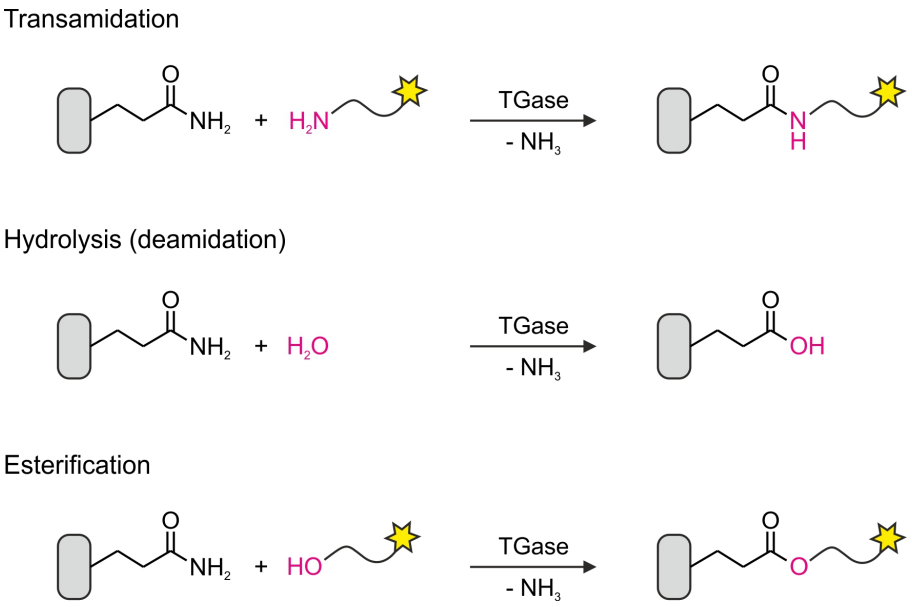

Fig. 1.8.: Possible TGase-mediated reactions. Transamidation of glutamine and a primary amine functionalized ligand, including lysines on proteins, directly competes with deamidation in presence of water or esterification in presence of alcohols.

by aromatic and acidic residues (Figure 1.9C) that influence the acyl-acceptor specificity of MTGase *i.e.,* substrates that comprise negative charges might be electrostatically repulsed [178].

Furthermore, it has also been shown that the sequence around the acyl-donor *i.e.,* glutamine residue directly influences the substrate specificity. Peptides containing hydrophobic amino acid residues at the -2, -1, +1 or +2, aromatic residues at the -5 to -3 positions and optionally arginine at the +1 position relatively to the glutamine were highly reactive substrate sequences for MTGase [179–181]. In addition, glutamines with negatively charged amino acids in close proximity are less likely to be modified by MTGase [182]. These experiments however, could not address the influence of the secondary and tertiary structure of a protein. Only solvent exposed glutamines that are located in a flexible or disordered chain segment are potential acyl-donors for MTGase [167, 183]. These experimental outcomes in combination with a rather broad acyl-acceptor specificity make it difficult to predict if a specific glutamine within the backbone of a given protein will be a site of modification or not. Conclusively, the selectivity of MTGase towards acyl-donors enables us to us to use it as a tool for site-specific protein modification.

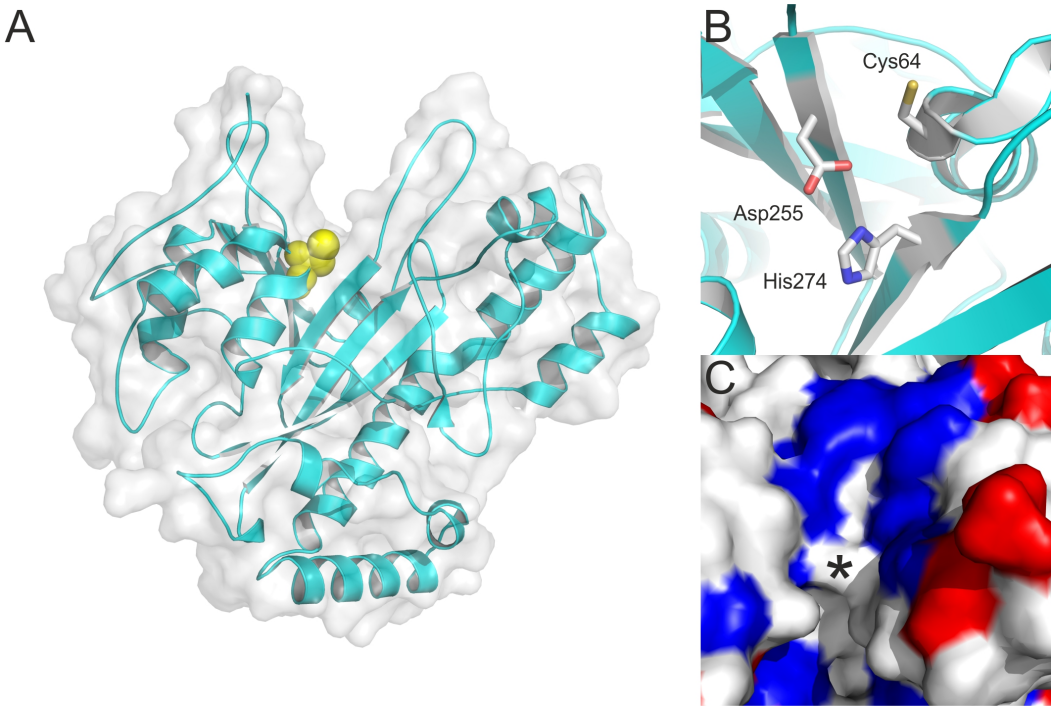

Fig. 1.9.: A) Overall structure of MTGase (1IU4) reveals a deep cleft harbouring the enyzme's active site at its bottom (yellow, reactive Cys64). B) Enlarged view of the Cys-His-Asp catalytic triad. C) Surface map of the active site region around the reactive cysteine (*). Surrounding aromatic (blue) and acidic (red) amino acid residues are highlighted.

1.8.2 MTGase as a tool for site-specific protein modification

Among a variety of different proteins that have been site-specifically modified by MTGase to develop PEGylated, fluorescently labeled, protein-DNA and protein-protein conjugates [174], only a few examples include antibodies. Josten *et al.* enzymatically biotinylated a murine IgG while Mindt and co-workers attached fluorescent dyes to chimeric antibodies [184, 185]. Both approaches yielded heterogeneous antibody conjugates with regard to ligand-to-antibody ratio and the site of conjugation remained unknown. It was not until the pioneering work of Jeger *et al.* who discovered a single glutamine in the human IgG heavy chain domain (Q295), which is next to the antibody glycosylation site (N297), to be the sole site of modification for MTGase-mediated bioconjugation. Furthermore, they showed that homogeneous antibody conjugates with a defined stoichiometry *i.e.,* exactly two ligands per antibody can be accomplished when the antibody was deglycosylated prior to the conjugation (Figure 1.10A). The introduction of a N297Q mutation enabled them to even express an aglycosylated antibody variant that displays four potential

acyl-donor sites for MTGase, thereby doubling the number of payloads that can be attached to the antibody [186].

Instead of exploiting the endogenous glutamine, Strop *et al.* introduced an artificial Gln-tag (XLLQGX, Figure 1.10B) into an IgG1 and investigated how the location of the conjugation site influences not only the *in vitro* but more importantly the *in vivo* characteristics of the antibody conjugate, a particularly interesting question for ADCs. The tag was incorporated at different sites, enzymatically modified with a toxin and the resulting ADCs stability and pharmacokinetics were evaluated. And indeed, they could demonstrate that ADCs where the toxin was attached at different sites exhibited different stabilities and pharmacokinetics when tested in rat plasma and rats, respectively [187].

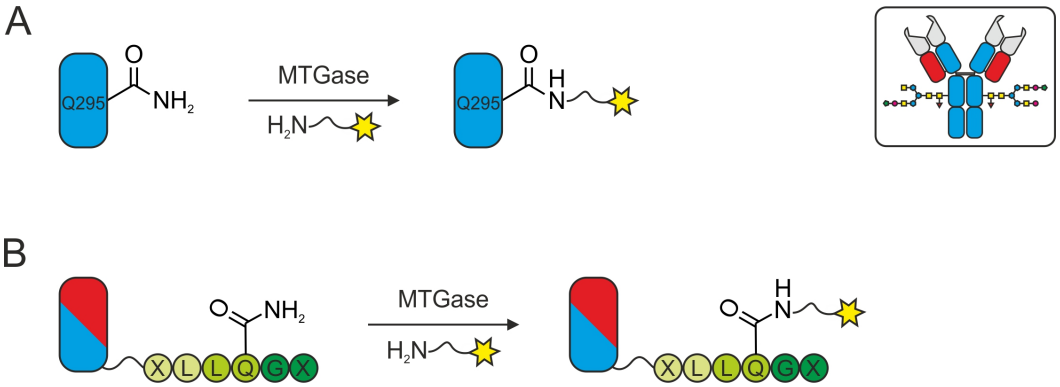

Fig. 1.10.: General scheme of MTGase-mediated antibody modification targeting A) the endogenous glutamine at position 295 or B) a glutamine-containing tag.

1.9 Aim of the thesis

The aim of this thesis was to expand the technology of site-specific MTGase-mediated protein modification based on work that had been previously conducted in our lab.

In the first phase of the thesis, we envisaged investigating the versatility of MTGase by evaluating its ability to modify antibodies, including subtypes other than IgG1, under varying reaction conditions which resulted in a general protocol for MTGase-based antibody modification. This technical chapter is supplemented with additional findings on MTGase properties that we made during the entire thesis, in particular the selectivity of the enzyme towards different acyl-acceptor substrates.

Previously, our lab employed MTGase to generate immunoconjugates with a defined chelator-to-antibody ratio. We aimed to exploit this conjugation approach to develop novel strategies for the generation of antibody-drug conjugates (ADCs) since product homogeneity is of special interest in this field. In addition, we focused on optimizing the conjugation conditions with regard to the excess of toxin that is required for the reaction because it is crucial to minimize hazardous waste. Therefore, we planned to explore different approaches including direct enzymatic and indirect chemo-enzymatic attachment of the toxin to the antibody. Finally, *in vitro* and *in vivo* properties of the resulting ADCs will be evaluated and compared with a clinically relevant ADC.

We also envisioned expanding our MTGase-based antibody modification technology by establishing a generic enzymatic bioconjugation platform. Based on the facts that (i) MTGase exclusively recognizes glutamines only as acyl-donors if they fulfil certain criteria and (ii) the glutamine of the c-myc-tag, a common protein tag, acts as such an acyl-donor, we reasoned that this tag, in combination with MTGase, could be the basis for a versatile protein conjugation platform. This technology would enable us to site-specifically modify virtually any given c-myc-tagged protein with a broad range of functionalities. We aimed to exploit the platform to generate various conjugates that are subsequently used in different assays to prove the applicability, versatility and usefulness of this bioconjugation approach.

Finally, we wanted to investigate the properties of non-covalent antibody conjugates. Exploiting antibody Fc binding domains (FcBDs) to generate non-covalent antibody conjugates is a valuable alternative to covalent antibody modification strategies. Although a few studies are published, not much is known about the *in vivo* stability of such conjugates. We wanted to address this lack of knowledge by radiolabelling FcBDs and assess the *in vitro* and *in vivo* behaviour of the final radioactive antibody conjugate by means of SPECT/CT imaging and quantitative biodistribution.

2

Enzymatic Antibody Modification by Microbial Transglutaminase: A General Protocol

Adapted from

Patrick Dennler, Roger Schibli and Eliane Fischer in *Antibody-Drug Conjugates* Vol. 1045 *Methods in Mol. Biol.* (ed Laurent Ducry) Ch. 12, 205-215 (Humana Press, 2013). With kind permission from Springer Science and Business Media, Licence No. 3563080192870.

Authors contribution

Patrick Dennler designed and carried out all experiments and wrote the chapter, Eliane Fischer wrote the chapter

2.1 Abstract

Enzymatic posttranslational modification of proteins permits more precise control over conjugation site than chemical modification of reactive amino acid side chains. Ideally, protein modification by an enzyme yields completely homogeneous conjugates with improved properties for research or therapeutic use. As an example, we here provide a protocol for microbial transglutaminase (MTGase)-mediated conjugation of cadaverine-derivatized substrates to an IgG1, resulting in stable bond formation between glutamine 295 of the antibody heavy chain and the substrate. This procedure requires enzymatic removal of N-linked glycans from the antibody and yields a defined substrate/antibody ratio of 2:1. Alternatively, a mutant aglycosylated IgG1 variant may be generated by site-directed mutagenesis. The mutation introduces an additional glutamine and yields a substrate/antibody ratio of 4:1 after coupling. Finally, we describe an ESI-TOF mass spectrometry based method to analyze the uniformity of the resulting conjugates. The presented approach allows the facile generation of homogeneous antibody conjugates and can be applied to any IgG1 and a wide range of cadaverine-derivatized substrates.

2.2 Introduction

Conventional approaches for coupling small molecules to monoclonal antibodies are based on chemical modification of lysine or cysteine residues, which typically yields heterogeneous products. In contrast, precise control over stoichiometry and conjugation sites gives rise to homogenous preparations with reduced batch-to-batch variation and favorable properties. Notably, optimization of drug load and the exclusive use of conjugation sites which do not impair targeting properties or stability have been shown to improve the therapeutic index of antibody-drug-conjugates [45, 188].

An elegant approach to reduce heterogeneity of antibody conjugates is site-specific linkage of substrates by enzymatic conjugation. Enzymes are restrictive in the acceptance of conjugation sites as they usually require a consensus sequence or are influenced by the tertiary structure of the protein. In addition to site-specificity, enzymatic conjugation has the advantage of being performed at physiological pH,

temperature and ionic strength, thus allowing mild reaction conditions. A variety of enzymes can potentially be used to form stable bonds between defined sites on a protein and a drug-derivative [189]. In many cases, the specificity of the enzyme requires introduction of a peptidic tag or mutation to the native antibody sequence prior to the conjugation step [108]. While introduction of such tags allows exact control over the conjugation site, it precludes direct modification of native antibodies and requires time-consuming recombinant engineering of the antibody sequence. In some cases, however, antibodies can be directly used for enzymatic conjugation without prior recombinant engineering. For example, glycosyltransferases have been used to modify the N-linked glycans on the Fc part of IgGs with sugar analogs resulting in relatively uniform conjugates [97, 100].

We recently described an approach for enzymatic modification of antibodies at a defined conjugation site using microbial transglutaminase (MTGase) from *Streptomyces mobaraensis* [186]. Transglutaminases (TGase) are a large family of enzymes (EC 2.3.2.13) that catalyze the covalent cross-linking of Gln- and Lys-containing peptides or proteins by formation of an isopeptide bond. There are eight different TGases in mammals (*e.g.,* factor XIIIa), but also lower organisms such as algae, fungi or bacteria express TGases. The advantage of using MTGase instead of mammalian TGases is its robustness, Ca^{2+} independency and high reaction rate. But most importantly, MTGase has a low substrate specificity and can therefore accept a wide range of lysine-containing substrates [158, 185]. It even accepts 5-aminopentyl groups and can therefore be used to couple cadaverine-derivatized entities to an antibody.

On the other hand, MTGase is much more selective towards the protein-bound Gln residues. Both protein chain flexibility and neighboring amino acids influence if a particular Gln can be modified by TGases [167]. Antibodies generally lack such a site and are not efficiently modifiable by MTGase. However, after removal of the carbohydrate moiety, a unique conjugation site is exposed, that allows attaching exactly one substrate to each heavy chain at amino acid Q295 (Figure 2.1A). By site-directed mutagenesis, we introduced an additional Gln-residue at position 297 (N297Q), resulting in an aglycosylated variant of the antibody which can then be modified with exactly two substrates per heavy chain (Figure 2.1B) [190].

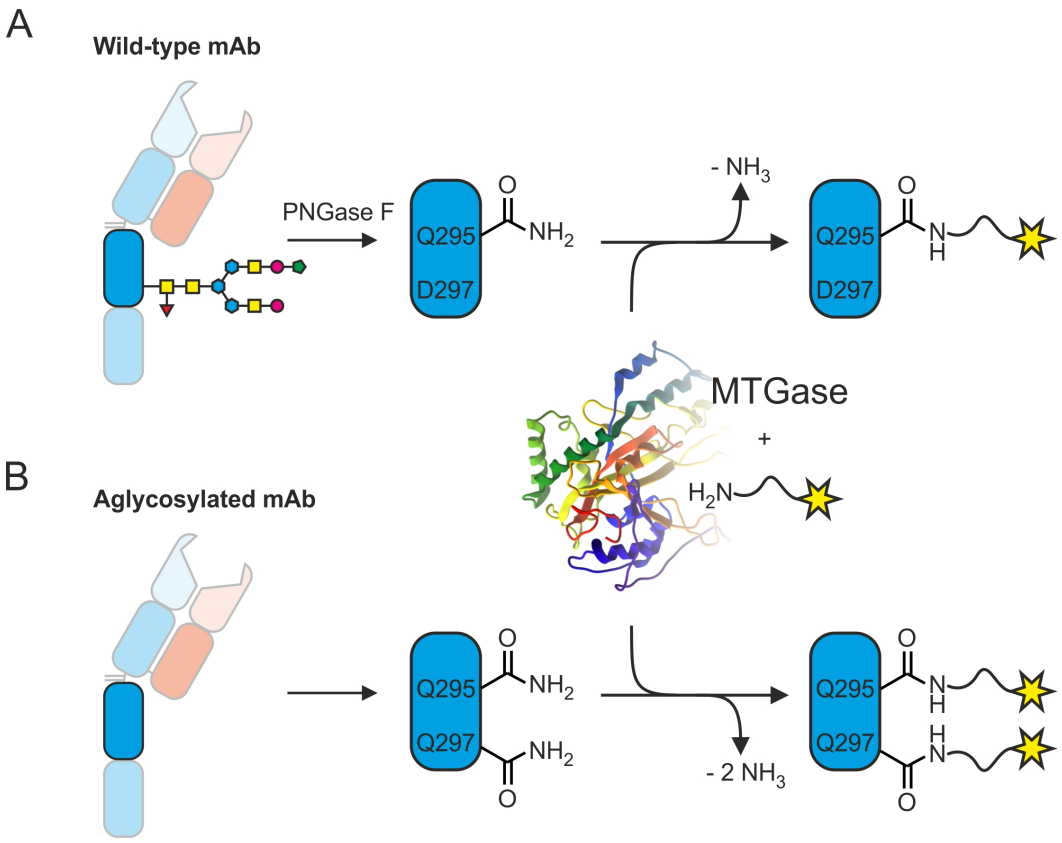

Fig. 2.1.: MTGase-mediated conjugation of cadaverine-derivatized substrates to A) an IgG1 and B) an aglycosylated variant. (Structure from RCSB Protein Data Bank, 11U4)

In this chapter, the enzymatic conjugation of cadaverine-derivatized molecules, including biotin-cadaverine, to a monoclonal antibody is described. The protocol includes deglycosylation of the antibody heavy chain by the enzyme PNGase F, subsequent modification by MTGase and a protocol for mass spectrometric identification of the conjugates. In addition, the impact of various parameters on the enzymatic conjugation reaction as well as on the analytics are described and discussed.

2.3 Materials

All buffers and solutions were prepared by using Millipore water unless indicated otherwise.

2.3.1 Antibodies and substrates

1. Antibody solution: Antibody in PBS or Tris-HCl, stored at -20 °C in 1.5-3 mg/mL stock solutions

2. *N*-(Biotinyl)cadaverine (biotin-cadaverine as white powder, Zedira), 20 mM in PBS, store aliquots at -20 °C
3. Cadaverine-derivatised substrates

2.3.2 Deglycosylation

1. 1.5 ml Eppendorf tubes
2. Deglycosylation buffer: PBS (10X): Weigh 2.1 g KH_2PO_4, 90 g NaCl, 4.8 g Na_2HPO_4 x $2H_2O$ and transfer to a 1 L glass bottle. Add water to a volume of 1 L. To get PBS 1X, use 100 mL PBS (10X) and add water to a volume of 900 mL. Adjust pH to 7.2.
3. PNGase F: *N*-Glycosidase F (EC 3.5.1.52) from *Flavobacterium meningosepticum*, recombinant, 1000 Units/mL, Roche
4. Centrifugal Ultrafiltration: Vivaspin 500, 50 kDa MWCO PES, Sartorius Stedim Biotech

2.3.3 Enzymatic conjugation

1. Assay buffer: PBS 1X
2. Transglutaminase: Microbial Transglutaminase (MTGase, EC 2.3.2.13) from *Streptomyces mobaraensis*, recombinant, 50 Units/mL, Zedira

2.3.4 Analysis by mass spectrometry

1. Guan-buffer: 7.5 M Guan-HCl, 0.1 M Tris-HCl, 1 mM EDTA buffer pH 8.5. Weigh 0.3152 g of Tris-HCl (Sigma) and transfer to a glass vial. Add 18.75 mL of 8 M Guanidine-HCl (Pierce) followed by 40 µL of 0.5 M EDTA (Fisher). Adjust the pH to 8.5 by addition of concentrated NH_4OH (28% aqueous solution). Add water to a final volume of 20 mL.
2. Reducing agent: 1 M DTT. Weigh 0.1543 g DTT, transfer it to a 1.5 mL Eppendorf vial and dissolve it in 1 mL of 50 mM NH_4HCO_3.
3. Column: Poros 10 R1 60 x 1mm, Dr. Maisch GmbH, Spherical Polystyrenedivinylbenzene
4. Mass spectrometer: Waters Micromass LCT Premier (LC-ESI-TOF)

5. LC parameters: Acetonitrile + 0.1% formic acid (solvent A), water + 0.1% formic acid (solvent B), isopropanol (solvent C). Gradient: 0 min to 3 min, 15% A, 80% B, 5% C; 3 min to 20 min, 15% A to 80% A, 80% B to 15% B, 5% C; 10 min re-equilibration time. Flow: 0.3 mL/min, column temperature: 25±2 °C
6. Analyze MS data with MassLynx V4.1 and deconvolute the raw data with MaxEnt1.

2.4 Methods

2.4.1 Deglycosylation of IgG1

1. Incubate the antibody (1 mg) in PBS buffer overnight at 37 °C with 6 units of PNGase F.
2. Remove the enzyme by ultrafiltration using a Vivaspin column MWCO 50 kDa. Apply the reaction mixture onto the column, centrifuge at 4000-6000 x g. Wash three times with buffer. Resuspend deglycosylated antibody in a suitable volume of buffer for further processing. Analyze deglycosylation by mass spectrometry.

2.4.2 Enzymatic conjugation by MTGase

1. Mix the antibody (final concentration: 1 mg/mL), 60 equivalents of cadaverine-derivatised substrate (biotin-cadaverine), MTGase (final concentration: 1 U/mL) and PBS buffer. Incubate the reaction mixture at 37 °C overnight.
2. Remove excess substrate and enzyme by ultrafiltration as described in section 2.4.1.
3. Under the experimental conditions described here, the coupling reaction was observed to be complete after 4 hours.

2.4.3 Quality control of the reaction by mass spectrometry

1. Mass Spectrometry: Mix 10 µg of antibody and 1 M DTT (final concentration: 20 mM) in an MS sample vial. Add Guan-buffer to a volume of 50 µL and incubate the mixture at 70 °C for 30 min. Inject 5 µL.

2. Process and analyze the data by using appropriate software (*e.g.,* MassLynxV4.1). Usually, two distinct peaks can be detected which correspond to light and heavy chain of the antibody (Figure 2.2A). Process the respective raw data (Figure 2.2C&D) using MaxEnt1 to get deconvoluted mass spectra of the light (Figure 2.2C) and heavy chain (Figure 2.2D). The expected mass difference between unconjugated and conjugated heavy chain represents the molecular weight of the substrate $MW_{substrate}$ minus 17 Da due to loss of ammonia during the conjugation reaction. Accordingly, an increase in mass of 2 x ($MW_{substrate}$ - 17 Da) is expected after conjugation to the mutant aglycosylated heavy chain.

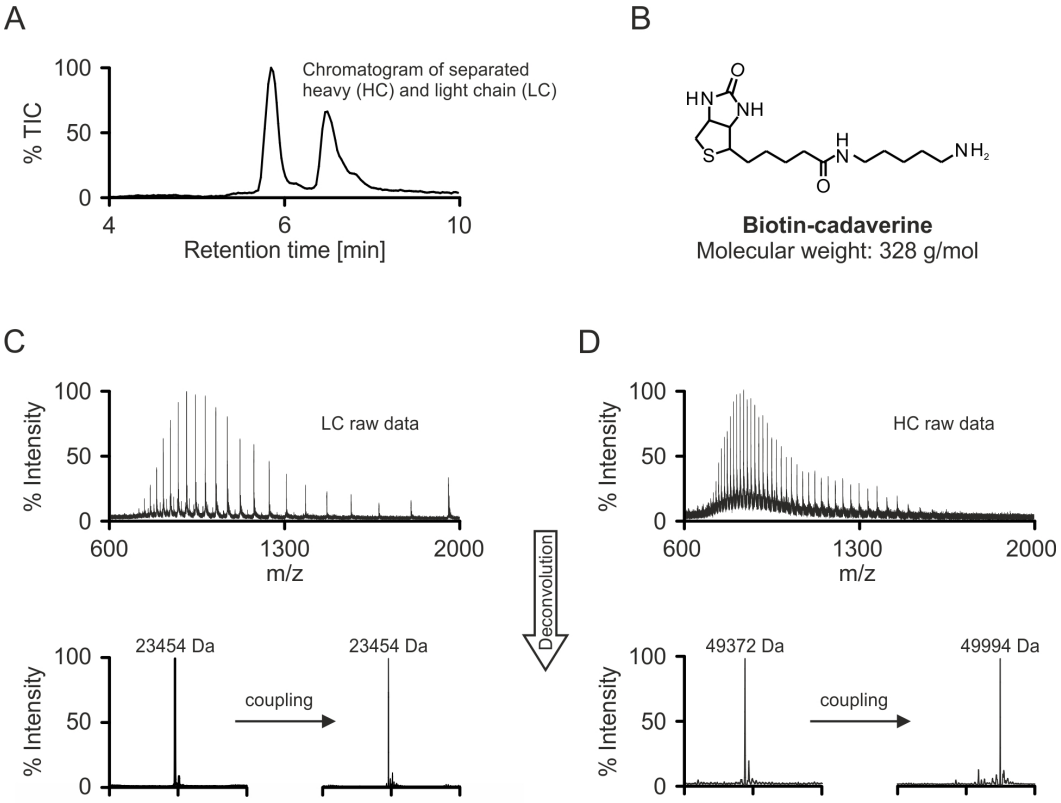

Fig. 2.2.: A) Liquid chromatography UV-trace (280 nm) of heavy and light chain. B) Chemical structure of biotin-cadaverine. C) Representative raw data of a chimeric IgG1 light chain (top) and deconvoluted data before (bottom, left) and after coupling (bottom, right). The light chain remains unaffected. D) Representative raw data of an aglycosylated chimeric IgG1 heavy chain (top) and deconvoluted data before (bottom, left) and after coupling (bottom, right). The mass difference between uncoupled and coupled heavy chain is 622 Da which corresponds to two biotin-cadaverine molecules (MW: 328 Da, 2 x 328 Da = 656 Da) attached to the heavy chain by MTGase under the loss of two ammonia molecules (2 x 17 Da = 34 Da).

2.5 Results and Discussion

The provided protocol represents a generalized instruction that can be used as a basis for MTGase-mediated antibody modification. However, if an extension of the protocol beyond the described parameters is required the corresponding conditions might need to be reassessed and adjusted. Some important and helpful findings with respect to reaction buffers, organic solvents, antibody isotypes, substrates and analytics are discussed in this section.

2.5.1 Reaction buffer and organic solvents

Alternatively to PBS, Tris-HCl pH 7.0 can be used for MTGase-mediated conjugation of antibodies. On the contrary, the following buffers are not recommended since they significantly decrease the conjugation yield: (i) 0.2 M Na_2HPO_4/NaH_2PO_4, pH 6 or 7 (ii) 0.1 M Citric acid/NaH_2PO_4, pH 6 or 7 (iii) 0.2 M Imidazole-HCl, pH 7. Other buffer systems such as 3-morpholinopropane-1-sulfonic acid (MOPS) or 2-[4-(2-hydroxyethyl)piperazin-1-yl]ethanesulfonic acid (HEPES) might represent valuable alternatives but have not been tested here. It is important to evaluate and if necessary to adjust the buffer capacity since the pH of the reaction mixture may rise or drop depending on the chemical properties of the substrate. We observed a decline in enzymatic acitivity at pH below 6 and above 8.

The addition of organic solvents to the enzymatic reaction mixture should be avoided since they decrease the activity of MTGase [191]. Nevertheless, it sometimes is inevitable because the corresponding substrate might not be soluble in an aqueous buffer. Our observations are in agreement with the published data by Mero et al. indicating that DMSO has the least influence on the enzymatic activity. Based on our experience, we recommend not exceeding 5% (v/v) DMSO in order to maximize the conjugation yield.

2.5.2 Antibody isotypes

We used a chimeric IgG1 which means that the site of modification (Gln 295) is located within the conserved human Fc region and hence the described protocol is valid for any chimeric, humanized or human antibody of the same isotype and subclass. In addition, the transferability of our MTGase-mediated conjugation tech-

nology to use it for human IgG4 and murine IgG1, IgG2a and IgG2b has been evaluated. The reported reaction conditions, including deglycosylation, were directly applicable to the human IgG4 and the murine IgG1. In comparison, deglycosylation conditions of murine IgG2a and IgG2b had to be adjusted and only partial conjugation yield could be accomplished. Interestingly, the murine IgG1 seems to have an additional glutamine per heavy chain that is accessible for MTGase compared to the human IgG1. Furthermore, the IgG2a and IgG2b could be modified with one substrate per heavy chain which was unexpected because they do not possess the conserved Gln 295. These two results prove that MTGase can target an extra glutamine on murine IgG1, IgG2a and IgG2b. We hypothesize that this additional site of modification must also be located in the CH2 domain because sequence alignment revealed only three positions where a glutamine is present in all murine but not in the human sequence (Figure 2.3). Site-directed mutagenesis of the potential glutamines could help to determine where exactly the murine IgGs are modified by MTGase.

2.5.3 Sample preparation impact on mass spectrometric analysis

Guanidine-HCl in the sample preparation buffer for mass spectrometry analysis causes denaturation of the antibody which, in combination with a reducing agent, leads to a complete monomerization of heavy and light chain. If the described sample preparation is too harsh for a given antibody conjugate *i.e.,* thermal instability of the conjugated substrate, a milder approach may be used. We have demonstrated that the guan-buffer can be easily substituted by PBS. Moreover, incubation at 37 °C instead of 70 °C is sufficient to completely reduce the antibody. The impact of the two different sample preparation methods on the downstream mass spectrometric analysis can directly be visualized by comparing the raw data. The observed shift of the charged protein species distribution from lower m/z ratios (guan-buffer) to higher m/z ratios (PBS) is a direct result of the lack of denaturation (Figure 2.4). Since the protein retains its tertiary structure in PBS, fewer amino acids that could potentially be ionized are available, leading to a decreased z-score and as a consequence to an increased m/z ratio. While both methods lead to the same result after raw data deconvolution, it is important however to note that potential antibody aggregates are not completely separated when applying the milder conditions. Accordingly, less

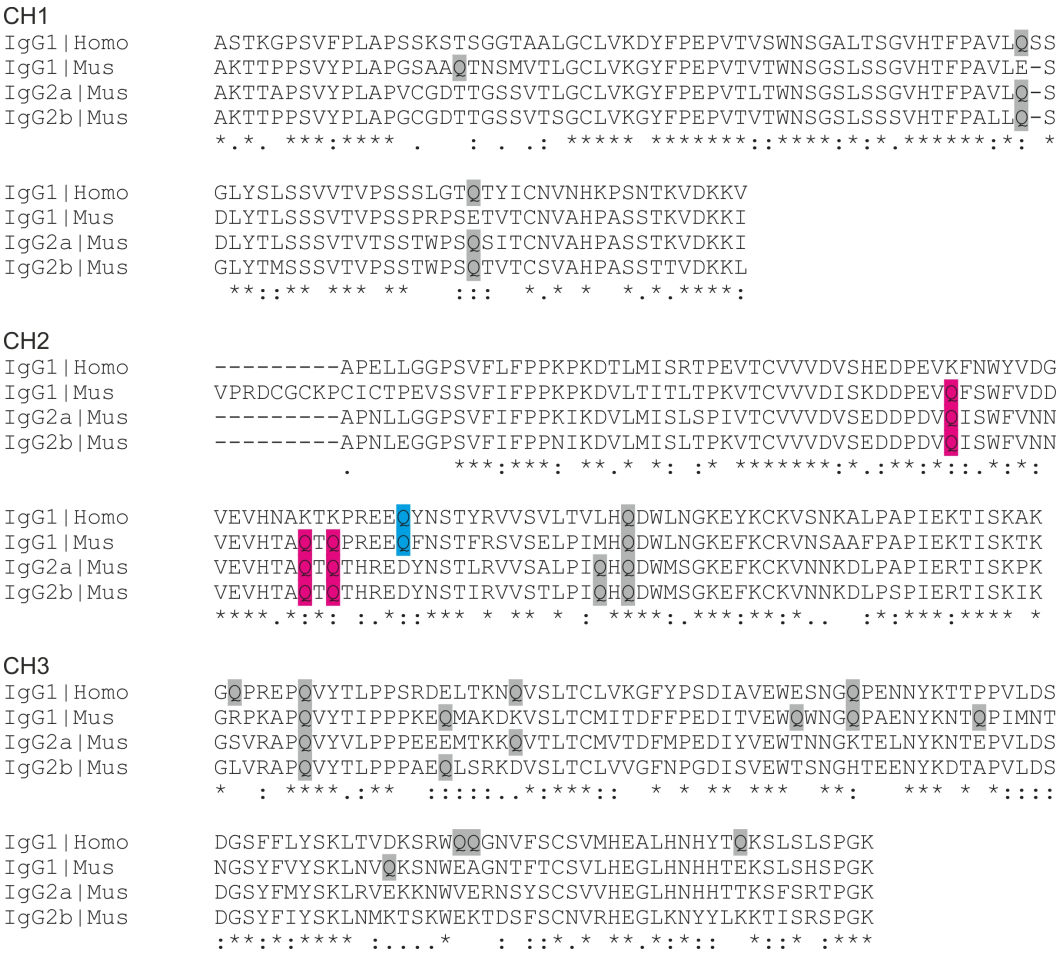

Fig. 2.3.: Constant heavy chain domains (CH1-3) sequence alignment of human IgG1, murine IgG1, IgG2a and IgG2b and highlighting of all glutamines (Q, gray, cyan, and magenta). The glutamine in position 295 (cyan) on the human IgG1, assigned as the site of MTGase-mediated modification [186], is also present in the murine IgG1 sequence and therefore most probably one of the two modification sites. Glutamines that are present in all murine subtypes but not in the human IgG1 and hence could potentially be Gln-donors for MTGase are highlighted in magenta. Sequences were aligned using Clustal Omega [192].

monomeric protein species are present in the sample and thus the signal intensity may be lower compared to a sample that has been treated with guan-buffer at elevated temperatures.

2.5.4 Substrates

Predicting whether a primary amine functionalized substrate is a suitable amine-donor for MTGase is not trivial since the enzyme has a low substrate specificity. Nevertheless, Gundersen *et al.* systematically tested a series of different substrates thereby gaining insight into the acyl-acceptor specificity of MTGase [178]. We focused on the applicability of MTGase to modify various proteins and not particularly

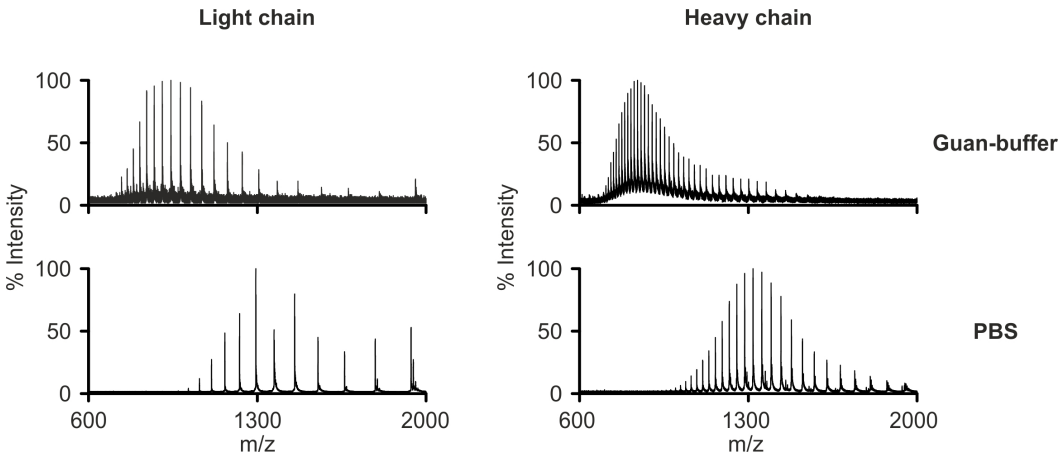

Fig. 2.4.: Representative raw data of an antibody light (left) and heavy chain (right) after sample preparation with either guan-buffer (top) or PBS (bottom).

on the substrate specificity. Nonetheless, some of our results can be used to extend the knowledge about MTGase, to estimate the performance and to support the design of novel substrates.

We observed that the extension of a spacer between the primary amine and a cyclic system such as chelating systems (DOTA) or toxins (epothilone) can lead to an elevated reaction yield. The addition of four carbon atoms between the primary amine and DOTA led to an increase of modified heavy chain from 30% to 70% (Figure 2.5A). The effect of extension on the conjugation efficiency was even more striking when we substituted a five carbon long linker between the primary amine and epothilone with a PEG4-spacer. While no modification could be observed with the carbon linker, quantitative (<95%) reaction yield could be accomplished with the PEG4 derivative (Figure 2.5B). Gundersend *et al.* observed the same trend of increasing conjugation yield when they prolonged the spacer of their substrates. In addition, they also hypothesized that the presence of an acidic functionality on the substrate *e.g.,* a carboxylic acid could be disadvantageous since there are negatively charged amino acids in close proximity to the active site of MTGase (Figure 1.9). Accordingly, the incomplete conjugation yield of the DOTA derivatives may be attributed to the three carboxylic acids present on the tetraazacyclododecan backbone.

We also aimed to use dendrimeric substrates in order to multiply the number of functionalities that can be attached to an antibody. While the small dendrimer precursor was well accepted (>95% conjugation yield) the final dendrimer, where

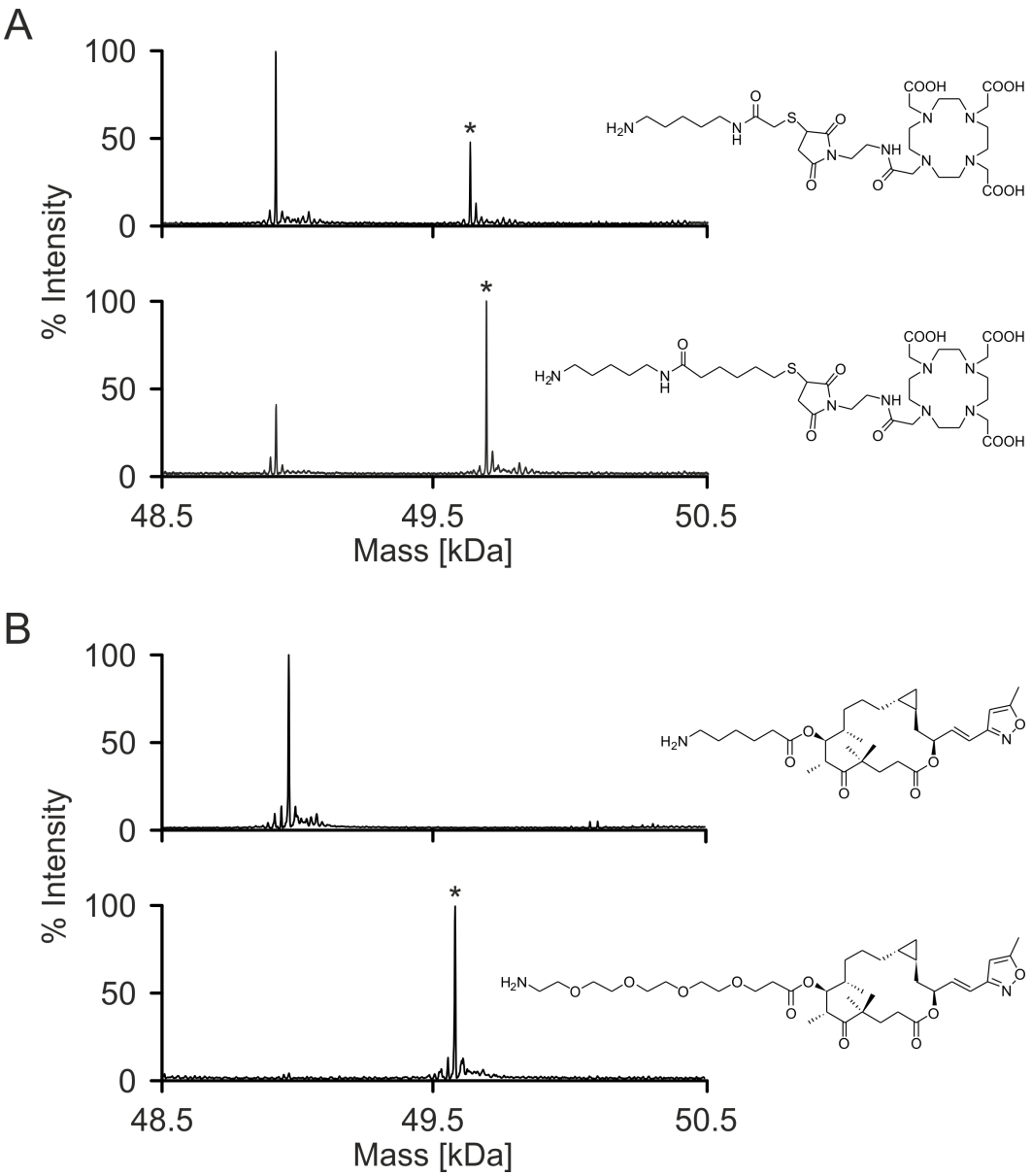

Fig. 2.5.: Deconvoluted mass spectra of an antibody heavy chain after MTG-mediated conjugation with A) DOTA derivates and B) epothilone derivatives. Extension of the linker between the primary amine and the cyclic system significantly increased the proportion of modified (*) compared to unmodified heavy chain.

the terminal alcohol was esterified with PEG4-azide, was no longer tolerated by MTGase which lead to a poor conjugation yield of <20% modified heavy chain (Figure 2.6).

These three examples demonstrate that bulky groups, including cyclic as well as branched systems, and negatively charged functionalites on the MTGase substrate are not advantageous with respect to the conjugation efficiency most probably because of steric hinderance (bulkiness) and electrostatic repulsion (negative charges)

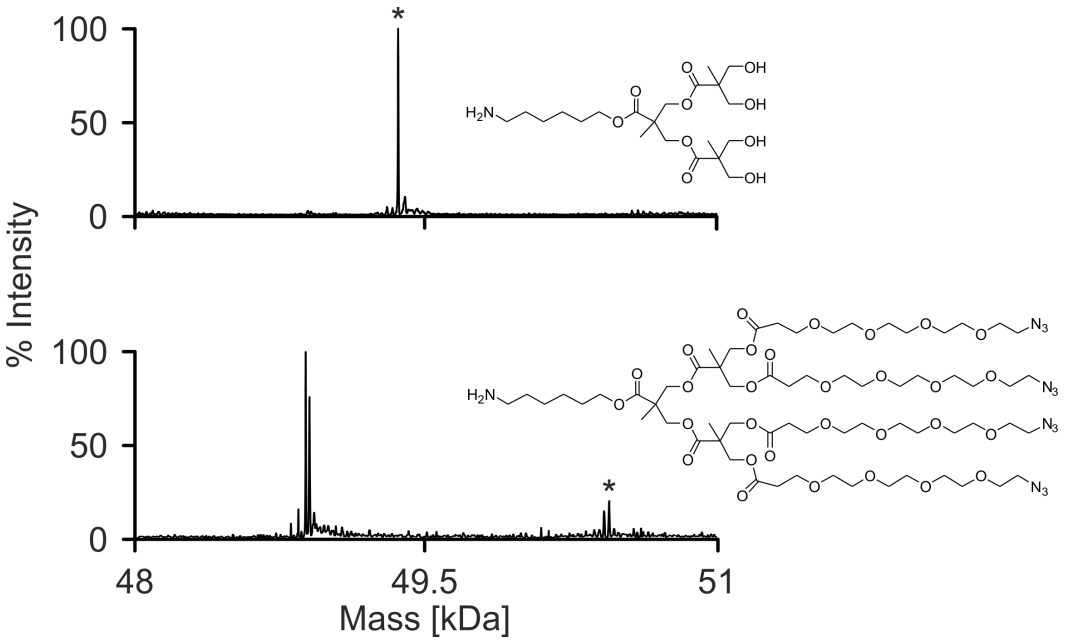

Fig. 2.6.: Deconvoluted mass spectra of an antibody heavy chain after MTG-mediated conjugation with a dendrimer precursor (top) and the corresponding azide-functionalized dendrimer (bottom). The esterification of the alcohol with PEG4-azide significantly decreased the enzymatic conjugation yield from >95% modified heavy chain (*) to <20%.

in the active pocket of MTGase (Figure 1.9). However, extended special separation of the primary amine and such functional groups by prolonging the linker region can help to circumvent poor conjugation yields.

3

A Transglutaminase-Based Chemo-Enzymatic Conjugation Approach Yields Homogeneous Antibody-Drug Conjugates

Adapted from

Patrick Dennler, Aristeidis Chiotellis, Eliane Fischer, Delphine Brégeon, Christian Belmant, Laurent Gauthier, Florence Lhospice, François Romagne, Roger Schibli. "A transglutaminase-based chemo-enzymatic conjugation approach yields homogeneous antibody-drug conjugates". *Bioconjugate Chem.* 2014, 25, 569-578.

Authors contribution

Patrick Dennler designed and carried out all experiments and wrote the paper, Aristeidis Chiotellis was responsible for the organic synthesis, Innate Pharma designed the experiments and provided the control antibody as well as the toxin.

3.1 Abstract

Most chemical techniques used to produce antibody-drug conjugates (ADCs) result in a heterogeneous mixture of species with variable drug-to-antibody ratios (DAR) which will potentially display different pharmacokinetics, stability and safety profiles. Here we investigated two strategies to obtain homogeneous ADCs based on site-specific modification of deglycosylated antibodies by microbial transglutaminase (MTGase), which forms isopeptidic bonds between Gln and Lys residues. We have previously shown that MTGase solely recognizes Gln295 within the heavy chain of IgGs as a substrate and can therefore be exploited to generate ADCs with an exact DAR of two. The first strategy included the direct, one-step attachment of the antimitotic toxin monomethyl auristatin E (MMAE) to the antibody via different spacer entities with a primary amine functionality that is recognized as a substrate by MTGase. The second strategy was a chemo-enzymatic, two-step approach whereby a reactive spacer entity comprising a bio-orthogonal thiol or azide function was attached to the antibody by MTGase and subsequently reacted with a suitable MMAE-derivative. To this aim, we investigated two different chemical approaches, namely thiol-maleimide and strain-promoted azide-alkyne cycloaddition (SPAAC).

Direct enzymatic attachment of MMAE-spacer derivatives at an 80 molar excess of drug yielded heterogeneous ADCs with a DAR of between 1.0 to 1.6. In contrast to this, the chemo-enzymatic approach only required a 2.5 molar excess of toxin to yield homogenous ADCs with a DAR of 2.0 in the case of SPAAC and 1.8 for the thiol-maleimide approach.

As a proof-of-concept, trastuzumab (Herceptin®) was armed with the MMAE via the chemo-enzymatic approach using SPAAC and tested *in vitro*. Trastuzumab-MMAE efficiently killed BT-474 and SK-BR-3 cells with an IC_{50} of 89.0 pM and 21.7 pM respectively. Thus, the chemo-enzymatic approach using MTGase is an elegant strategy to form ADCs with a defined DAR of two. Furthermore the approach is directly applicable to a broad variety of antibodies as it does not require prior genetic modifications of the antibody sequence.

3.2 Introduction

Antibody-drug conjugates (ADCs) are promising therapeutics since their tumor selectivity is increased when compared to classical chemotherapy or combination therapy [12, 13, 193–196]. Targeted delivery of toxic payload to the tumor leads to a potential reduction of off-target toxicity and therefore an increased therapeutic index.

Antibody conjugation methods typically include chemical reaction of lysines or cysteines with activated esters or maleimide functionality respectively. However, these reactions are difficult to control with regard to site-specificity and stoichiometry which leads to heterogeneous products [30]. Moreover, each subpopulation of antibody conjugates produced in this manner will have different pharmacokinetic, efficacy and safety profiles [16, 17].

Various technologies have been developed in recent years to improve the production of homogeneous ADCs. Junutula *et al.* endowed antibodies with additional cysteines that can be reacted with maleimide-functionalized toxins, thereby yielding nearly homogeneous conjugates with improved therapeutic indexe [45]. However, this method includes a reduction-reoxidation step that can potentially lead to unpaired, reactive sulfhydryl groups. Furthermore, depending on the location of the engineered cysteines, maleimide exchange processes can lead to drug loss and thus decrease the potency of the ADC [47]. Incorporation of non-natural amino acids into the backbone of an antibody represents another promising technology towards homogeneous ADCs. To this aim, p-acetylphenylalanine was introduced into an antibody, thereby creating a bioorthogonal functionality that was exploited for site-specific modification with a drug [70, 71]. Although this is an elegant approach, it is a rather complex process and has yet to prove its general applicability.

By targeting the carbohydrate moiety of an antibody Zuberbühler *et al.* established a method to generate uniform ADCs while using native antibodies. A selective periodate oxidation of the fucose residue yielded an aldehyde functionality that could then be selectively reacted with a hydrazide-functionalized dolastatin analogue [84]. A major draw-back of this approach is the huge excess (100-fold molar excess) of toxin that is required for the reaction since toxins are expensive and may cause hazardous waste during the manufacturing procedure. Okeley *et al.* also

targeted the carbohydrate moiety as a potential site to attach drugs. In contrast to Zuberbühler *et al.* they introduced unnatural sugars by producing their antibodies by CHO cells in the presence of 6-thiofucose and subsequently conjugated the toxin to the antibody by using thiol-maleimide chemistry. Even though the excess of toxin could be reduced to a minimum here, incomplete incorporation of 6-thiofucose (60-70%) resulted in heterogeneous ADC product [104].

Enzymatic modification of antibodies and other proteins represents an alternative approach to the chemical modification strategies outlined above [109]. Transglutaminases (TGase) are a family of enzymes (EC 2.3.2.13) that catalyze the formation of a covalent bond between the γ-carbonyl amide group of glutamines and the primary amine of lysines (Figure 3.1) [158]. Since some TGases also accept substrates other than lysine as the amine donor, they have been used to modify proteins [167, 183, 197] including antibodies [184–186, 198]. Recently, Strop *et al.* investigated the conjugation of drugs to antibodies using microbial transglutaminase (MTGase). By genetically introducing glutamine tags *i.e.,* a minumun of 4 amino acid, at various positions in an antibody they could demonstrate the impact of conjugation site on the drug-to-antibody ratio (DAR), stability and pharmacokinetics of ADCs [187]. Here we report a procedure to obtain homogeneous ADCs that does not

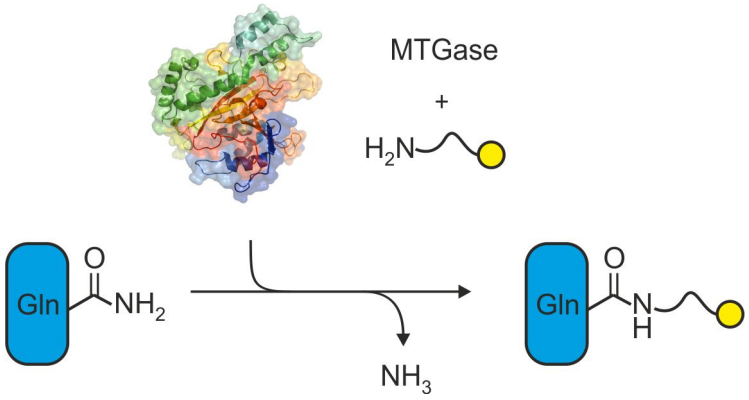

Fig. 3.1.: Microbial transglutaminase (MTGase) catalyzes the formation of a covalent bond between primary amines and the γ-carbonylamid group of glutamines under the loss of ammonia. (Structure from RCSB Protein Data Bank, 1IU4)

require prior engineering of the immunoglobulin at the DNA level. Our group has previously demonstrated that a conserved glutamine located in the constant domain of the heavy chain is the sole γ-carbonyl amide donor for MTGase within the backbone of a deglycosylated IgG1 [186]. Small molecular weight substrates including cadaverin-derivatized chelators or biotin were efficiently coupled to this site [199].

We adapted this strategy to generate ADCs with a known site of conjugation and uniform stoichiometry. Furthermore, we investigated and compared two different conjugation strategies with regard to the amount of toxin that is required and the reaction efficiency (Figure 3.2). In addition to the direct enzymatic coupling of the toxin to the antibody, we established a novel chemo-enzymatic approach whereby a small linker with a synthetic functional group was first attached to the antibody by MTGase. A toxin was then chemically conjugated to the antibody to generate the desired ADC. Finally, the toxicity of the novel conjugate was evaluated *in vitro*.

In addition to the direct enzymatic coupling of the toxin to the antibody, we established a novel chemo-enzymatic approach whereby a small linker with a synthetic functional group was first attached to the antibody by MTGase. A toxin was then chemically conjugated to the antibody to generate the desired ADC. Finally, the toxicity of the novel conjugate was evaluated *in vitro*.

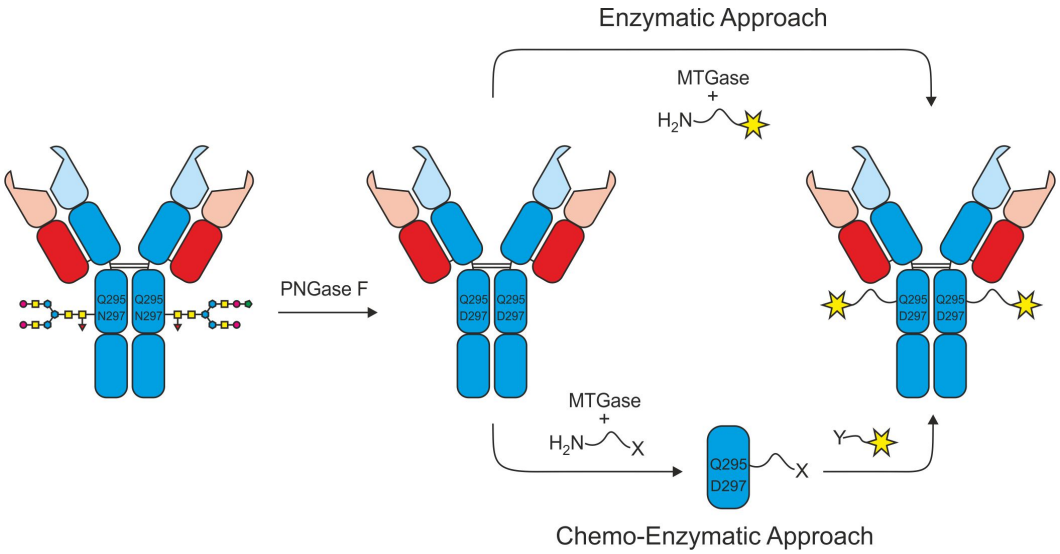

Fig. 3.2.: Schematic illustration of the two different strategies to generate homogeneous antibody-drug conjugates (ADCs). The N-linked glycans are cleaved by N-Glycosidase F (PNGase F). The enzymatic approach includes direct conjugation of an amine-functionalized toxin (yellow star, top panel) to the deglycosylated antibody. For the chemo-enzymatic approach, a bioorthogonal functionality is enzymatically attached to a deglycosylated antibody (amine-X, bottom panel) in a first reaction. In a second step, the toxin (Y-yellow star), which is modified with a suitable functionality Y, is conjugated to the antibody.

3.3 Materials and Methods

3.3.1 Chemistry

All solvents used for reactions were purchased as anhydrous grade from Acros Organics (puriss., dried over molecular sieves, H_2O<0.005%) and were used without further purification unless otherwise stated. Solvents for extractions, column chromatography and thin layer chromatography (TLC) were purchased as commercial grade. All non-aqueous reactions were performed under an argon atmosphere using flame-dried glassware and standard syringe/septa techniques. Commercially available reagents were used without further purification. In general, reactions were magnetically stirred and monitored by TLC performed on Merck TLC glass sheets (silica gel 60 F254). Spots were visualised with UV light (λ = 254 nm) or by staining with either anisaldehyde solution or $KMnO_4$ solution and subsequent heating. Chromatographic purification of products was performed using Fluka silica gel 60 for preparative column chromatography.

11-Azido-3,6,9-trioxaundecan-1-amine (Azido-PEG3-Amine) and dibenzylcyclooctyneamine (DBCO-amine) were purchased from Click Chemistry Tools (Scottsdale, USA). Amine-PEG4-vc-PAB-MMAE, DBCO-PEG4-vc-PAB-MMAE and maleimide-vc-PAB-MMAE were purchased from ADC Biotechnology (St Asaph, UK), maleimide-vc-PAB-MMAF was purchased from Concortis (San Diego, USA). All of the toxins were equipped with a valine-citrulline 4-aminobenzyl alcohol (vc-PAB) cleavable linker unit.

Nuclear magnetic resonance (NMR) spectra were recorded in $CDCl_3$ or CD_3OD on a Bruker Av-400 spectrometer at room temperature (RT). The measured chemical shifts are reported in δ (ppm) and the residual signal of the solvent was used as the internal standard ($CDCl_3$ ^{1}H: δ = 7.26 ppm, ^{13}C: δ = 77.0 ppm, CD_3OD ^{1}H: δ = 3.31 ppm, ^{13}C: δ = 49.1 ppm). All ^{13}C NMR spectra were measured with complete proton decoupling. Data of NMR spectra are reported as follows: s = singlet, d = doublet, t = triplet, m = multiplet, dd = doublet of doublets, dt = doublet of triplets, br = broad signal. The coupling constant *J* is reported in Hertz (Hz). High resolution mass spectra (HR-MS) were recorded on a Waters Micromass Autospec Ultima (EI-sector) or a Varian Ionspec Ultima (MALDI/ESI-FT-ICR) (both

MS service of Laboratory of Organic Chemistry (LOC) at the ETH Zurich). Low resolution mass spectra (LR-MS) were obtained with a Micromass Quattro micro API LC-ESI instrument

HPLC was performed on a Merck-Hitachi L-7000 system equipped with a L-7400 tunable absorption detector. Analytical HPLC was performed with a reverse phase column (Ultimate XB C-18, 4.6 x 250 mm, 5 µm, Welch Materials Inc.) using 50 mM NH_4HCO_3 solution (solvent A) and acetonitrile (solvent B) with the following gradient system; 0-22 min: 5-80% B; 22-25 min: 80% B; 25-27min: 80-5% B; 27-30 min: 5% B; flow: 1 mL/min; UV: 254 nm. Semipreparative HPLC purifications were performed with a reverse phase semipreparative column (Xbridge C18, 10 x 150 mm, 5 µm, Waters) with 50 mM NH_4HCO_3 solution (solvent A) and acetonitrile (solvent B) with the following gradient systems; system 1: 0–5 min: 40% B, 5-20 min: 40–80% B; flow: 4 mL/min; UV: 254 nM. system 2: 0–5 min: 30% B, 5-20 min: 30–70% B; flow rate: 4 min/mL and UV=254 nm.

di-*tert*-butyl(((6,6'-disulfanediylbis(hexanoyl))bis(azanediyl))bis(pentane-5, 1-diyl))dicarbamate (1).

In a solution of 6,6'-disulfanediyldihexanoic acid (250 mg, 0.849 µmol, *tert*-butyl (5-amino-pentyl)carbamate (412 mg, 2.038 mmol) and DIPEA (0.890 mL, 5.09 mmol) in DMF (4.7 mL), HBTU (1.29 g, 3.40 mmol) was added portionwise at RT. After stirring for 20 hours, the yellowish reaction mixture was diluted with ethyl acetate (70 mL) and washed with cold HCl 0.1N (3 x 50 mL), $NaHCO_3$ (sat) (1 x 50 mL) water (1 x 50 mL) and brine (1x 50 mL). The organic layer was dried over sodium sulfate, filtered and evaporated to dryness. The crude was purified by flash column chromatography on silica using $CHCl_3$/EtOH 95:5 to yield 525 mg (93%) of compound as a yellow sticky solid. ^{1}H NMR (400 MHz, $CDCl_3$): δ 5.87 (br, 2 H), 4.64 (br, 2 H), 3.22 (dt, J_1 = 7.3 Hz, J_2 = 6.8 Hz, 4H), 3.09 (dt, J_1 = 8.1 Hz, J_2 = 6.7 Hz, 4H), 2.65 (t, J = 7.2 Hz, 4H), 2.16 (t, J = 7.2 Hz, 4H), 1.73 – 1.59 (m, 8H), 1.55 – 1.45 (m, 8H), 1.42 (s, 18H), 1.37 – 1.28 (m, 4H). ^{13}C NMR (100 MHz, CDCl3): δ 172.9, 156.1, 79.0, 40.2, 39.2, 38.8, 36.5, 29.7, 29.1, 28.8, 28.4, 28.0, 25.3, 23.9. ESI-QTOF MS m/z calculated for $C_{32}H_{62}N_4O_6S_2$ $[M+H]^+$ 663.4184, measured 663.4185.

***tert*-butyl (5-(6-mercaptohexanamido)pentyl)carbamate (2)**

To a solution of di-*tert*-butyl(((6,6'-disulfanediylbis(hexanoyl))bis(azanediyl)) bis

(pentane -5,1-diyl))di-carbamate (196 mg, 0.296 mmol) in a mixture of tetrahydrofurane (3 mL) and water (0.31 mL, 17.21 mmol), tributylphosphine (272 µl, 1.035 mmol) was added dropwise at RT, within 1 min. The reaction mixture was stirred for 1 h and then the volatiles were removed under reduced pressure at 33 °C. The crude was azeotroped once with 50 mL benzene to remove traces of water and the residue was purified with flash column chromatography on silica with chloroform/ethanol 95:5 to yield a slightly yellow clear oil. NMR revealed that the compound was contaminated with oxidized tributylphosphine byproducts so the crude was purified again with flash column chromatography with hexane/ethyl acetate 2:8 to yield 180 mg (91%) of product as a colorless oil which solidified after storage at -25 °C. ^{1}H NMR (400 MHz, $CDCl_3$): δ 5.88 (br, 1 H), 4.57 (br, 1 H), 3.23 (dt, J_1 = 7.3 Hz, J_2 = 6.9 Hz, 2H), 3.09 (dt, J_1 = 7.8 Hz, J_2 = 6.5 Hz, 2H), 2.52 (dt, J_1 = 8.0 Hz, J_2 = 7.6 Hz, 2H), 2.16 (t, J = 7.5 Hz, 4H), 1.69 – 1.57 (m, 4H), 1.56 – 1.46 (m, 4H), 1.43 (s, 9H), 1.36 – 1.28 (m, 3H). ^{13}C NMR (100 MHz, $CDCl_3$): δ 172.8, 156.1, 79.1, 40.2, 39.2, 36.5, 33.6, 29.7, 29.1, 28.4, 27.9, 25.1, 24.4, 23.9. ESI-QTOF MS m/z calculated for $C_{16}H_{32}N_2O_3S$ $[M+H]^+$ 333.2206, measured 333.2198.

S-(6-((5-((*tert*-butoxycarbonyl)amino)pentyl)amino)-6-oxohexyl)ethanethioate (3)

To a solution of *tert*-butyl (5-(6-mercaptohexanamido)pentyl)carbamate (180 mg, 0.541 mmol) and dry potassium carbonate (150 mg, 1.083 mmol) in degassed (freeze-pump-thaw) ethyl acetate (2.2 mL), acetic anhydride (61 µl, 0.650 mmol) was added and the reaction was stirred for 16 h. The reaction was then diluted with ethyl acetate (20 mL), filtered and washed with cold water (1 x 10mL) and brine (1 x 10 mL), dried over sodium sulfate and evaporated to dryness. The crude was purified by flash column chromatography using chloroform/ethanol 96:4 to yield 182 mg (90%) of a white solid. ^{1}H NMR (400 MHz, $CDCl_3$): δ 5.68 (br, 1 H), 4.61 (br, 1 H), 3.21 (dt, J_1 = 7.3 Hz, J_2 = 6.9 Hz, 2H), 3.09 (dt, J_1 = 7.7 Hz, J_2 = 6.4 Hz, 2H), 2.83 (t, J =7.2 Hz, 2H), 2.30 (s, 1H), 2.14 (t, J = 7.2 Hz, 2H), 1.67 – 1.44 (m, 8H), 1.42 (s, 9H), 1.40 – 1.27 (m, 4H). ^{13}C NMR (100 MHz, $CDCl_3$): δ 196.0, 172.8, 156.1, 79.3, 40.2, 39.2, 36.4, 30.6, 29.7, 29.2, 29.1, 28.8, 28.4, 28.3, 25.1, 23.9. ESI-QTOF MS m/z calculated for $C_{18}H_{34}N_2O_4S$ $[M+H]^+$ 375.2312, measured 375.2312

S-(6-((5-aminopentyl)amino)-6-oxohexyl) ethanethioate (4, C6-SAc linker)

To a solution of S-(6-((5-((*tert*-butoxycarbonyl)amino)pentyl)amino)-6- oxohexyl) ethanethioate (187 mg, 0.5 mmol) in dichloromethane (6.6 mL), trifluoroacetic acid (0.77 mL, 5.34 mmol) was added dropwise at 0 °C. After stirring for 10 min, the reaction mixture was allowed to reach RT where it was stirred for 1 h. The volatiles were removed under reduced pressure at 30 °C and the residue was azeotroped with toluene and dried under high vacuum for 30 min. Lyophilization yielded a white solid (185 mg) which was sufficiently pure by NMR. ^{1}H NMR (400 MHz, CD_3OD): δ 3.18 (t, *J* = 7.0 Hz, 2H), 2.92 (t, *J* = 7.8 Hz, 2H), 2.86 (t, *J* =7.3 Hz, 2H), 2.30 (s, 3H), 2.17 (t, *J* = 7.3 Hz, 2H), 1.72 – 1.50 (m, 8H), 1.45 – 1.33 (m, 4H). ^{13}C NMR (100 MHz, CD_3OD): 197.7, 176.2, 40.7, 40.0, 37.0, 30.64, 30.61, 30.0, 29.8, 29.4, 28.3, 26.6, 24.8. ESI-QTOF MS m/z calculated for $C_{13}H_{26}N_2O_2S$ $[M+H]^+$ 275.1788, measured 275.1785.

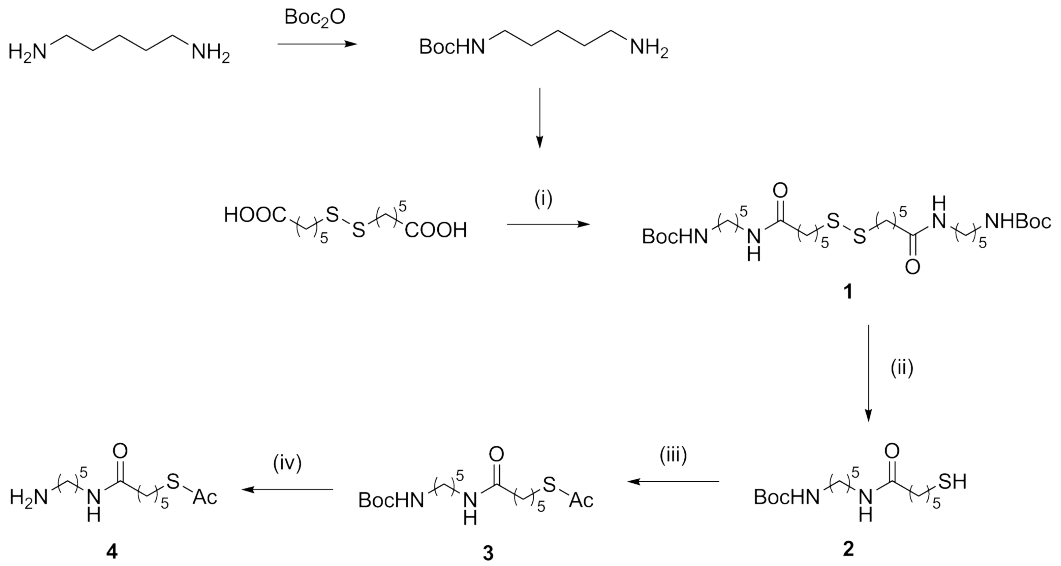

Fig. 3.3.: Synthesis of S-protected thiol-linker C6-SAc bearing a primary amine function. Reagents: (i) HBTU, DIPEA, DMF, r.t., 20 h, 93%; (ii) Bu_3P/H_2O, THF, r.t., 1 h, 91%; (iii) Ac_2O/K_2CO_3, AcOEt, r.t., 16 h, 90%; (iv) TFA, DCM, 0 °C to r.t., 1 h, quantitative

Boc-C6-vc-PAB-MMAF (7)

To a solution of maleimide-valine-citrullin-PAB-MMAF (8.8 mg, 6.61 µmol) in DMF (0.6 mL) was added 6.6µl of a 0.1 M solution of triethylamine in DMF (0.66 µmol Et_3N), followed by the dropwise addition of a solution of *tert*-butyl (5-(6-mercapto-hexanamido)pentyl)carbamate **2** (3 mg, 9.02 µmol) in acetonitrile (0.3 mL). The reaction was stirred for 3 h while being monitored by HPLC (t_R = 18.5 min). After the reaction was complete it was diluted with water (2 mL) and purified with semi-

preparative RP-HPLC with gradient system 1 (t_R = 10.3 min). The product was obtained as a white solid after lyophilization (8.7 mg, 79% yield). MS (ES+) m/z 832.44 $[M+H]^{2+}$

C6-vc-PAB-MMAF (8)

Compound **7** (8 mg, 4.81 µmol) was dissolved in an ice cold solution of CH_2Cl_2/TFA 95:5 (8 mL). The reaction mixture was allowed to reach RT and stirred for 40 min (reaction monitoring by HPLC, t_R = 16.8 min) after which time the volatiles were removed under reduced pressure and dried under high vacuum. The residue was purified by semi-preparative HPLC with gradient system 2, t_R = 11.7 min. The product was obtained as a white solid after lyophilization (4.86 mg, 65% yield). ESI-QTOF MS m/z calculated for $C_{79}H_{127}N_{13}O_{17}S$ $[M+2H]^{2+}$ 781.9670, measured 781.9667.

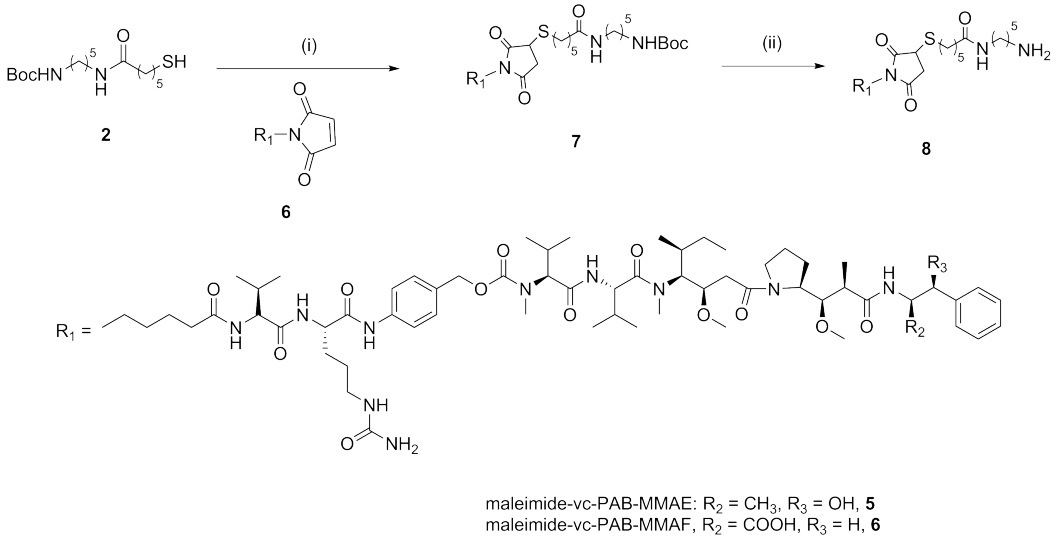

Fig. 3.4.: Synthesis of C6-vc-PAB-MMAF and structures of maleimide-MMAE/F. Reagents: (i) DMF/MeCN 1:1, Et_3N, r.t., 3 h, 79%; (ii) TFA, DCM, 0 °C to r.t, 40 min, 65%

3.3.2 LC-ESI-MS analysis

LC-ESI-MS analysis was performed on a Waters LCT Premier mass spectrometer. Prior to analysis, 10 µg of antibody was mixed with DTT (20 mM final concentration) and incubated at 37 °C for 30 min to separate heavy and light chains. Samples were chromatographed on an Aeris WIDEPORE XB-C18 column (3.6 µm, 100 mm x 2.1 mm; Phenomenex) heated to 80 °C using the following gradient: 0 min to 1 min, 10 to 20% A; 1 min to 30 min, 20 to 60% A; 30 min to 31 min, 60 to 10% A (solvent A: 1:1 acetonitrile:isopropanol + 0.1% formic acid, solvent B: water + 0.1% formic

acid) at a flow rate of 0.5 mL/min. The eluent was ionised using an electrospray source (ESI+). Data were collected with MassLynx 4.1 and deconvolution was performed using MaxEnt1. Unless stated otherwise, the following equations were used to estimate the relation between two mass peaks

$$\%\ \text{Mass Peak A} = \frac{\text{Intensity}_{\text{Mass Peak A}}}{\text{Intensity}_{\text{Mass Peak A}} + \text{Intensity}_{\text{Mass Peak B}}} \times 100 \tag{3.1}$$

and

$$\%\ \text{Mass Peak B} = 100 - \%\ \text{Mass Peak A} \tag{3.2}$$

3.3.3 Deglycosylation of antibodies

Antibody in phosphate buffered saline (PBS) was incubated with 6 Units/mg protein of *N*-glycosidase F (PNGase F) from *Flavobacterium meningosepticum* (Roche, Switzerland) overnight at 37 °C. The enzyme was then removed by centrifugation-dialysis (Vivaspin MWCO 50 kDa, Vivascience, Winkel, Switzerland). The reaction was monitored by LC-ESI-MS.

3.3.4 Enzymatic modification of antibodies

1 mg/mL deglycosylated antibody in PBS was incubated with 80 molar equivalents (40 molar equivalents per conjugation site) of the corresponding amine-functionalized chemical entity and 6 U/mL microbial transglutaminase (MTGase, Zedira, Darmstadt, Germany) overnight (16 h) at 37 °C. Excess substrate and the MTGase were removed by centrifugation-dialysis (for analytical purposes) or by size exclusion chromatography (SEC, Superdex 200 10/300 GL, GE Healthcare, 0.5 mL/min flow) for batch production.

3.3.5 Deacetylation of protected thiol linkers and maleimide-thiol conjugation

The method for deacetylation of the protected thiol linker was adapted from published procedures [21]. Briefly, deprotection stock solution containing 0.5 M hydroxylamine and 25 mM EDTA was prepared in PBS. The antibody-linker conjugate was combined with 10 - 40% v/v of the prepared deprotection stock solution in a final volume of 1 mL and the pH was adjusted to 7.7 - 8.8. The reaction mixture was

then incubated for 2 - 6 h at RT or 37 °C (Table A.1, supplementary information) and subsequently purified on a desalting column. The protein was eluted with PBS containing 10 mM EDTA. Conditions for maleimide-thiol coupling were adopted from previously described experiments [45]. Briefly, the deglycosylated antibody was reacted with a five-fold molar excess of maleimide-toxin (per thiol group) in PBS for 2 h at RT.

3.3.6 Strain-Promoted Azide-Alkyne Cycloaddition (SPAAC)

20 µM of azide-functionalized antibody was incubated with 50 µM to 200 µM (1.25 to 5 molar equivalents per azide group) of DBCO-amine at RT for 0.5 - 6 h. Excess of DBCO-PEG4-vc-PAB-MMAE was removed by SEC. The final ADC was formulated in citrate buffer (20 mM sodium citrate, 1 mM citric acid, pH 6.6) containing 0.1% polysorbate 80 and 70 mg/mL trehalose.

3.3.7 Linker cleavage assay (Cathepsin B)

Human liver cathepsin B (1.25 U/µL, Sigma Aldrich) was activated by incubating 3 µL of the protease with 84 µL water, 30 µL 0.5 M sodium acetate pH 5.0 and 6 µL 0.1 M dithiothreitol (DTT) at 37 °C. After 15 min, 28 µL ADC (1 mg/mL) was added and the reaction mixture was incubated at 37 °C for 6 h. Samples were taken after 2 and 6 h and analyzed by LC-ESI-MS.

3.3.8 Cell lines and antibodies

The human breast cancer cell lines BT-474 and SK-BR-3 were obtained from the American Type Culture Collection (ATCC) and maintained in RPMI 1640 and McCoy's 5a (BioConcept), respectively. Media was supplemented with 10% fetal calf serum (FCS), 2 mmol/L glutamine, 100 units/mL penicillin, 100 µg/mL streptomycin and 0.25 µg/mL fungizone (BioConcept, Allschwil, Switzerland). The cells were maintained at 37 °C. with 5% CO_2. Trastuzumab (Herceptin®) was obtained from the University Hospital Zurich and a non-specific chimeric IgG1 (Innate Pharma, France) was used as control IgG.

3.3.9 Fluorescence-Activated Cell Sorting (FACS)

The binding ability of native antibodies and ADCs was determined by flow cytometry using an indirect fluorescent staining method. The cells were harvested by trypsin/EDTA, washed with PBS supplemented with 1% BSA (PBS/BSA) and incubated with 10 µg/mL antibody for 30 min at 4 °C. Cells were washed three times with PBS/BSA on ice and incubated with a goat anti-human IgG-FITC (1:200 dilution in PBS/BSA, Santa Cruz Biotechnology) for 30 min at 4 °C in the dark. The cells were washed again three times with PBS/BSA, resuspended in 200 µL PBS/BSA and directly submitted to flow cytometry (Guava easyCyte™ Flow Cytometer, Merck Millipore). Data was analyzed with FlowJo software (Tree star Inc.).

3.3.10 Cell toxicity assay

Cells were plated in 96-well plates ($\sim$ 2000 and 3000 cells per well for SK-BR-3 and BT-474 respectively) and allowed to attach to the plates overnight at 37 °C. A serial dilution of wild-type antibody or ADC ranging from 66.6 nM (10 µg/mL) to 63.5 fM (9.5 pg/mL) was added and the cells were incubated at 37 °C. After 96 h, 30 µL of 5 mg/ml MTT-solution ((3-(4,5-dimethylthiazol-2-yl)-2,5-diphenyltetrazolium bromide, Sigma-Aldrich) was added to each well for 2 - 3 h at 37 °C in the dark. The supernatant was removed and the purple formazan crystals were dissolved in 200 µL DMSO. The absorption of the colored solution was measured at 506 nm on a Multilabel Plate Reader (VICTOR™ X3, Perkin Elmer). The raw data was processed using GraphPad Prism 5.0 (GraphPad Software, San Diego, USA).

3.4 Results and Discussion

3.4.1 Chemical syntheses of the spacer entities

The synthesis of the C6-SAc linker (**4**) is shown in Scheme 1. Two equivalents of N-Boc cadaverine were coupled to 6,6'-disulfanediyldihexanoic acid with HBTU in DMF to provide the disulfide **1** in excellent yield (93%). The starting material 6,6'-disulfanediyldihexanoic acid was synthesized from 6-bromo hexanoic acid by following a reported procedure [200]. N-Boc cadaverine was synthesized from cadaverine according to a published protocol with slight modifications [201]. Treat-

ment of compound **1** with Bu_3P/H_2O in THF afforded efficiently the free thiol **2** in 91% yield which was successively protected with an acetyl group by reacting it with acetic anhydride in AcOEt under basic conditions (**3**, 90% yield). Finally, cleavage of the Boc group in **3** with TFA in DCM afforded quantitatively linker **4** (C6-SAc) which was used for coupling with the antibody.

The synthesis of C6-vc-PAB-MMAF is depicted in Scheme 2. First, the Boc-protected-free thiol **2** was coupled with the MMAF toxin by reacting it with maleimide-vc-PAB-MMAF **6** in DMF to provide intermediate **7** in good yield (79%) after HPLC purification. Treatment of **7** with TFA in DCM and HPLC purification afforded C6-vc-PAB-MMAF in excellent purity (>98%).

3.4.2 Direct enzymatic conjugation of linker-toxins

We previously demonstrated that various small molecular weight cadaverin-derivatized substrates can be coupled by MTGase to a unique site on the heavy chains of deglycosylated mAbs [186]. Here, we tested if direct conjugation to chimeric and humanized IgG1 could also be achieved with cadaverin-derivatives of the auristatins MMAE and MMAF, both containing the cleavable dipeptide linker valine-citrulline. To this aim, we introduced two different spacers (C6 and PEG4) between the cleavable linker and the terminal amine and monitored the enzymatic conjugation by mass spectrometry.

The direct enzymatic conjugation reactions using a 40-fold excess C6-vc-PAB-MMAF (**8**) and PEG4-vc-PAB-MMAE (**9**) (Figure 3.5A) over conjugation site yielded approximately 50% and 80% of modified heavy chain for mAb-C6-MMAF and mAb-PEG4-MMAE respectively. While PEG4-MMAE seems to be a better amine-donor for MTGase than C6-MMAF (Figure 3.6), both toxin-derivatives are less reactive than the small molecular weight control substrate biotin-cadaverine. The coupling yield could theoretically be optimized by increasing the molar excess of the substrate or the units of MTGase. However, there are three critical issues that do not favour this direct enzymatic conjugation approach: (i) The acceptance of MTGase towards larger, amine-functionalized chemical entities such as toxins is unpredictable. Thus, reaction parameters have to be evaluated for each toxin individually. (ii) Lipophilic toxins might need to be dissolved in an organic solvent. However, these co-solvents can negatively influence the MTGase activity [191].

(iii) The large excess of toxin required for the reaction is another disadvantage with regard to large-scale production since these cytotoxic agents are expensive.

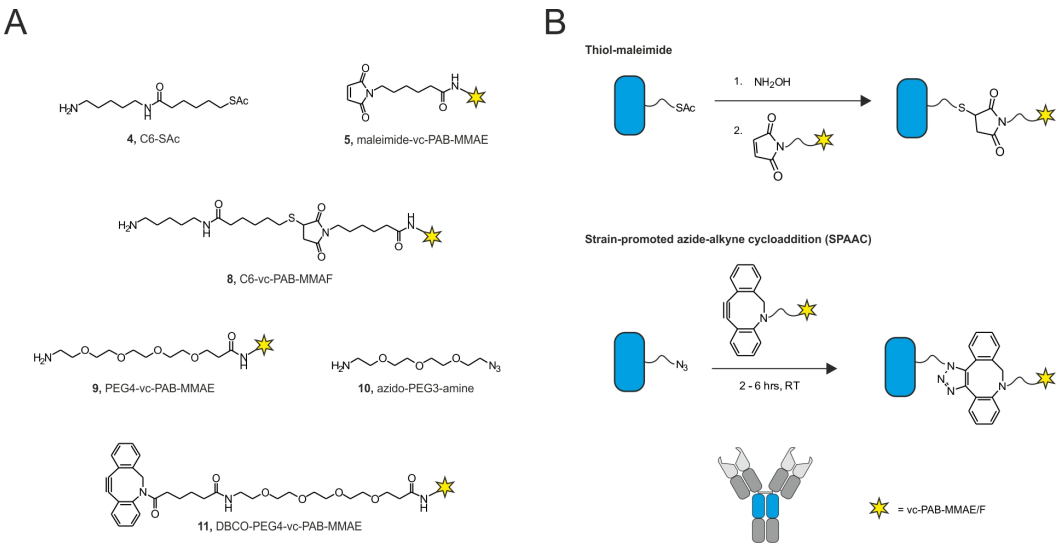

Fig. 3.5.: A) Chemical structures of the different substrates for the enzymatic- and chemo-enzymatic approach. B) General strategies for the chemo-enzymatic approaches. The thiol linker (**4**) and the azide linker (**10**) were enzymatically conjugated to the heavy chain (HC, cyan rectangle) of the antibody. Thiol-maleimide chemistry (top panel): The protected thiol was deacetylated under basic conditions. The free thiol was then further reacted with the maleimide-functionalized toxin (**5**) to yield the desired ADC. SPAAC reaction (bottom panel): The azide was reacted with the DBCO-functionalized toxin (**11**) in a Cu(I)-free [2+3] cycloaddition under mild conditions to yield the final ADC.

3.4.3 A chemo-enzymatic method to produce ADCs

To circumvent the problems outlined above, we developed a novel chemo-enzymatic approach whereby a small linker suitable for the enzymatic reaction by MTGase was used to introduce an additional thiol or azide functionality onto the antibody in a first step. The toxin, which was equipped with a functional group reactive towards the linker, could then be reacted with the antibody-linker conjugate to yield the desired ADC (Figure 3.2, bottom panel). We chose two different chemistries for this novel strategy: (i) Thiol-maleimide chemistry is a very popular chemistry to modify proteins via natural or engineered cyteines. Hence, numerous maleimide-functionalized chemical entities are commercially available, including toxins. (ii) Strain-promoted azide-alkyne cycloaddition (SPAAC), a Cu(I)-free [2+3] cycloaddition reaction, is an emerging tool for protein modification [24, 112]. Both chemistries should be fast, efficient and can be performed under mild conditions.

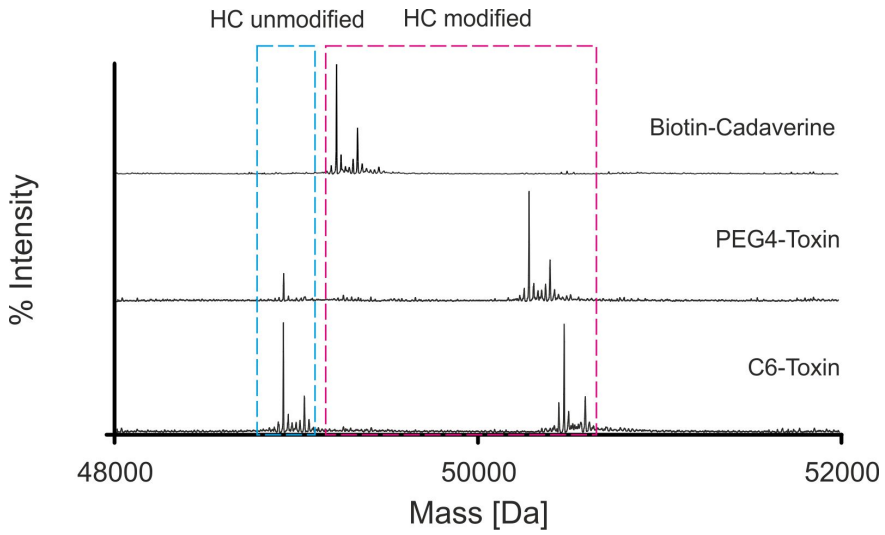

Fig. 3.6.: Deconvoluted mass spectra of different reactions. The smaller peaks with an increased mass correspond the TFA adduct of the main peak. The PEG4-Toxin seems to be a better amine donor for MTGase than C6-Toxin because there is less unmodified heavy chain (HC, cyan dashed box) left after the enzymatic reaction. However, no unmodified HC (cyan dashed box) but only heavy chain with the expected mass shift of 311 Da (328 Da [molecular weight of biotin-cadaverine] - 17 Da [ammonia] = 311 Da; magenta dashed box) could be found after the enzymatic reaction with biotin-cadaverine. This indicates that the linker length and the size of the entire chemical entity have a influence on the enzymatic reaction outcome.

Thiol-maleimide approach (Figure 3.5B, top lane). First, we attached the commercially available thiol linker 6-amino-1-hexanethiol to the antibody by MTGase but observed major side products by LC-MS that could be assigned to dimerized linker attached to heavy chain (data not shown). Hence, we protected the thiol with an acetyl group to circumvent dimerization issues.

The protected thiol-linker C6-SAc (**4**) could be quantitatively conjugated to the antibody. We observed the expected mass shift for the heavy chain and there was no unmodified heavy chain remaining after the enzymatic reaction (Figure A.1A, supporting information). In order to establish quantitative removal of the protection group, different conditions have been tested (Table S1, supporting information) with the antibody-C6-SAc conjugate. However, residual acetylated heavy chain species were detected in all of the conditions tested. We reacted the antibody-C6-SH/antibody-C6-SAc conjugate mixture with a 3-fold molar excess of maleimide-vc-PAB-MMAE and found approximately 80-90% heavy chains with the desired mass shift (Figure A.1B, supporting information). While these results demonstrate the potential of this approach as a tool for the production of homogeneous ADC, the deacetylation of the thiol prevents this method from being entirely successful.

Additionally, two aspects have to be considered when maleimide-thiol chemistry is used (i) immunoglobulin aggregation may be influenced by free thiols that can form disulfide bonds between antibodies and (ii) depending on the site of conjugation, maleimide exchange processes can influence the performance of the antibody conjugate [47].

Strain-promoted azide-alkyne cycloaddition (SPAAC, 3.5B, bottom lane). The enzymatic reaction with the small linker azido-PEG3-amine (**10**) quantitatively yielded the desired antibody conjugate (Figure 3.7). DBCO-amine was used as a model substrate to determine optimal reaction conditions for the Cu(I)-free [2+3] cycloaddition. We varied the molar equivalents of DBCO-amine and monitored the progress by analyzing reaction aliquots after different time intervals by LC-ESI-MS. The SPAAC reaction was very fast and yielded homogeneous antibody conjugates after 6 h at RT with a minimal molar excess of 1.25 equivalents per azide group (Figure A.2, supporting information). We applied these conditions to attach DBCO-PEG4-vc-PAB-MMAE (**11**) and obtained uniform ADCs (Figure 3.7).

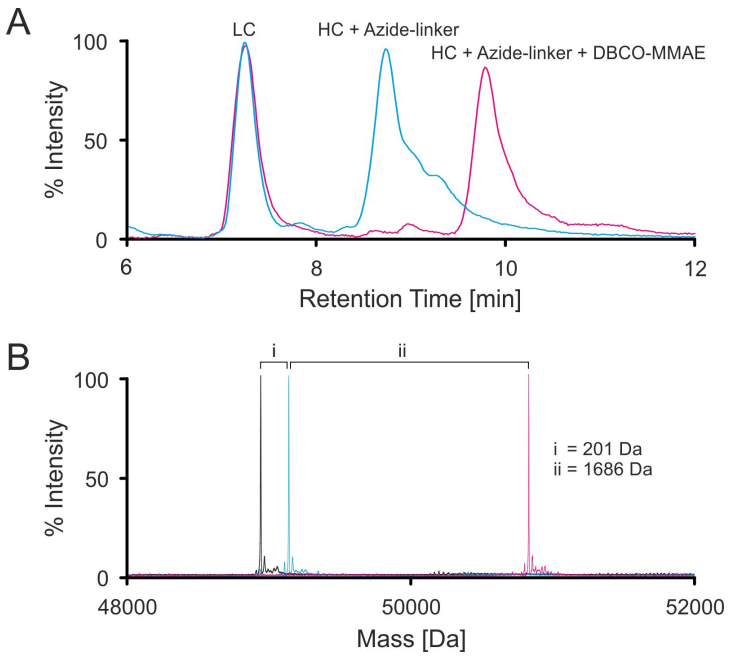

Fig. 3.7.: A) Liquid chromatrography UV trace of the antibody before (cyan) and after (magenta) the SPAAC reaction with the toxin. B) Deconvoluted mass spectra of different reactions. The SPAAC reaction was monitored by LC-MS and showed expected mass shifts between (i) unmodified HC (black) and HC after the enzymatic reaction with MTGase and amine-PEG3-azide linker (cyan) of 201 Da (218 Da [molecular weight of amine-PEG3-azide linker] - 17 Da [ammonia] = 201 Da) and (ii) HC + azide-linker (cyan) and the HC after SPAAC reaction with DBCO-PEG4-vc-PAB-MMAE (magenta) of 1686 Da ([molecular weight of DBCO-PEG4-vc-PAB-MMAE]). Moreover, yields of both the enzymatic (1st step) and the chemical (2nd step) reaction are quantitative (>95%)

These results impressively demonstrate the ability of our chemo-enzymatic approach to produce homogeneous ADCs with respect to site-specificity and stoichiometry. A defined DAR is important for ADCs since a heterogeneous drug load can have a negative influence on the *in vivo* properties [16, 17]. Moreover, ADCs obtained by SPAAC conjugation are potentially more stable *in vivo* than thiol-maleimide coupled ADCs, because of maleimide exchange processes with reactive thiols on serum proteins [47]. Furthermore, the minimal excess of expensive toxin used is clearly advantageous with respect to scaled-up production of ADCs. Our method can also be applied to a broad variety of IgGs since the site of modification is located within the constant heavy chain domain and is conserved in human IgG1-4, murine IgG1/3 and rat IgG1/2a-c.

Deglycosylation of the antibody is, however, inevitable when exploiting our chemo-enzymatic approach since the site of modification (Q295) is adjacent to the glycosylation site (N297). It has been reported that carbohydrate removal influences the structural stability of antibodies thereby leading to an increased aggregation rate [202]. Nevertheless, several aglycosylated antibodies are currently evaluated in clinical trials [203]. Moreover, the lack of the carbohydrate moiety can even be advantageous since hepatic toxicities of ADCs seem to be driven by interactions of the antibody glycans with the mannose receptor, resulting in off-target cellular uptake [204]. In addition, abrogated FcR+ interaction can potentially be advantageous as a lower uptake by FcR+ cells can lead to a limited off-target toxicity and improve tumor specific targeting [205, 206].

3.4.4 Biological evaluation of the ADC

In order to prove the applicability of our novel technology we selected two different antibodies, a humanized anti-HER2/neu IgG1 (Trastuzumab, Herceptin®) and a non-specific IgG1 (control IgG), and transformed them into ADCs according to the established protocol. These conjugates were then used to assess the biological activity.

Mass spectrometric analysis of trastuzumab-PEG3-N3-DBCO-PEG4-vc-PAB-MMAE (trastuzumab-MMAE) after the incubation with human liver cathepsin B revealed complete cleavage of the toxin after 6 hours (Figure 3.8). These results demonstrate

that the introduction of a PEG4 spacer or a DBCO functionality does not inhibit the enzymatic cleavage of the dipeptide valine-citrulline.

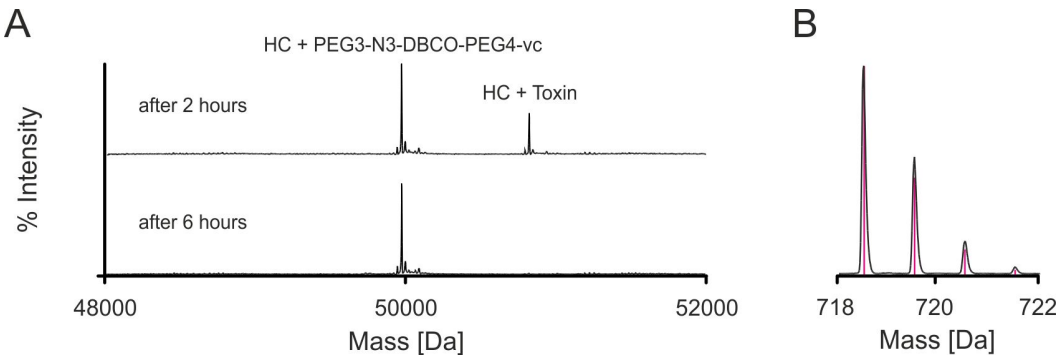

Fig. 3.8.: A) Deconvoluted mass spectra of reaction monitoring. The toxin was completely cleaved after 6 hours by cathepsin B and a single peak that corresponds to HC + PEG3-N3-DBCO-PEG4-vc could be observed. B) The cleaved toxin fragment could be identified in the reaction mixture. The isotopic model (magenta) is congruent with the measured data.

Next, we examined the ability of trastuzumab-MMAE to bind to HER2/neu by flow cytometry on HER2/neu+ cell lines (BT-474, SK-BR-3) and observed binding of the ADC to both cell lines (Figure 3.9A, left). This result is not surprising because the site of drug attachment (CH2 domain) is distant from the antigen-binding site. In addition, no variant of the control IgG1 (unmodified and ADC) bound to BT-474 or SK-BR-3 cells (Figure 3.9A, right).

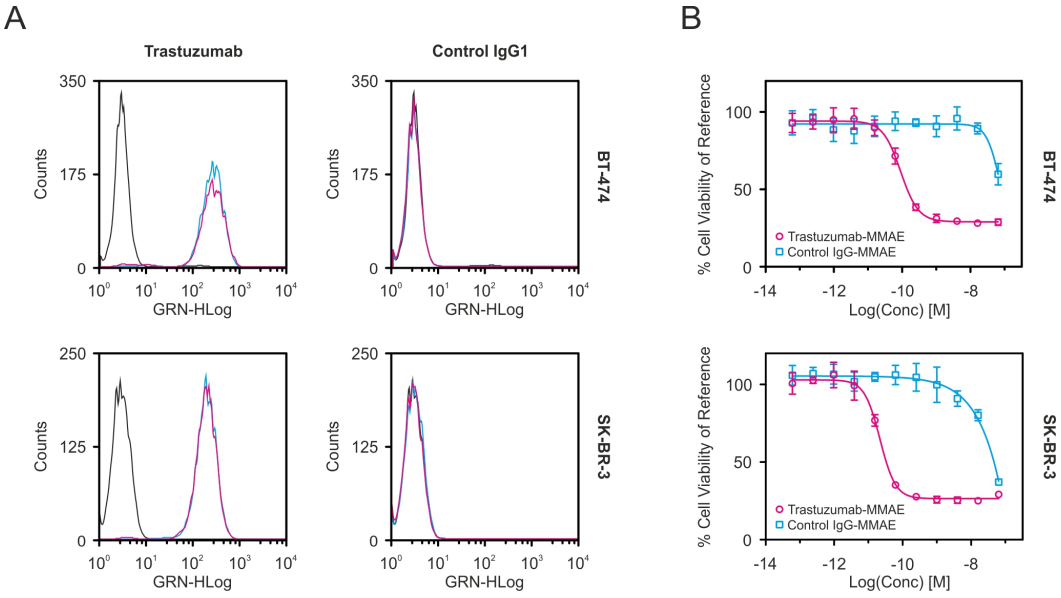

Fig. 3.9.: A) Fluorescence-activated cell sorting (FACS) analysis of trastuzumab/control IgG1 wild-type (cyan) and trastuzumab-MMAE/control IgG1-MMAE (magenta) on human breast cancer cell lines BT-474 (top) and SK-BR-3 (bottom). B) Trastuzumab-MMAE (circles) effectively inhibits cell proliferation of both BT-474 and SK-BR-3 cells whereas the control IgG1-MMAE (diamonds) shows cytotoxic effect only at high concentrations

Finally, the ADC was tested for cytotoxicity and selectivity to prove its functionality. Trastuzumab-MMAE effectively killed BT-474 and SK-BR-3 cells with an IC_{50} of 89.0 pM and 21.7 pM respectively, whereas the control IgG-PEG3-N3-DBCO-PEG4-vc-PAB-MMAE (control IgG-MMAE) did not kill BT-474 or SK-BR-3 cells (IC_{50} > 700-fold higher). These IC_{50} values are comparable with published values where a similar cell toxicity assay setup was used [70]. However, a non-specific effect on cell proliferation was observed with the highest ADC concentration, (10 µg/mL, Figure 3.9B). As an inhibitory effect arising from the antibody itself cannot be ignored, the impact of both unconjugated trastuzumab and control antibody on cell proliferation was evaluated in parallel on both cell lines. While the control IgG1 had no effect on cell proliferation, trastuzumab influenced the proliferation of both BT-474 and SK-BR-3 cells (Figure A.3, supporting information). Nevertheless, trastuzumab-MMAE showed an approximately 10-fold lower IC_{50} for both cell lines, clearly demonstrating the enhanced potency of the ADC in comparison to the unmodified antibody.

3.5 Conclusion

In this article we have described different approaches to endow antibodies with MMAE in a site-specific and stoichiometric uniform manner. The chemo-enzymatic approach using SPAAC chemistry was superior to the other evaluated methods with respect to product homogeneity and amount of MMAE required. The fact that a minimal amount of toxin is needed using a two-step, chemo-enzymatic approach can be a crucial argument with regard to large-scale production of ADCs because of reduced costs and prevention of hazardous waste. Our results demonstrate the versatility and potential of this conjugation method. It allows not only the transformation of virtually any IgG1 into a functional ADC but also enables a direct comparison of *e.g.,* different antibodies, linker systems or toxins because of the known site of drug attachment and the uniform stoichiometry. Therefore, the chemo-enzymatic procedure is a powerful tool for both ADC production and development of next generation ADCs.

4

Microbial Transglutaminase and c-myc-Tag: A Strong Couple for the Functionalization of Antibody-Like Protein Scaffolds from Discovery Platforms

Adapted from

Patrick Dennler, Laura K. Bailey, Philipp R. Spycher, Roger Schibli and Eliane Fischer. "Microbial Transglutaminase and c-myc-Tag: A Strong Couple for the Functionalization of Antibody-Like Protein Scaffolds from Discovery Platforms". *ChemBioChem* 2015, in press

Authors contribution

Patrick Dennler designed and performed experiments and wrote the paper, Laura Bailey designed and cloned the ESC11-Fab into the new expression system and established the expression, Philipp Spycher performed the surface immobilization, provided the patterned surfaces and operated the microscope, Eliane Fischer worked on the manuscript

4.1 Abstract

Functionalization of lead candidates selected from antibody discovery platforms is preferentially accomplished by site-specific bioconjugation. This approach preserves the binding abilities of functionalized proteins and allows a direct side-by-side comparison of multiple conjugates during early stage development. Here we present a generic, enzymatic bioconjugation platform that targets the c-myc-tag peptide sequence (EQKLISEEDL) as a handle for site-specific modification of antibody-like proteins. Microbial transglutaminase (MTGase) was exploited to form a stable isopeptide bond between the glutamine on the c-myc-tag and various primary amine functionalized substrates. We attached biotin, fluorescent dyes, chelating systems for radiolabeling and bioorthogonal functionalities to a c-myc-tagged antibody fragment and used these bioconjugates for downstream applications such as protein multimerization and immobilization on surfaces, fluorescence microscopy, fluorescence-activated cell sorting (FACS) and *in vivo* nuclear imaging. The results demonstrate the versatility of our conjugation strategy to transform a c-myc-tagged protein into any desired probe.

4.2 Introduction

Display libraries are a virtually inexhaustible source of affinity reagents for research and drug development [207]. The biomolecules selected from such discovery platforms include antibody fragments, but also alternative antibody-like protein scaffolds, for example affibodies, nanobodies or DARPins [208]. These small proteins are invaluable tools in early drug development because they are easy to produce and are thus perfectly suited for screening drug candidates.

Transformation of lead candidates into functional entities for downstream applications often requires site-specific bioconjugation. This is particularly important for the functionalization of small proteins, because random modification is more likely to affect their binding properties. Furthermore, site-specific bioconjugation enables the direct comparison different antibody-like proteins as highly specific molecular probes in a range of applications. For example, biotinylation is a widely used approach for protein detection, multimerization, surface immobilization for

biosensor technologies or pretargeting strategies *in vivo* and takes advantage of the exceptionally high binding affinity between biotin and (strept)avidin ($K_d \sim 10^{-15}$ M) [209–212]. Also, antibody-like proteins are frequently functionalized with fluorescent dyes or radiolabels for molecular imaging *in vitro* and *in vivo*. Radiometals are particularly interesting for positron emission tomography (PET) or single-photon emission computed tomography (SPECT) imaging but the protein must generally be functionalized with a chelator prior to radiolabeling. Furthermore, an antibody-like protein can also be indirectly functionalized by first introducing a chemical functionality that is then reacted with a second entity *e.g.,* a protein or a drug.

Methods to attach chemically reactive amino acids *e.g.,* cysteines, non-canonical amino acids or genetically encoded tags to the C or N-terminus of proteins are currently used technologies to generate site-specifically modified bioconjugates [69, 109]. The addition of a terminal cysteine is the most basic approach but the resulting maleimide-thiol bond after conjugation is prone to *in vivo* instability [52]. While the incorporation of non-natural amino acids requires reestablishment of protein expression conditions, tagging of proteins is simple and straightforward. Formylglycine-generating enzymes (FGE) convert the cysteine of a terminal CXPXR-tag to formylglycine, thereby creating a bioorthogonal functionality that can be used for site-specific protein modification [110]. However, the conjugation yield is limited due to hydration of the formylglycine to diol-formylglycine [114]. Another innovative approach exploits the transpeptidic activity of sortase A to join a LPXTG-tag with a polyglycine-linked substrate [213, 214]. However, the necessity of a polyglycine motif restricts the commercial availability of substrates because they usually have to be tailor made.

Transglutaminases are a family of enzymes (EC 2.3.2.13) that catalyze the covalent formation of an isopeptide bond between the γ-carbonyl amide group of glutamines and the primary amine of lysines [158]. Unlike other enzymes that are used for site-specific bioconjugation [109], MTGase does not require a consensus sequence and targets various glutamines in a protein backbone. However, these residues are rare since they must be located in a flexible or disordered region of the polypeptide [167, 183]. For this reason, MTGase can be used as a valuable tool for site-specific protein modification by targeting either endogenous glutamine residues that fulfill

the aforementioned requirements or terminal glutamine-containing tags [187, 215, 216].

We established a versatile, MTGase-based bioconjugation platform that exploits the C-terminal c-myc-tag (EQKLISEEDL, Figure 4.1A) on proteins as the glutamine donor for the enzymatic attachment of various functionalities (Figure 4.1B). The c-myc-tag is widely used for sensitive detection of the recombinant proteins with a high-affinity anti-c-myc antibody and thus already integrated in a broad variety of pro- and eukaryotic expression vectors. Therefore, proteins and in particular antibody-like scaffolds that derive from phage display libraries, are often c-myc-tagged [217]. Additionally, MTGase recognizes only one glutamine, located in the CH2 domain, as acyl-donor within the sequence of a native IgG. Consequently, our conjugation strategy can be exploited to site-specifically functionalize c-myc-tagged antibody fragments that lack the CH2 domain such as Fab fragments or scFvs.

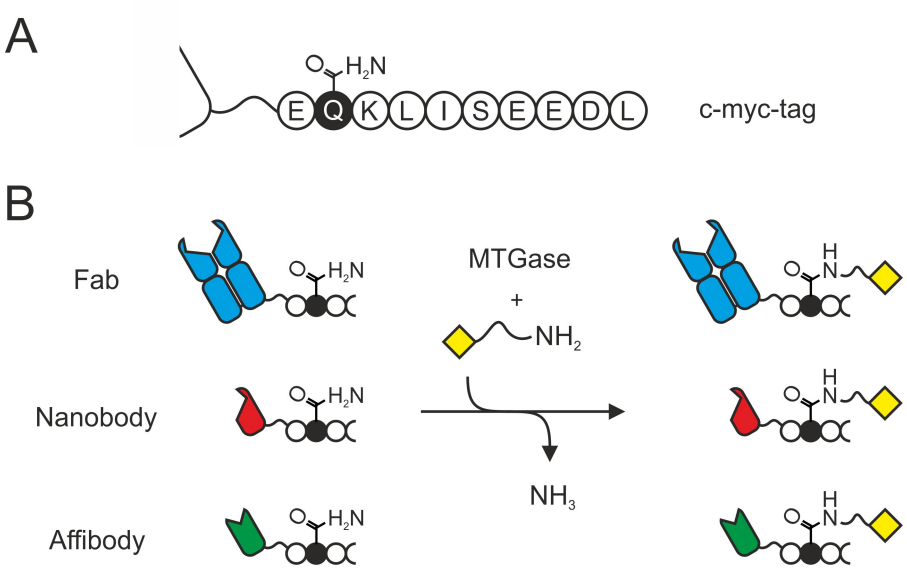

Fig. 4.1.: A) Amino acid sequence of the c-myc-tag. B) Various c-myc-tagged antibody-like protein scaffolds from discovery platforms can be site-specifically modified with a broad variety of primary amine functionalized substrates (yellow square) by MTGase.

4.3 Results and Discussion

To demonstrate the applicability of our enzymatic bioconjugation platform, we functionalized a c-myc-tagged Fab-fragment and two c-myc-tagged antibody-like scaffolds *i.e.,* a nanobody and an affibody with biotin (Figure B.1, supporting information) and monitored the reaction by mass spectrometry. We observed an

increase in mass of 311 Da for all three proteins, which corresponds to the attachment of exactly one biotin per protein (Figure 4.2). Conversely, no biotinylation was observed after incubation of the corresponding untagged nanobody with MTGase and biotin (Figure B.2, supporting information), indicating that MTGase selectively targets the glutamine of the c-myc-tag also on different protein scaffolds. The identification of the biotinylated c-myc-tag by peptide mapping ultimately proved the site-specificity of our enzymatic bioconjugation platform (Table B.1, supporting information).

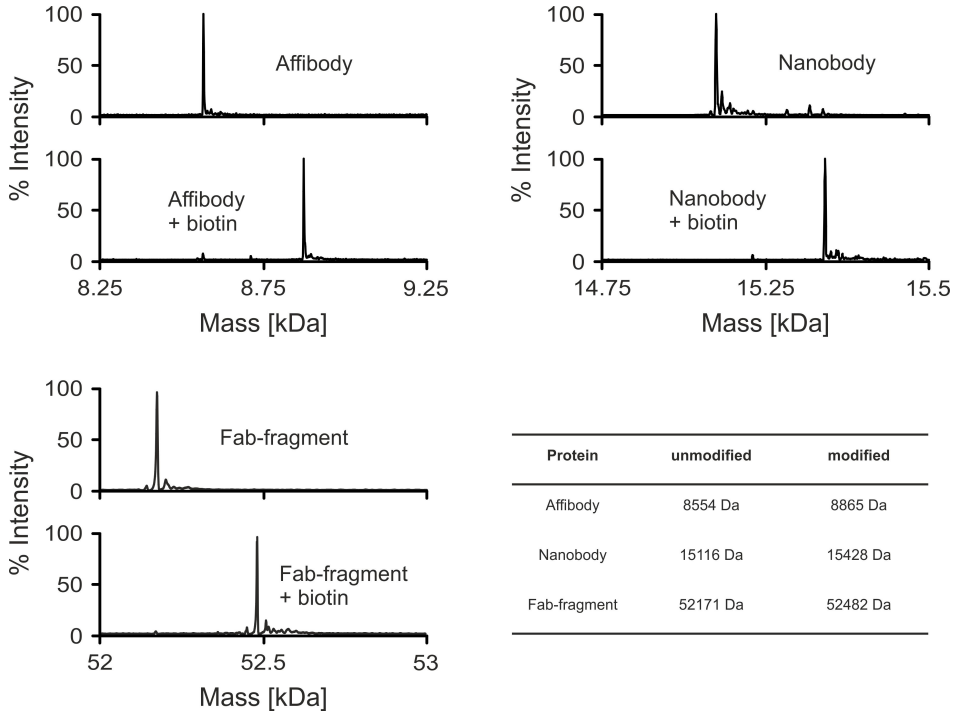

Protein	unmodified	modified
Affibody	8554 Da	8865 Da
Nanobody	15116 Da	15428 Da
Fab-fragment	52171 Da	52482 Da

Fig. 4.2.: Mass spectrometric monitoring of MTGase-catalyzed protein conjugation. MaxEnt1 deconvoluted mass spectra of an affibody, a nanobody and a Fab-fragment before and after incubation with MTGase and *N*-(Biotinyl)cadaverine (designated as biotin). The mass shift corresponds to the attachment of exactly one biotin (311 Da).

Encouraged by the finding that virtually every c-myc-tagged protein can be functionalized by using our MTGase-based technology we chose the Fab-fragment, derived from the anti-fibroblast activation protein (α-FAP) antibody ESC11 [218], as a model protein to demonstrate the versatility of the conjugation platform. We aimed to modify the c-myc-tagged Fab-fragment, designated as ESC11-Fab, with a variety of different functionalities that are useful for a range of downstream applications (Figure 4.3).

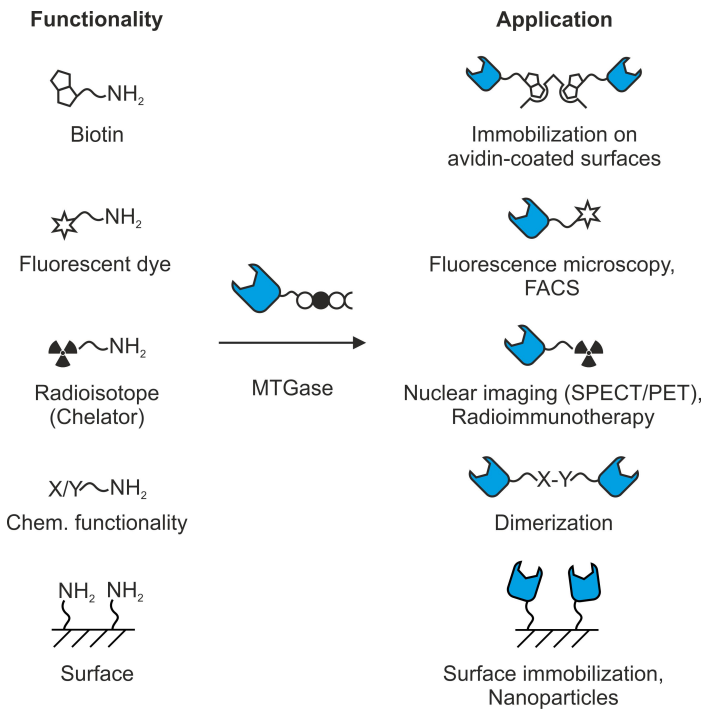

Fig. 4.3.: The different functionalities (left) that have been used in this study to modify a c-myc tagged targeting protein and a selection of possible downstream applications (right).

Eight different functionalities were attached to the ESC11-Fab by incubation with MTGase and the corresponding amine-derivatized substrate (Figure B.1,supporting information). Mass spectrometric analysis revealed that all chemical entities could be attached to the ESC11-Fab (Figure 4.4). While the reaction yield with biotin, both fluorescent dyes and the azide linker was quantitative (>95%), we observed a lower yield with the DBCO functionality (∼50%). Among the three different chelating systems that were tested, NH_2-PEG4-DOTA gave the highest conjugation yield (∼80%) compared to ∼75% and ∼65% for NH_2-PEG4-DOTA-GA and NH_2-PEG4-NODA-GA, respectively and was therefore selected for further studies (Figure B.3, supporting information). It has been shown that acidic residues on the acyl-acceptor are not favorable for MTGase-mediated conjugation [178]. Based on the conjugation result of the DBCO linker and our experience we hypothesize that the same is true for bulky cyclic structures. We subsequently used the generated conjugates for a panel of different *in vitro* and *in vivo* applications.

The biotinylated ESC11-Fab, for example, was incubated with streptavidin to show that the interaction between biotin and streptavidin is retained after the enzymatic modification process. As expected, streptavidin formed a tetrameric complex when incubated with 4 molar equivalents biotinylated ESC11-Fab (Figure B.4, support-

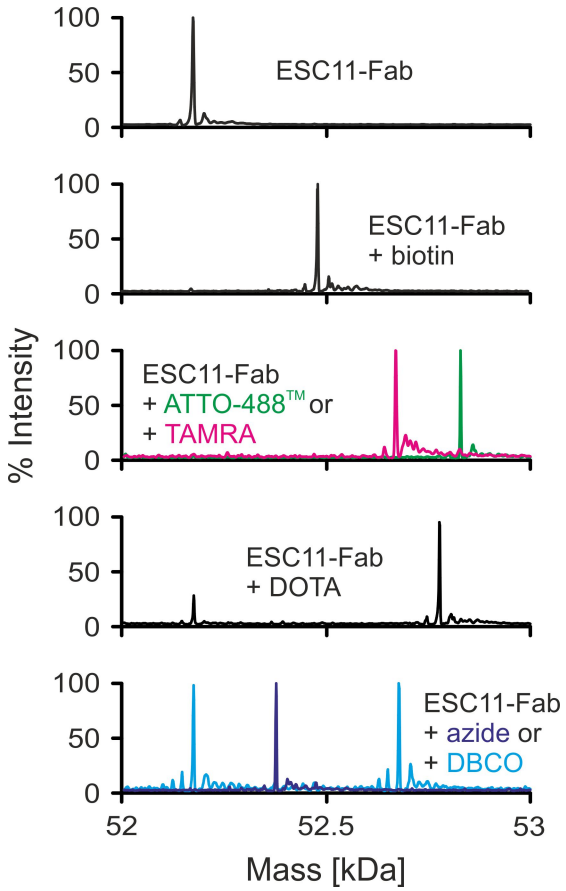

Fig. 4.4.: Mass spectrometric monitoring of MTGase-catalyzed protein conjugation. Mass spectrometric monitoring of MTGase-catalyzed protein conjugation. MaxEnt1 deconvoluted mass spectra showing the successful conjugation of different functionalities to the ESC11-Fab. The two individual spectra of ESC11-Fab-ATTO-488™ and ESC11-Fab-TAMRA as well as ESC11-Fab-azide and ESC11-Fab-DBCO are merged into one spectrum.

ing information). We then tested the ability of ESC11-Fab to bind to its antigen once it was immobilized on a streptavidin-coated surface by adding recombinant FAP (Figure B.5A, supporting information). Highly quenched fluorescein-labeled gelatin revealed the specific capturing of enzymatically active FAP by the biotinylated immobilized ESC11-Fab (Figure B.5B, supporting information). Finally, we demonstrated that the biotinylated ESC11-Fab could be specifically immobilized on an avidin-coated patterned surface (Figure 4.5A, Figure B.6, supporting information). This site-specific *in vitro* biotinylation approach enables us to immobilize proteins in an oriented manner, which can contribute to an increased sensitivity of biosensors [219]. Additionally, it also overcomes common problems of the classical BirA-mediated biotinylation in *E.coli e.g.,* decreased protein expression levels, because it does not rely on variable cellular processes [220].

ESC11-Fab equipped with (ATTO-488™)cadaverine was used for FACS analysis of HT1080FAP cells. FAP+ cells could be specifically stained while FAP- cells did not show any fluorescent signal (Figure 4.5B). We further functionalized ESC11-Fabs with another dye, *N*-(TAMRA)cadaverine, and could directly stain a series of FAP+ cell lines including activated fibroblasts, melanoma and liposarcoma cells with the two bioconjugates (Figure 4.5C, Figure B.7, supporting information). While this direct staining helps to streamline and shorten immunofluorescence experiments, we envisage our conjugation strategy being also applied in assays where it is not possible to use a secondary antibody and direct fluorescence labeling of the protein is required *e.g.,* fluorescence anisotropy, analytical ultracentrifugation or even for optical *in vivo* imaging.

In order to transform the ESC11-Fab-DOTA into a radiotracer suitable for SPECT imaging, we radiolabeled it with $^{111}InCl_3$ and yielded ^{111}In-ESC11-Fab-DOTA with a specific activity of $\sim$0.9 MBq/µg protein (Figure B.8, supporting information). We then injected $\sim$18 MBq into liposarcoma tumor-bearing mice and successfully visualized the subcutaneous tumors by SPECT imaging (Figure 4.5D). These radioactive conjugates can also be used for biodistribution studies and moreover, therapeutic probes could easily be generated by using a suitable radionuclide.

Homodimeric ESC11-Fab complexes were produced by incubating ESC11-Fabs that have been conjugated with either an azide or DBCO functionality. We could detect a band of approximately 100 kDa by SDS-PAGE, which corresponds to the molecular weight of the desired bivalent product (Figure 4.5E). The rather low reaction yield may be attributed to steric clashing of the two ESC11-Fabs. Furthermore, it has been shown that the coupling yield depends on the localization of the azide- and DBCO functionality [112]. The development and usage of novel bioorthogonal chemical handles could help to overcome these limitations.

The fusion of two proteins with different functionalities can be employed to increase their therapeutic index, to alter their pharmacokinetics or to be used for a pretargeting approach [221–223]. Our strategy circumvents the genetic fusion of proteins and is therefore more flexible because different combinations of protein-protein conjugates can easily be accomplished. Moreover, this strategy is not limited to the attachment of a second protein but can even be used to conjugate toxins or other more complex entities [224].

As a last example we aimed to directly immobilize the ESC11-Fab onto a surface. We used supported lipid bilayers (SLBs) as a model because they are compatible with a number of characterization tools *e.g.,* quartz crystal microbalance with dissipation monitoring (QCM-D). In combination with patterning technologies, SLBs represent a potent option in the field of biosensor design [225]. To accomplish SLBs that display amine donors for MTGase, we mixed maleimide-functionalized (PE-MCC) phospholipids and phosphocholine lipids (POPC) to generate liposomes that, when exposed to a solid support, formed a SLB. A peptide, containing a cysteine (reactive towards the maleimide) and lysine (amine donor for MTGase, Figure B.1, supporting information) was coupled to the SLB in a second step that enabled us to covalently attach the ESC11-Fab to the SLB using MTGase (Figure B.9, supporting information). The ESC11-Fab could then be efficiently anchored on the membrane as indicated by a fast decrease of the resonant frequency of the quartz crystal, which corresponds to an increase of mass on the surface (Figure 4.5F). The possibility to determine the ratio between the PE-MCC and POPC enables us to control the incorporation rate of amine functionalities and, as a consequence, the density of immobilized and oriented proteins on an SLB. Moreover, it is also conceivable to directly functionalize liposomes with a targeting protein and use them as a drug delivery system.

4.4 Conclusion

In conclusion, we have established a versatile enzymatic conjugation platform that allows the site-specific functionalization of any c-myc-tagged antibody-like protein. Furthermore, we demonstrated that the very same protein can be easily transformed into different probes. Ultimately, these different conjugates can be used for *in vitro* or *in vivo* applications such as immunofluorescence assays, FACS, nuclear imaging, surface immobilization and multimerization. While we have only used a selection of functionalities for our studies, there are, nevertheless, numerous additional possibilities that are conceivable. Toxic agents, for example, could be used to transform a given protein into a therapeutic agent. As long as a primary amine functionality can be incorporated into a molecule, it is a potential substrate for MTGase. Consequently, there are virtually no limits to which extent our enzymatic bioconjugation platform can be expanded.

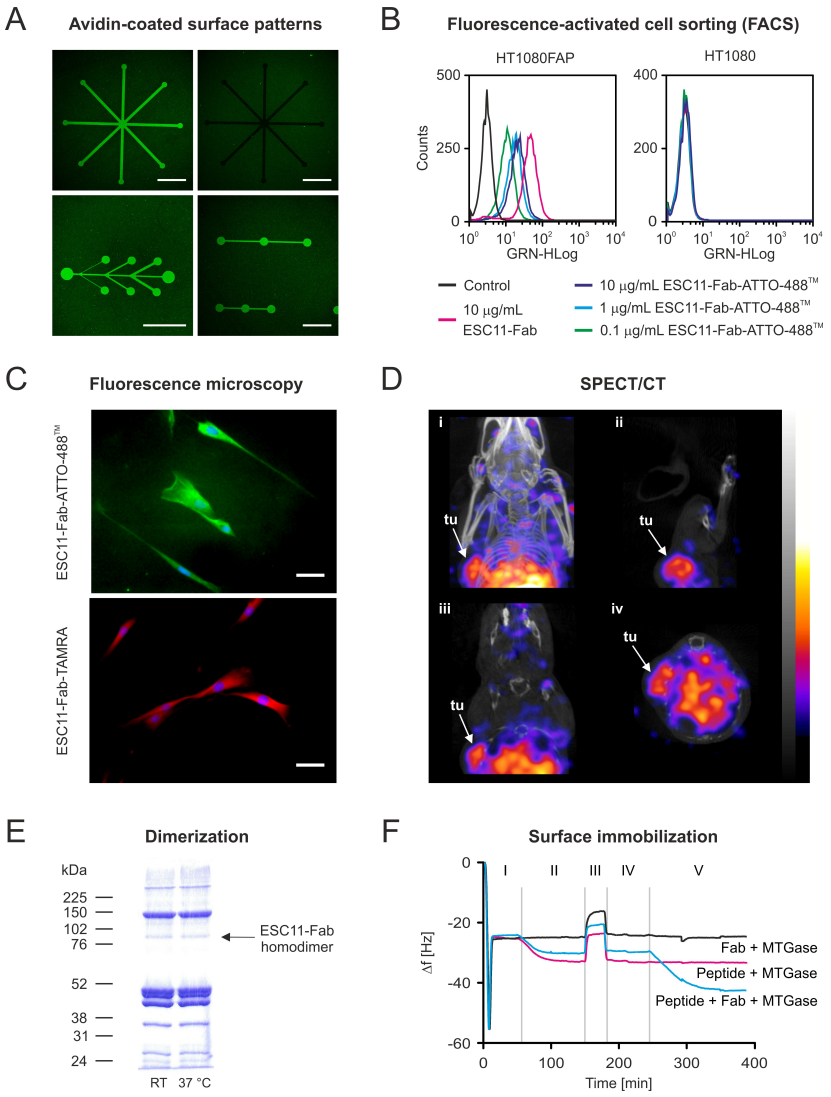

Fig. 4.5.: Downstream applications with different ESC11-Fab conjugates. A) Specific immobilization of biotinylated ESC11-Fab (Alexa Fluor® 488 labeled) on different avidin-coated micropatterns and a negative control (top right image, non-biotinylated Alexa Fluor® 488 labeled ESC11-Fab). Scale bar: 50 µm. B) FACS analysis of FAP+ (HT1080FAP) and FAP- (HT1080) cells using different concentrations of ESC11-Fab-ATTO-488™ and ESC11-Fab as positive control. C) Immunofluorescence microscopy of FAP-expressing activated fibroblasts with ESC11-Fab-ATTO-488™ (green), ESC11-Fab-TAMRA (red) and Hoechst 33342 (blue) to visualize cell nucleus. Scale bar: 50 µm. D) *In vivo* SPECT imaging of liposarcoma (SW-872) tumor-bearing mouse with ^{111}In-ESC11-Fab-DOTA. Tumor cells (tu) were injected s.c. on the left shoulder. (i) Maximum intensity projection (MIP) (ii) sagittal (iii) coronal (iv) transverse views. E) Coomassie-stained SDS-PAGE gel after incubation of ESC11-Fab-PEG3-azide and ESC11-Fab-PEG4-DBCO at RT and 37 °C. Clicked homodimer can be observed at ~100 kDa size. F) QCM-D sensogram of direct MTGase-mediated ESC11-Fab immobilization on a SLB (cyan). Additionally, unspecific adsorption (black) and MTGase self-immobilization (magenta) were tested. Different phases of the immobilization experiment, I: formation of the SLB II: cysteine-maleimide coupling of Lys-containing peptide to the SLB III: quenching of unreacted maleimides IV: buffer exchange V: MTGase-mediated immobilization of ESC11-Fab on SLB. A decrease in frequency corresponds to an increase of mass and hence, conjugation of protein onto the SLB surface.

4.5 Experimental Section

4.5.1 General

All restriction enzymes were purchased from Fermentas (Thermo Fischer) and used according to manufacturer′s instructions. Microbial transglutaminase (MTGase), *N*-(Biotinyl)cadaverine, (ATTO-488™)cadaverine and *N*-(Tetramethylrhodaminyl)cadaverine (TAMRA) were purchased from Zedira (Darmstadt, Germany), Dibenzylcyclooctyne-PEG4-Amine (DBCO-PEG4-Amine) and 11-Azido-3,6,9-trioxaundecan-1-amine (Azido-PEG3-Amine) from Jena Bioscience GmbH (Jena, Germany) and 2,2′,2″-(10-(17-amino-2-oxo-6,9,12,15-tetraoxa-3-azaheptadecyl)-1,4,7,10-tetraazacyclododecane-1,4,7-triyl)triacetic acid (NH_2-PEG4-DOTA) from CheMatech (Dijon, France). The myc-tagged nanobody and affibody were kindly donated by collaborative partners.

4.5.2 Plasmid Construction for ESC11-Fab

Primers specific for the 5′ end of ESC11 VL (5′AGTGCACTTGAAACGACACTCACG CAGTCTCCAGGCA) and the 3′ end of ESC11 VH (5′ CTACCTCAGCGAAAAC TATAGACCCCGGTTCCCTGTTCCAGTGGCAG) were used to amplify the Fab VL-CL-VH sequence using the pCES1 ESC11-Fab DNA [218] as a template. The taq-amplified PCR product (REDTaq® DNA Polymerase, Sigma) was cloned into the pCR2.1™-TOPO vector (Invitrogen) and transformed into *E. coli* TOP10F′, after which blue/white screening was performed. Positive clones were verified by sequencing (Microsynth AG). *Sfi*I sites were introduced at the 5′ and 3′ ends of the Fab using a two-step PCR reaction. In the first step, HUVK5 and hujh3 primers [226] were used to introduce the 5′ *Sfi*I site. The PCR product was purified (illustra GFX PCR DNA and Gel Band Purification Kit, GE Healthcare) and used as a template for the second PCR step. Here, HUVK5 and c-3′fivh primers [226] were used to introduce the 3′ *Sfi*I site, after which the PCR product was cloned into pCR2.1™-TOPO vector as before. A *Sfi*I digest was performed to remove the ESC11-Fab insert, after which it was ligated into *Sfi*I-digested pC3C vector (a kind gift from Prof. C. Rader, NIH, USA) that had been engineered to include a myc/His6 tag. Clones were verified by sequencing.

4.5.3 Expression and Purification of ESC11-Fab

pC3C ESC11-Fab was transformed into *E. coli* Top10F′. Stationary overnight cultures were diluted 1:10 into fresh 2TY media, grown until an OD_{600} ~0.5 was reached and induced with 1 mM isopropyl β-D-1-thiogalactopyranoside (IPTG, Sigma). The protein was expressed for 20 h at 37 °C, 250 rpm, after which the cells were pelleted. The media containing the ESC11-Fab was removed, filtered and applied directly onto 2 mL CaptureSelect™ LC-Kappa agarose (Life Technologies) using a peristaltic pump at a flow rate of 1.5 mL/min. The resin was washed extensively with phosphate-buffered saline (PBS) before 0.5 mL fractions of ESC11-Fab were eluted with 0.1 M glycine pH 2.7 directly into neutralization buffer (1 M Tris-HCl pH 8) to achieve a final pH of ~7.4. Fractions were analyzed by SDS-PAGE and those containing ESC11-Fab were pooled and concentrated on a Vivaspin® 6 column (10 kDa MWCO, LuBio Science) prior to purification by size exclusion chromatography (SEC) on a Superdex 75 10/300 GL column (GE Healthcare), 0.5 mL/min flow. Fractions were analyzed by SDS-PAGE and those containing only ESC11-Fab were pooled and concentrated as before. LC-ESI-MS analysis was performed to establish the purity of the protein.

4.5.4 Enzymatic functionalization of recombinant proteins

Recombinant proteins were functionalized as previously described [198, 224]. Briefly, 6.6 µM protein in PBS was incubated with 80 molar equivalents of the corresponding amine-functionalized chemical entity and 6 U/mL MTGase for 16 h at 37 °C. Unless stated otherwise, excess substrate and the MTGase were removed by SEC on a Superdex 75 10/300 GL column, 0.5 mL/min flow.

4.5.5 Chemical functionalization of ESC11-Fab with a fluorescent dye

10 molar equivalents of Alexa Fluor® 488 NHS Ester (Life Technologies, 10 mg/mL stock in DMSO) were added to the ESC11-Fab (biotinylated and non-biotinylated, ~4.5 mg/mL in 100 mM sodium bicarbonate buffer pH 8.3) and incubated for 1 h at RT with vigorous shaking before the reaction mixture was purified on a NAP-5 column (GE Healthcare). The degree of labelling was determined on a

NanoPhotometer® P-Class (Implen GmbH, Munich, Germany) using the default settings for Alexa Fluor® 488 (on average 2 dyes per ESC11-Fab).

4.5.6 LC-ESI-MS analysis proteins

LC-MS analysis was performed on a Waters LCT Premier mass spectrometer. Samples were chromatographed on an Uptisphere 5BP1#15QS C18, 150 x 2 mm column (Interchim, Montluçon, France) heated to 40 °C using a linear gradient from 20 to 80% A in 20 min plus 5% solvent C (solvent A: acetonitrile + 0.1% formic acid, solvent B: water + 0.1% formic acid, solvent C: 2-propanol) at a flow rate of 0.5 mL/min. The eluent was ionized using an electrospray source. Data were collected with MassLynxV4.1 and deconvolution was performed using MaxEnt1.

4.5.7 Peptide mapping

The protocol for tryptic digestion was adapted from a previously published paper [227]. Briefly, to a solution of 6.6 nmol protein in 50 µL 50 mM ammonium bicarbonate pH 8.0 containing 0.1% Rapidgest SF (Waters Corp.) was added 0.96 µL 1 M dithiothreitol (DTT) and the mixture was incubated for 30 min at 55 °C. After the sample was cooled to room temperature (RT) 1.92 µL 1 M iodoacetamide (IAM) was added and the samples were incubated for 40 min at RT (protected from light). Sequencing grade modified trypsin (1:20 w/w ratio, Promega AG) was added and the protein was digested for 16 h at 37 °C. Prior to LC-ESI-MS measurement the samples were diluted 1:1 (v:v) with 1% formic acid in 10% acetonitrile (ACN). An auxiliary pump was used to spray a solution of 50 pmol/mL leucine enkephalin in 50/50 ACN/water containing 0.1% formic acid for mass accuracy (lockmass channel). The system was calibrated using a sodium formate infusion (0.05 M NaOH + 0.5% formic acid). The peptide mixture was then separated on a AerisPEPTIDE 3.6 µm XB-C18, 150 x 2.1 mm column (Phenomenex) heated to 80 °C using the following gradient: 0-5 min, 3% solvent A; 5-60 min, 3% to 45% solvent A; 60-65 min, 45% to 90% solvent A, 65-70 min, 90% to 3% solvent A (solvent A: acetonitrile + 0.1% formic acid, solvent B: water + 0.1% formic acid). Data were collected and analyzed with MassLynxV4.1.

4.5.8 Native gel of streptavidin-ESC11-Fab complex

Different molar ratios of streptavidin (Thermo) to biotinylated ESC11-Fab (1:1, 1:2, 1:3, 1:4, 1:5, 1:8) were incubated for 1.5 h at RT, an aliquot of the reaction mixture was subsequently loaded onto a native gel (7.5% polyacrylamide, pH 8.8, 160 V, 50 min) and the gel was then stained with Coomassie Brilliant Blue.

4.5.9 ESC11-Fab immobilization on a streptavidin coated surface and functionality test

100 µL of biotinylated ESC11-Fab (10 µg/mL) in reaction/wash buffer (25 mM Tris-HCl, 150 mM NaCl, pH 7.2, 0.1% BSA, 0.05% Tween20) was added to a streptavidin-coated 96-well plate (Reacti-Bind™-Streptavidin coated plate, Pierce, Thermo Scientific) and incubated for 2 h at RT, 220 rpm. The wells were washed three times with 200 µL wash buffer before incubation with 100 µL fibroblast activation protein (FAP, 5 µg/mL, Sigma) for 1 hour at RT, 220 rpm. The wells were washed three times with 200 µL wash buffer and subsequently incubated with 100 µL DQ™ Gelatin (0.1 mg/mL in PBS, Life Technologies) at 37 °C for 88 h. The fluorescent intensity was measured on a Multilabel Plate Reader (VICTOR™ X3, Perkin Elmer) using a preset protocol for fluorescein (485/535 nm, 0.1 s, bottom). The raw data was processed using GraphPad Prism 6.0 (GraphPad Software, San Diego, USA).

4.5.10 ESC11-Fab immobilization on avidin-coated micropatterns

Micropatterns were created as previously described [228]. Briefly, the clean patterned glass slides were incubated with 100 µg/mL nitrodopamine-mPEG (SuSoS AG, Dübendorf, Switzerland) in high salt MOPS buffer (100 mM 3-(*N*-morpholino)propane-sulfonic acid at pH 6, 600 mM NaCl and 600 mM K_2SO_4 readjusted to pH 6) for 4 h at 80 °C. After incubation, the samples were rinsed with ultrapure water before they were washed in HEPES buffer (10 mM (4-(2-hydroxyethyl)-1-piperazine-ethanesulfonic acid, 150 mM NaCl, pH 7.4) for 24 h at RT and gentle agitation to remove unbound PEG-polymer. The glass slides were rinsed with ultrapure water, dried with nitrogen and mounted in to a tailor-made microscopy cell where they were incubated with 40 µg/mL avidin (Sigma Aldrich) in tris-buffered saline buffer (TBS,

10 mM Tris(hydroxymethyl)aminomethane, 150 mM NaCl, pH 7.4) for 1 h at RT, washed with 10 mL TBS, incubated with 30 µg/mL biotinylated or non-biotinylated, Alexa Fluor® 488-conjugated ESC11-Fab and finally washed with 10 mL TBS. Images of the patterns were captured with a Leica SP5 confocal microscope and raw data was processed with ImageJ (NIH, USA).

4.5.11 Cell lines

All cell lines were kindly donated by Prof. C. Renner. Rheumatoid arthritis synovial fibroblasts (RASFs), melanoma cell line SK-Mel-187, fibrosarcoma cell line HT1080 (FAP-) and HT1080FAP (FAP+) were maintained in RPMI 1640 (Bioconcept). The liposarcoma cell line SW-872 was maintained in DMEM high glucose. Media was supplemented with 10% fetal calf serum (FCS), 2 mmol/L glutamine, 100 units/mL penicillin, 100 µg/mL streptomycin, and 0.25 µg/mL fungizone (BioConcept). In addition, 3% normal human serum (NHS, Millipore) and 1% non essential amino acids (NEAA, Bioconcept) were added to the media for RASFs and SW-872, respectively. The cells were maintained at 37 °C with 5% CO_2.

4.5.12 Fluorescence-activated cell sorting (FACS)

Cells were harvested with Accutase (Millipore), washed with 1% BSA-supplemented PBS (PBS/BSA) and incubated with ESC11-Fab or ESC11-Fab-ATTO-488™ (10 µg/mL, 1 µg/mL or 0.1 µg/mL) for 2 h at RT. Cells were washed on ice with PBS/BSA (3x 200 µL) and those treated with ESC11-Fab only were incubated with a goat anti-human IgG-FITC (1:200 dilution in PBS/BSA, Santa Cruz Biotechnology) for 30 min at 4 °C in the dark and washed as before. All cells were resuspended in 200 µL PBS/BSA and directly submitted to flow cytometry (Guava easyCyte™ Flow Cytometer, Merck Millipore). Data was analyzed with FlowJo software (TreeStar Inc.).

4.5.13 Fluorescence microscopy

Cells were seeded in Nunc™ 8-well Lab-Tek™ II Chamber Slides™ (Thermo Scientific) with a density of 5000 cells/well and allowed to attach overnight at 37 °C, 5% CO_2. The cells were washed with PBS (3x 400 µL), fixed with 400 µL of pre-warmed (37 °C) 4% paraformaldehyde for 15 min at 37 °C, washed with PBS (3x 400 µL), in-

cubated with 1 drop of ImageitFX (Invitrogen) for 30 min at RT, washed with PBS (3x 400 µL) and incubated with either ESC11-Fab-ATTO-488™ or ESC11-Fab-TAMRA (250 µL, 10 µg/mL in PBS/BSA) for 2 h at RT. The cells were then washed with ice-cold PBS (3x 400 µL), incubated with 250 µL 1 mM Hoechst 33342 for 10 min at RT and washed with deionized water (3x 400 µL). The media chamber was dismounted, slides were drained and dried with a tissue and the cells were covered with one drop of Prolong Gold (Invitrogen). The coverslip was sealed with nail polish and the slides were stored protected from light at 4 °C. Images were captured with a Zeiss Axiovert 200M microscope and raw data was processed with ImageJ (NIH, USA).

4.5.14 Radiolabeling

NH_2-PEG4-DOTA was enzymatically conjugated to the ESC11-Fab as described above. After 16 h incubation at 37 °C, MTGase activity was blocked by the addition of MTGase-blocker (500 µM final concentration, Zedira). The reaction mixture was buffer-exchanged into 0.5 M ammonium acetate (NH_4OAc) pH 5.5 using a Vivaspin® 6 column (10 kDa MWCO), radiolabelled with 1 MBq $^{111}InCl_3$ / µg ESC11-Fab-DOTA for 1 h at 37 °C after which it was purified by SEC on a Superdex 75 10/300GL column, 0.5 mL/min flow and the major peak fractions were pooled.

4.5.15 SPECT imaging

Animal studies were conducted in compliance with the Swiss laws on animal protection. All experiments were approved by the animal welfare commission of the cantons BS-BL-AG, Switzerland, and permitted by the local government (Departement Gesundheit und Soziales, Veterinärdienst des Kantons Aargau, Switzerland; permission number 75528). All efforts were made to minimize suffering. Housing and animal husbandry was conducted according to local law on animal protection.

Female CB17/Icr-Prkdc scid/Crl mice, 5 weeks old (Charles River, Sulzfeld, Germany) were inoculated subcutaneously (right shoulder) with $5x10^6$ liposarcoma cells SW-872 each and tumors were allowed to grow for 4 weeks before mice were randomly divided into two groups (n=4) and injected with ∼18 MBq ^{111}In-ESC11-Fab-DOTA (∼20 µg protein). SPECT/CT (NanoSPECT/CT, Bioscan Europe, Paris, France) imaging was performed 1 h and 24 h p.i.. The scans were acquired using

Nucline software (version 1.02, Bioscan, Inc.) and the data sets were analyzed with the InVivoScope post-processing software (version 2.0, Bioscan, Inc.).

4.5.16 Multimerization

The reaction conditions to generate homobifunctional Fab-fragments using copper-free click chemistry was adapted from a previously published procedure [112]. Briefly, 20 µM ESC11-Fab-PEG3-azide was reacted with 40 µM ESC11-Fab-PEG4-DBCO at RT or 37 °C. An aliquot of the reaction mixture was analyzed by SDS-PAGE (10% polyacrylamide) after 5 h incubation time.

4.5.17 Supported Lipid Bilayers

Production of liposomes:

Lipids 1-palmitoyl-2-oleoyl-sn-glycero-3-phosphocholine (POPC), 1,2-dioleoyl-*sn*-glycero-3-phosphoethanolamine-*N*-(4-(*p*-maleimidomethyl) cyclohexanecarboxy-amide) (PE-MCC) (Avanti Polar Lipids, USA) were mixed in the ratio of 10 mol% PE-MCC and 90 mol% POPC. The solvent was evaporated under a gentle stream of argon gas for 1 h to obtain a dried lipid film which was rehydrated with tris-buffered saline (TBS; 50 mM Tris(hydroxymethyl)aminomethane, 150 mM NaCl, pH 7.2) such that a final lipid concentration of 2 mg/ml was reached. The liposome suspension was then extruded 31 times through two polycarbonate filters (Avestin, Canada) with a pore size of 100 nm using a LiposoFast extruder (Avestin, Canada).

Quartz Crystal Microbalance with dissipation monitoring (QCM-D):

To investigate supported lipid bilayer functionalization a Q-Sense E4 quartz crystal microbalance with dissipation monitoring (QCM-D; Q-Sense AB, Sweden) was used. SiO_2-coated 4.95 MHz QCM-D crystals (Q-Sense AB, Sweden) were first sonicated for 20 min in toluene followed by sonication for 20 min in isopropanol. The crystals were then washed with Milli-Q water and blow-dried with nitrogen followed by exposure to UV/ozone for 30 min (UV/Ozone Procleaner, Bioforce Nanosciences, USA). All buffers were degassed prior to use and measurements were performed at 25 °C. A multichannel dispenser equipped with 0.51 mm tygon tubing (IPC Ismatec SA, Switzerland) was used to inject all the solutions. The measurement cell was rinsed with TBS pH 7.2 or 7.6 between all steps at a flow rate of 50 µL/min for 20 min. The cleaned crystals were mounted into the cells and the baseline was equilibrated

with TBS pH 7.2. Afterwards, a liposome solution (100 µg/mL) was injected at a flow rate of 376 µL/min for 30 s followed by 10 µL/min for 50 min. The lipid bilayer was then exposed to the lysine-containing peptide (168 µM in TBS 7.2, Ac-FKGGERCG-NH_2, Genscript, United States) for 50 min (10 µL/min). Unreacted maleimides were quenched with 5 mM β-mercaptoethanol (Sigma Aldrich, Switzerland) for 5 min. The buffer was then changed to TBS pH 7.6 for the enzymatic immobilization of the ESC11-Fab. The peptide-modified SLB was exposed to a mix of MTGase (0.2 units/mL) and to ESC11-Fab (50 µg/mL) at a flow rate of 376 µL/min for 30 s and then 10 µL/min for 50 min. The stock mixture of ESC11-Fab and MTGase was kept on ice to avoid deamination of the reactive glutamine. The represented graphs are measured at the 5^{th} overtone (f5$\approx$25 MHz).

5

In Vitro and *In Vivo* Characterization of Targeted Non-Covalent Antibody-Z-Domain Conjugates

Adapted from

Patrick Dennler, Ivo Grgic, Roger Schibli, and Eliane Fischer. "*In Vitro* and *In Vivo* Characterization of Targeted Non-Covalent Antibody-Z-Domain Conjugates". Sumbitted to *J. Controlled Release*

Authors contribution

Patrick Dennler designed and carried out experiments and wrote the paper, Ivo Grgic (Master student) performed experiment under the supervision of Patrick Dennler, Eliane Fischer worked on the manuscript

5.1 Abstract

Immunoglobulin Fc binding domains (FcBDs) are small proteins that can interact with antibodies to form non-covalent conjugates which have been extensively used for a variety of *in vitro* applications including targeted delivery of proteins, fluorescent dyes or toxins. However, only a few reports describe the *in vivo* application of such conjugates. In this study we aimed to investigate the *in vitro* and *in vivo* stability of the Z-domain (ZD), a synthetic FcBD, and the ZZ-domain (ZZD), an FcBD dimer of the ZD, by means of radiolabeling with ^{111}In for quantitative assessment of their biodistribution and to evaluate their targeting capacity by SPECT imaging. ZD ($\sim$8.5 kDa) and ZZD ($\sim$15.6 kDa) could be easily expressed in *E.coli*, purified, modified with a DOTA chelator for radiolabeling and refolded properly after being heated to 90 °C for 30 min. While the ZZD promoted crosslinking when incubated with antibodies (IgG1), the ZD formed defined antibody conjugates with a ZD-to-IgG ratio of two. When incubated with the anti-L1CAM antibody chCE7, the binding to L1CAM-expressing ovarian carcinoma cells was not influenced by the bound ZD. Assessment of the plasma stability showed significant interspecies variation. The conjugates were stable in human plasma for at least 72 h, while partial instability was observed in rat plasma and no intact conjugate could be found in mouse plasma after 72 hours. *In vivo* SPECT imaging revealed that the non-covalent conjugate was unstable in both BALB/c and tumor-bearing CD1/nu mice. The major fraction of the injected radioactivity accumulated in the kidneys, which indicates that the domain dissociates from the antibody. Our qualitative and quantitative studies indicate that non-covalent ZD-IgG1 conjugates are not sufficiently stable in rodent plasma for targeted delivery of diagnostic or therapeutic cargos in mouse models. Further investigation and development of the ZD and eventually other FcBDs is required in order to discover novel domains that overcome the reported limitations.

5.2 Introduction

Antibody conjugates are entities that combine the targeting properties of a larger biomolecule and the effector functions of a smaller moiety. *In vivo* applications of such bioconjugates predominantly include optical and nuclear imaging, radioimmunotherapy or targeted delivery of cytotoxic payloads for the treatment of

cancer [32]. Dyes, chelating systems and toxins have all been attached to antibodies in order to generate immunoconjugates that can be used for the aforementioned applications. Current conjugation approaches to link these functionalities to the immunoglobulin include chemical conjugation *via* amino acids or (chemo)enzymatic approaches [21, 108, 109]. Small domains that bind non-covalently to antibodies represent an alternative methodology since they can be exploited as versatile adaptor molecules and thus, covalent modification of the antibody is no longer a prerequisite. The general high stability of these immunoglobulin Fc binding domains (FcBD) allows the use of harsher modification conditions. Moreover, the fact that they bind to a conserved sequence in the antibody backbone means that they form a complex with any given antibody of the same isotype. A widely used FcBD is the Z-domain (ZD), an analog of the subdomain B of *Staphylococcal* protein A [122, 229, 230]. The ZD is a three-helix bundle that binds to the Fc of IgGs with a high affinity [231, 232]. Interestingly, the binding affinity could be increased tenfold from a K_d of $\sim$17 nM to $\sim$1.5 nM by using the domain in a dimeric form, designated as ZZ-domain (ZZD) [229].

Both domains have been employed for antibody purification since they exhibit improved properties with respect to antibody yield and purity [233, 234]. Furthermore, mutated variants of the ZD allow milder elution conditions *i.e.,* antibody elution at pH 4.5 instead of pH 3.3 [235]. Beyond that, the ZD and ZZD have been exploited for a variety of other *in vitro* applications. Fusion proteins of the ZZD with fluorescent proteins, enzymes and various bait proteins were used for enzyme-linked immunosorbent assays (ELISA), immunofluorescence microscopy, flow cytometry and pull-down assays [134, 236–238]. Kurata *et al*. genetically fused enhanced green fluorescence protein (EGFP) to the C-terminus and the ZZD to the N-terminus of the L protein, a hepatitis B virus surface antigen that is used to form bionanocapsules (BNCs). Simple incubation of the ZZD-BNC-EGFP with an anti-epidermal growth factor receptor (EGFR) antibody yielded antibody displaying BNCs that could specifically deliver EGFP to HeLa cells *in vitro* and therefore demonstrated its importance as a tool for targeted protein delivery [125]. The same strategy was adapted by Iijima and co-workers and revolutionized the simultaneous detection of multiple antigens in Western blot, immunocytochemistry and flow cytometric analysis [126]. Furthermore, they used the same approach to create immunosensor

chips with enhanced sensitivity as well as to evaluate and visualize the orientation of immobilized antibodies [127, 128, 239].

In vivo applications of pre-formed non-covalent antibody conjugates, in particular *in vitro* formed complexes between antibodies and ZDs or ZZDs, are rare. Different research groups have exploited FcBDs to extend the plasma half-life of proteins. By fusing FcBDs to various proteins, which are usually cleared quickly, they were able to increase their residence time in circulation. This effect relies on the non-covalent, reversible binding of the fusion protein to antibodies that are present in the blood of the mice [222, 240, 241]. The aforementioned method to use particles which are decorated with FcBDs for the targeted delivery of *e.g.,* proteins or dyes has also been employed for *in vivo* purposes [129, 242]. Nevertheless, Benhar and co-workers were the first to exploit FcBDs as cargo molecules for *in vivo* applications. They fused the ZZD to *Pseudomonas* exotoxin A, designated as ZZD-PE38, and generated non-covalent IgG conjugates *in vitro* that were subsequently injected into mice for targeted drug delivery to a tumor site [130–132]. Despite the promising results of this cancer therapy, little is known about the *in vivo* stability of such non-covalent immunoconjugates where the FcBD is not immobilized on a particle but acts as an adaptor molecule on its own.

In the present study, we characterize non-covalent antibody conjugates consisting of an IgG1 and the ZD / ZZD (Table 5.1) *in vitro* and *in vivo* by radiolabeling the domains with ^{111}In. To minimize the influence of the chelator on the interaction of the domains and the antibody, we adapted a site-specific enzymatic protein modification technology that has been developed in our group [198]. Therefore, a glutamine-containing peptide sequence (c-myc-tag, EQKLISEEDL) was attached at the C-terminus of the domains serving as a unique conjugation site for the chelating system. The domains were then radiolabeled, mixed with antibodies (IgG1) to yield a radioactive non-covalent antibody conjugate and their *in vitro* and *in vivo* properties were evaluated (Figure 5.1).

Tab. 5.1.: Amino acid sequence of the different FcBDs used in this work. Bold: ZD sequence, Astericks: Site of chelator attachment. [a]C-terminal cysteine (CTC)

Domain	Amino acids sequence
ZZD	A Q H D E A **V D N K F N K E Q Q N A F Y E I L H L P N L N E E Q R N A F I Q S L K D D P S Q S A N L L A E A K K L N D A Q A P K V D N K F N K E Q Q N A F Y E I L H L P N L N E E Q R N A F I Q S L K D D P S Q S A N L L A E A K K L N D A Q A P K** V D A N S E Q* K L I S E E D L
ZD	G S **V D N K F N K E Q Q N A F Y E I L H L P N L N E E Q R N A F I Q S L K D D P S Q S A N L L A E A K K L N D A Q A P K** V I E S R E Q* K L I S E E D L
CTC-ZD[a]	G S **V D N K F N K E Q Q N A F Y E I L H L P N L N E E Q R N A F I Q S L K D D P S Q S A N L L A E A K K L N D A Q A P K** C*

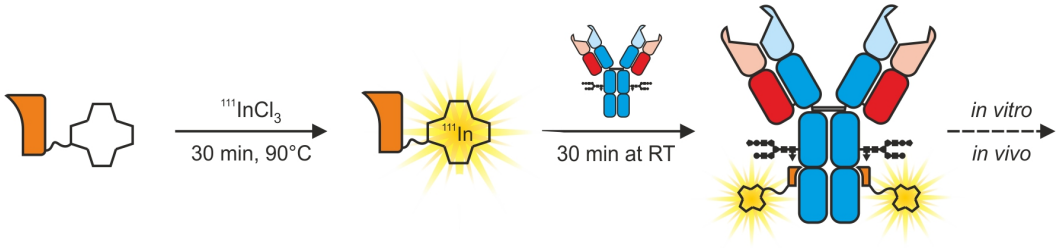

Fig. 5.1.: Schematic representation of the work-flow to generate radiolabeled non-covalent antibody conjguate. The FcBD (orange) is site-specifically modified with a chelating system. Labeling of the domain with $^{111}InCl_3$ and subsequent incubation with an antibody yields the radioactive non-covalent antibody conjugate that can be used for *in vitro* and *in vivo* experiments.

5.3 Material and Methods

5.3.1 General

The anti-L1CAM antibody chCE7 (chimeric IgG1 isotype) was produced in-house. The control antibody (chimeric IgG1 isotype) was kindly donated by collaborative partners. Unless stated otherwise, raw data was processed using GraphPad Prism 6.0 (GraphPad Software, San Diego, USA).

5.3.2 Construction of Z-Domains (ZDs)

The DNA encoding the various ZDs was synthesized by GeneArt. *Bam*HI and *Eco*RI restriction sites were added at the 5' and 3' ends, respectively, for directional

cloning into the bacterial expression vector pGEX-2T (GE Healthcare) downstream of glutathione S-transferase (GST).

5.3.3 Expression and purification of ZDs

The vector containing the GST-ZD fusion was transformed into the *E. coli* strain BL21. Stationary overnight cultures were diluted 1:40 into LB/Amp, grown until an OD_{600} ~0.5 was reached and induced with 1 mM Isopropyl β-D-1-thiogalactopyranoside (IPTG, Sigma). The protein was expressed for 18 h at 37 °C, 220 rpm. The cells were pelleted, resuspended in ice-cold phosphate buffered saline (PBS; 140 mM NaCl, 2.7 mM KCl, 10 mM Na_2HPO_4, 1.8 mM KH_2PO_4, pH 7.4) and lysed using a Sonifier® (30% duty cycle, 30-40 output, 15 min, Branson Ultrasonics, USA). Cell debris were pelleted, the supernatant was filtered and incubated with glutathione sepharose beads (GE Healthcare) for 2 h at RT using gentle agitation. The beads were transferred into a column, washed with PBS and the fusion protein was eluted with 50 mM Tris-HCl, 10 mM reduced glutathione, pH 8.0. Fractions were analyzed by SDS-PAGE (12.5% polyacrylamide) and those containing the protein of interest were pooled and concentrated on a Vivaspin® 6 column (10 kDa MWCO, LuBio Science). The concentrated fraction was rebuffered into PBS using a PD10 column (GE Healthcare) and the GST was cleaved from the ZD by the incubation with 100 U of thrombin (GE Healthcare) for 18 h at RT using gentle agitation. The cleaved protein mixture was applied onto IgG sepharose beads (GE Healthcare), washed with Tris-saline Tween 20 (TST; 50 mM Tris buffer, pH 7.6, 150 mM NaCl and 0.05% Tween 20) and the ZZD was eluted from the beads with 0.5 M acetic acid pH 3.4 (adjusted with 1 M ammonium acetate). Fractions were analyzed by SDS-PAGE (16% tricine [243]) and those containing the cleaved ZD were pooled and lyophilized.

5.3.4 Construction of a c-myc-tagged ZZ-Domain (ZZD)

Two oligonucleotides (5' CGG AAT TCG GAA CAA AAA CTC ATC TCA GAA GAG GAT CTG and 5' ATT CCC AAG CTT TTA TTA CAG ATC CTC TTC) were used in an overlap extension PCR to generate the DNA sequence for the c-myc-tag flanked by 5' *Eco*RI and 3' *Hind*III sites and to introduce a stop codon. The PCR product was *Eco*RI / *Hind*III digested, purified (illustra GFX PCR DNA and Gel Band Purification

Kit, GE Healthcare) and ligated into the *Eco*RI / *Hind*III- digested pEZZ-18 vector (GE Healthcare) to yield pEZZ-18-c-myc-tag.

5.3.5 Expression and purification of ZZD

The vector pEZZ-18-c-myc-tag was transformed into the *E. coli* strain HB101. Stationary overnight cultures were diluted 1:100 into TYE/Amp (30 g/L tryptic soy broth, 5 g/L yeast extract) and the protein was expressed for 18 h at 37 °C, 250 rpm. The cells were pelleted and the supernatant was decanted and filtered before purification. The supernatant was then applied onto IgG sepharose beads (GE Healthcare) and the domain was purified as described above. Fractions were analyzed by SDS-PAGE (15% polyacrylamide) and those containing the ZZD were pooled and directly lyophilized.

5.3.6 Site-specific enzymatic functionalization of domains

The domains were enzymatically functionalized on the terminal c-myc-tag with 2,2',2"-(10-(1-amino-19-carboxy-16-oxo-3,6,9,12-tetraoxa-15-azanonadecan-19-yl)-1,4,7,10-tetraazacyclododecane-1,4,7-triyl)triacetic acid (NH_2-PEG4-DOTA-GA) (CheMatech, Dijon, France) by microbial transglutaminase (MTGase, Zedira, Darmstadt) as previously reported [198]. Briefly, domain in PBS (0.5 mg/mL, 58.8 µM) was incubated with 80 molar equivalents of NH_2-PEG4-DOTA-GA and 3 U/mL MTGase for 18 hours at 37 °C. Excess NH_2-PEG4-DOTA-GA and MTGase were removed by purifying the domain-PEG4-DOTA-GA on IgG sepharose beads as described above.

5.3.7 Chemical functionalization of C-terminal cysteine Z-domain (CTC-ZD)

The chemical conjugation of maleimide-NODA-GA (CheMatech, Dijon, France) to CTC-ZD was performed according to a previously published procedure [244]. Briefly, CTC-ZD (5 mg/mL) was incubated with 30 mM dithiothreitol (DTT) for 2 h at 40 °C and subsequently rebuffered into 0.2 M ammonium acetate pH 6.5 using a NAP-5 column (GE Healthcare). The reduced CTC-ZD was incubated with 3 molar equivalents of maleimide-NODA-GA for 4 h at 40 °C after which excess of chelator

was removed by NAP-5 column rebuffering into 0.5 M ammonium acetate buffer pH 5.5 (buffer for radiolabeling).

5.3.8 LC-MS analysis

LC-MS analysis was performed on a Waters LCT Premier mass spectrometer (Waters Corp., Millford, USA). Samples were chromatographed on an Uptisphere BP1 column (50 µm, 150 mm x 2 mm; Interchim, Montluçon, France) heated to 40 °C using a linear gradient starting from 2.5 % A, 95 % B and 2.5 % C changing to 52.5 % A, 45 % B and 2.5 % C in 10 min at a flow rate of 0.5 mL/min (solvent A, 0.1 % formic acid in acetonitrile, solvent B, 0.1 % formic acid in water, solvent C, isopropanol). The eluent was ionised using an electrospray source in the positive ionisiation mode (ESI+). Data were collected with MassLynx V4.1 and deconvolution of the raw data was performed using MaxEnt1.

5.3.9 Circular dichroism (CD)

CD spectra (200 to 280 nm) of ZD-PEG4-DOTA-GA (20 µM) in PBS were recorded on a Chirascan spectropolarimeter (Applied Photophysics, UK) with a 0.1 cm path length. The first set of spectra was recorded at 20 °C (baseline) after which the protein was heated to 90 °C for 30 min, cooled to 20 °C, and a second data set acquired.

5.3.10 Multi Angle Light Scattering (MALS) of ZZD-IgG complexes

ZZD-PEG4-DOTA-GA was incubated with the IgG (3:1 molar ratio) for 30 min at RT and 100 µg of the non-covalent complex was injected onto a Superdex 200 10/300GL column (GE Healthcare), 0.5 mL/min PBS flow, coupled to a TriStar MiniDawn light scattering detector and an Optilab Rex refractometer (Wyatt Technology).

5.3.11 Radiolabeling of ZD-PEG4-DOTA-GA and non-covalent conjugate formation

The domain-PEG4-DOTA-GA (2 mg/mL) in 0.5 M ammonium acetate buffer pH 5.5 was incubated with 4 MBq/µg $^{111}InCl_3$ (Mallinckrodt Pharmaceuticals) for 30 min at 90 °C. The reaction mixture was quenched with EDTA (5 mM final concentration)

and washed three times with PBS using an Amicon® Ultra 4 mL centrifugal filter (3 kDa MWCO, EMD Millipore) after which 3 molar equivalents of ^{111}In-domain-PEG4-DOTA-GA were incubated with the antibody for 30 min at RT. The radioactive complex was separated from unbound ^{111}In-domain-PEG4-DOTA-GA by size exclusion chromatography (SEC) on a Superdex 200 10/300 GL, 0.75 mL/min PBS flow, and the major peak fractions were collected and pooled.

5.3.12 Cell binding assay

Human ovarian cancer cells (1x10^5 IGROV cells) were incubated with a dilution series of radioactive complex ranging from 67 nM to 30 pM for 2.5 h at 37 °C, 200 rpm. The cells were washed three times with PBS and subsequently measured in a gamma counter. Non-specific binding was assessed by co-incubation of the radioactive conjugate with 6.7 µM native chCE7.

5.3.13 Plasma stability

Murine, rat and human plasma were depleted of antibodies by incubation with a mixture of protein A and protein G sepharose for 16 h at 4 °C. The radioactive complex was added to non-depleted and depleted plasma (20 kBq/µL plasma) and incubated for 72 h at 37 °C. Aliquots of plasma (50 µL) were injected onto an analytical SEC column (TSKgel G3000$_{SWXL}$, Tosoh Bioscience, 1 mL/min 0.3 M NaCl, 0.05 M NaH_2PO_4, pH 6.2) at 24 h intervals.

5.3.14 *In vivo* SPECT imaging

Animal studies were conducted in compliance with the Swiss laws on animal protection. All experiments were approved by the animal welfare commission of the cantons BS-BL-AG, Switzerland, and permitted by the local government (Departement Gesundheit und Soziales, Veterinärdienst des Kantons Aargau, Switzerland; permission number 75528). All efforts were made to minimize suffering. Housing and animal husbandry was conducted according to local laws on animal protection.

Female CD1/nu mice were injected subcutaneously with 7x10^6 SK-OV-3ip ovarian cancer cells and tumors were allowed to grow for 20 days before ∼3.5-4.5 MBq ^{111}In-domain-PEG4-DOTA-GA-IgG1 (∼30-40 µg) was injected i.v. in the tail vein

and SPECT data was acquired 1 h, 24 h and 48 h p.i. For blocking experiments, a 10-fold molar excess of IgG1 was co injected. BALB/c mice were injected i.v. with ∼3.5 MBq ^{111}In-domain-PEG4-DOTA-GA-IgG1 (∼30 µg) and SPECT data was acquired 1 h and 24 h p.i. A hybrid SPECT/CT with a four-head multi-pinhole camera (Nanospect/CT Plus, Bioscan) was used for *in vivo* imaging. The scans of anesthetized mice (Isoflurane, Provet AG, Lyssach) were acquired for 25 to 35 min. The raw data was reconstructed with HiSPECT software (v1.2.3049, Scivics GmbH). Fused SPECT/CT images were analyzed with Vivoquant 1.23 (Invicro).

5.4 Results

5.4.1 Expression and *in vitro* characterization of the ZD and the ZZD

While the ZZD could directly be purified from the supernatant using IgG sepharose, the ZD was, due to its smaller size, expressed as a GST-fusion. The fusion protein was purified using glutathione sepharose after which the GST was cleaved from the ZD by thrombin. In a second step, the cleaved ZD was separated from the enzyme and GST using IgG sepharose. Both the direct one-step purification of the ZZD and the two-step purification approach resulted in highly pure domains (>95% by SDS-PAGE, Figure 5.2A-C) with a yield of ∼3 mg/L. The mass of the ZD (expected: 8554 Da, found: 8554 Da) and the ZZD (expected: 15586 Da, found 15585 Da found) was confirmed by mass spectrometry. Furthermore, the congruent CD-spectrum of the domains after heating to 90 °C for 30 min demonstrates their high thermal stability *i.e.,* their ability to refold properly after being completely denatured (Figure 5.2D and F). The ZD formed defined non-covalent conjugates within 30 min when incubated with an IgG1, indicated by a small decrease in retention time when analyzed by SEC. Moreover, by incubating the same amount of IgG (15 µM) with increasing molar equivalents of ZD (1.5 to 45 µM), it could be demonstrated that the non-covalent IgG-ZD conjugate consists of one antibody and two ZDs (Figure 5.2E). Conversely, the UV peak of the ZZD-IgG complex exhibited a shift towards the range where high molecular weight species (>200 kDa) would elute. MALS analysis of the reaction mixture revealed that the protein species were not composed of a single antibody with two ZZDs (∼180 kDa). Molecular masses of ∼380 kDa and bigger

indicated that two or more antibodies were crosslinked by the ZZD. The second peak in the chromatogram can be assigned to unbound domain deriving from the excess of ZZD that has been used (Figure 5.2G). Based on these results, the ZZD was not used for *in vivo* experiments.

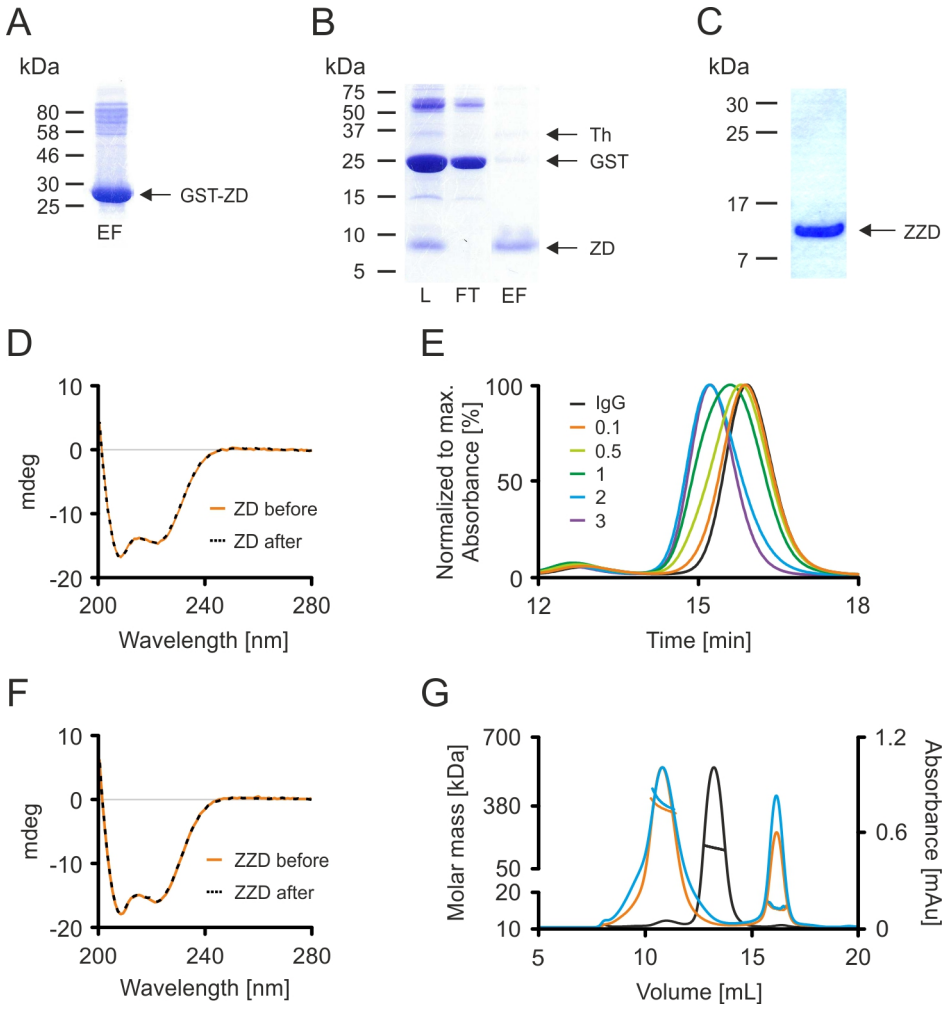

Fig. 5.2.: *In vitro* characterization of the domains. A) 12.5% polyacrylamide SDS-PAGE analysis of the GST-ZD fusion protein (eluted fraction, EF) after GST purification. B) 16% tricine SDS-PAGE analysis of the IgG purification process (after thrombin cleavage of GST-ZD). Protein bands were visualized by staining the gels with Coomassie Blue. Load [L]: protein mixture after thrombin cleavage, Flow-through [FT]: containing non-bound GST and thrombin [Th], eluted fraction [EF]: containing the highly pure, cleaved ZD. C) 15% polyacrylamide SDS-PAGE analysis of purified ZZD. D) CD spectra of ZD before (orange) and after (black, dashed) exposure to 90 °C for 30 min. E) SEC analysis of antibody that was pre-incubated with different molar equivalents of the ZD (0.1-3 molar equivalents). The antibody alone (IgG, black) was injected as a reference. F) CD spectra of ZZD before (orange) and after (black, dashed) exposure to 90 °C for 30 min. G) MALS analysis of chCE7 (black), ZZD-chCE7 (orange) and ZZD-control IgG (cyan). The lines under the UV peaks indicate the molar mass.

The ZD was then enzymatically modified with NH_2-PEG4-DOTA-GA by MTGase. Mass spectrometric analysis revealed a relative mass shift that corresponds to

exactly one chelator indicating that the ZD was site-specifically modified at its C-terminus on the c-myc-tag (Figure 5.3A). The radiolabeled ZD was buffer-exchanged, subsequently incubated with the antibody (chCE7 or control antibody) and yielded non-covalent antibody conjugates with a specific activity of ∼0.1 MBq/µg after SEC purification. Moreover, we successfully employed the labeled ZD to form non-covalent radioactive conjugates with different antibodies of the same subtype under the same conditions (Figure 5.3B). The immunoreactivity of the antibody conjugate was assessed with a cell-binding assay on human ovarian cancer cells and the K_d was determined to be 2.3 nM (Figure 5.3C).

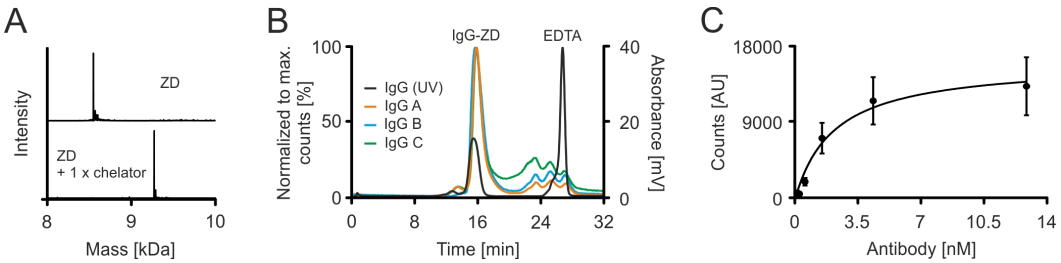

Fig. 5.3.: *In vitro* evaluation of the ZD and the corresponding radioactive ZD-IgG conjugate. A) Deconvoluted mass spectra of ZD before (top spectrum) and after (bottom spectrum) enzymatic modification with NH_2-PEG4-DOTA-GA. B) Radioactivity and traces of labelled ZD-IgG conjugate with different IgGs (orange, cyan and green). The black trace represents the corresponding UV signal of IgG A. C) Saturation binding curve of the purified, active ZD-IgG1 conjugate to determine its immunoreactivity.

5.4.2 Plasma stability of the ZD-chCE7 conjugate and *in vivo* SPECT imaging

To test the plasma stability, samples of plasma containing the radioactive ZD-IgG conjugate were subjected to size-exclusion chromatography and traced by a radiodetector. The non-covalent antibody conjugates were stable in human plasma for at least 72 h at 37 °C since no degradation product of smaller size or aggregation product of larger size could be detected by analytical SEC. The retention time of the radioactive peak corresponds to a molecular size of ∼160 kDa, which could derive from either the intact ZD-IgG conjugate or ZD that dissociated from the parent IgG and interacts with an IgG from the plasma. However, no difference was observed between the stability in non-depleted or IgG-depleted plasma which indicates that the ZD interacts exclusively with chCE7 (Figure 5.4A and Figure C.1, supplementary material). Analysis in rat plasma revealed a radioactivity pattern that remained constant over time, indicating that a fraction of the conjugate was stable

for 72 h at 37 °C. However, a broad second activity peak could be detected that most likely derive from ZD that has dissociated from the antibody (Figure 5.4B and Figure C.2, supplementary material). On the contrary, ZD-IgG conjugates were not stable in murine plasma since time-dependent appearance of radioactive species with a lower molecular weight (corresponding to a longer retention time on the SEC column) could be observed for all conjugates (Figure 5.4C and Figure C.3, supplementary material).

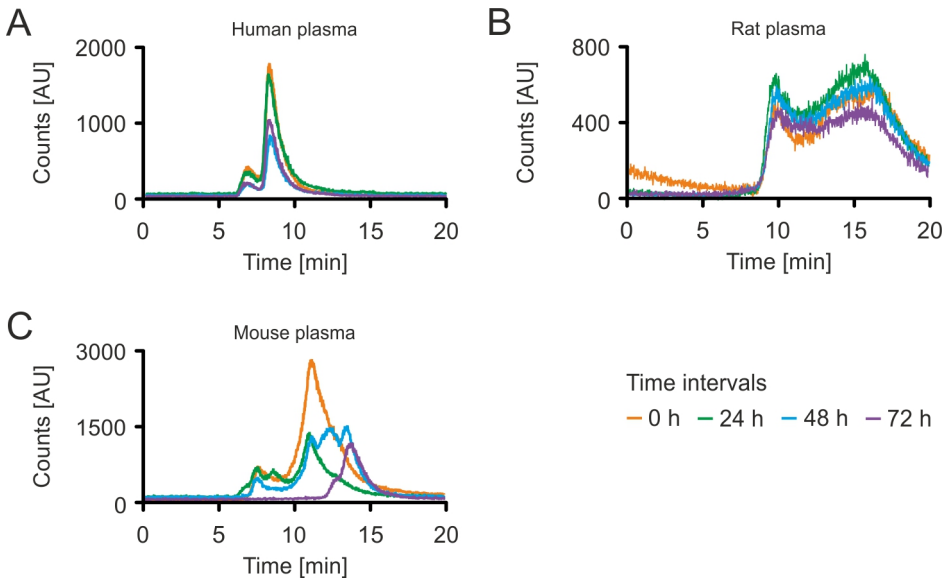

Fig. 5.4.: Representative (here: ZD-chCE7, non-depleted plasma) radioactivity trace of analytical SEC to evaluate the time dependent stability of the non-covalent antibody conjugate in A) human, B) rat and C) mouse plasma. The first peak in the rat plasma trace (around 10 min) corresponds to the ZD-IgG conjugate

The *in vivo* properties of the tumor targeting ZD-chCE7 conjugate were evaluated in tumor-bearing CD1/nu mice. Time-dependent SPECT data revealed that the major fraction of the activity was localized in the kidneys after one hour while only a minor amount of activity could be detected in the tumor (Figure 5.5A and B). Furthermore, comparison between the biodistribution of ZD-chCE7 and ZD-control IgG conjugates revealed that the tumor uptake of ZD-chCE7 was not specific and that both conjugates behaved in a similar manner since equivalent levels of radioactivity could be detected in the corresponding tissues (Figure 5.5C). To ascertain whether the ZD would dissociate from the parent antibody (chCE7) and bind to other antibodies present in the circulation of the mouse we injected BALB/c mice, a mouse strain that has higher antibody titers compared to athymic CD1/nu mice, with the ZD-chCE7 conjugate. Aside from a slightly higher activity in the

blood pool after 1 hour, there was no difference between the two strains. The major fraction of the radioactivity could again be found in the kidneys shortly after injection (Figure 5.6A).

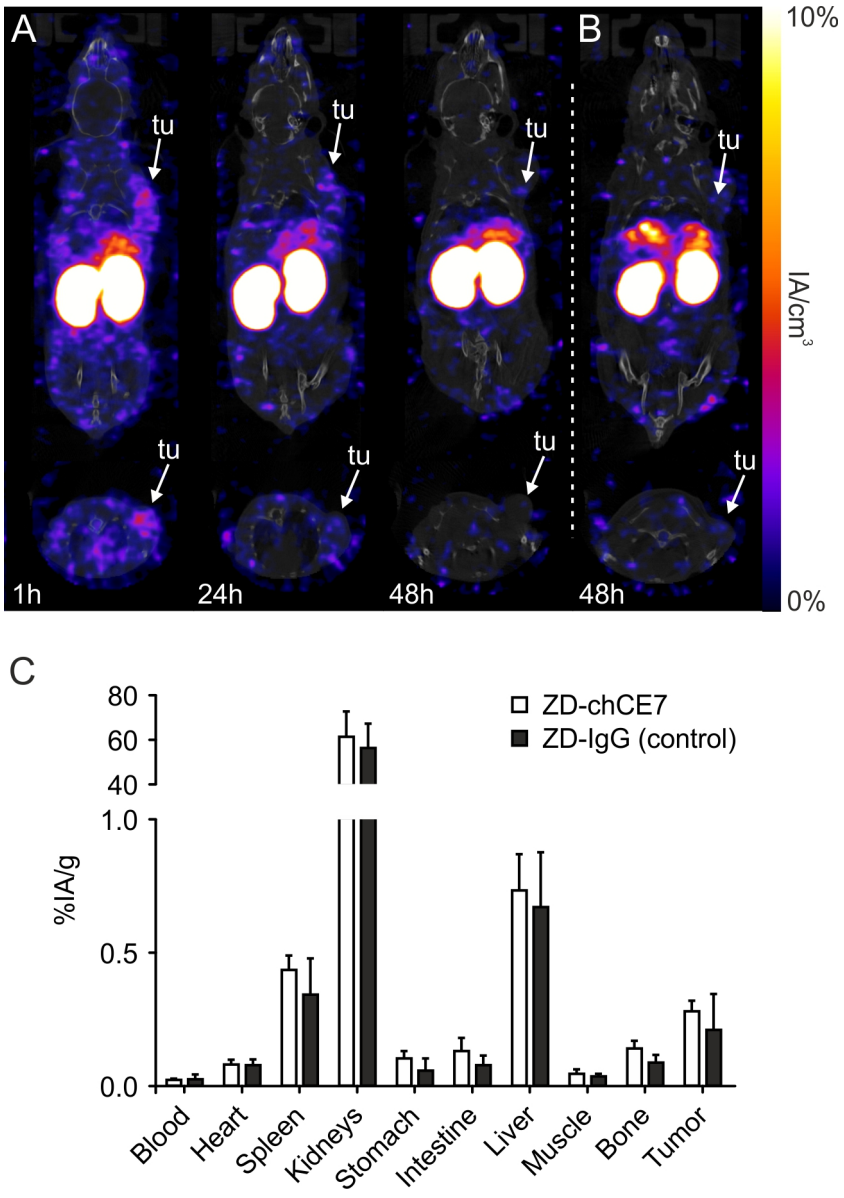

Fig. 5.5.: *In vivo* SPECT imaging of the non-covalent ZD-IgG conjugate and biodistribution study. A) Time dependent SPECT images of radiolabeled ZD-chCE7 and B) ZD-IgG (control antibody) in SK-OV-3ip tumor-bearing CD1/nu mice (tu, right shoulder). C) Biodistribution of ZD-chCE7 and ZD-IgG (control antibody) in SK-OV-3ip tumor-bearing CD1/nu mice, n=4

5.4.3 Generation and *in vivo* application of the C-terminal cysteine ZD derivative (CTC-ZD)

It was then tested whether the enzymatic conjugation strategy could be the problem for the unexpected instability of the antibody conjugate. For this reason, the

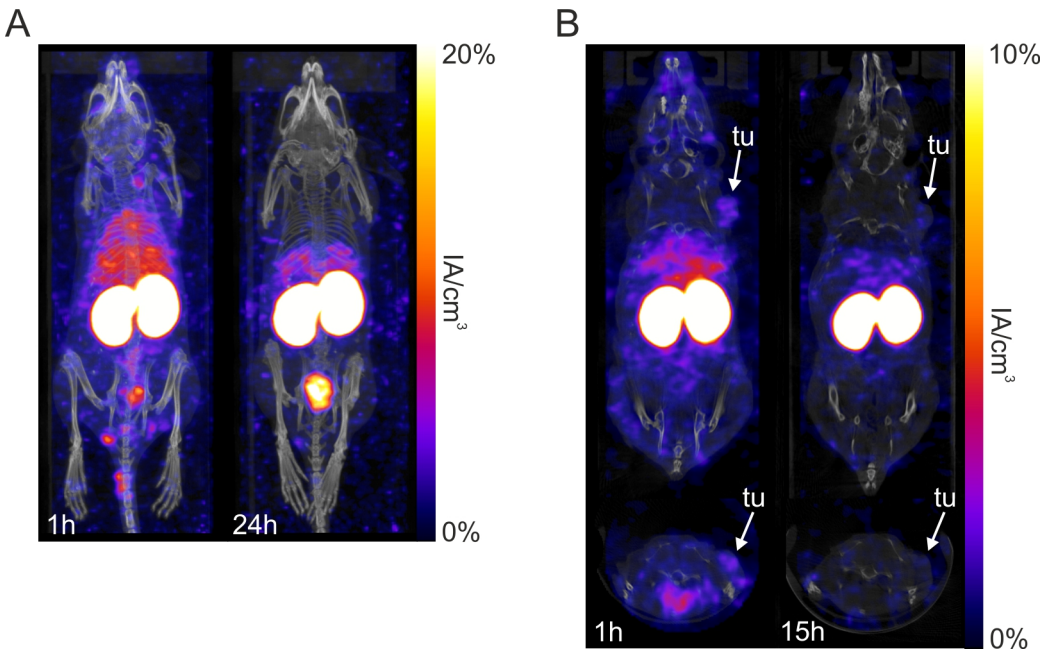

Fig. 5.6.: A) Time dependent *in vivo* SPECT imaging of a BALB/c mouse injected with radiolabeled ZD-chCE7 conjugate. B) Time dependent *in vivo* SPECT imaging of radiolabeled CTC-ZD-chCE7 in SK-OV-3ip tumor-bearing CD1/nu mice (tu, right shoulder).

C-terminal c-myc-tag on the ZD was replaced with a cysteine residue suitable for maleimide-thiol chemistry. Expression and purification of the CTC-ZD worked in the same manner as for the ZD (data not shown). The chemical modification at the terminal cysteine was very efficient (>95% reaction yield, Figure C.4, supplementary material) and non-covalent antibody conjugates with a specific activity of ∼0.3 MBq/µg after SEC purification could be generated. Nevertheless, *in vivo* SPECT imaging of tumor-bearing CD1/nu mice showed no difference compared to the antibody conjugates including the c-myc-tagged ZD. Again, the major fraction of the injected activity was located in the kidneys shortly after administration and did not get cleared from the mouse (Figure 5.6B).

5.5 Discussion

Using FcBDs to form non-covalent antibody conjugates is a powerful alternative to conventional approaches that form covalent bonds between the immunoglobulin and a given substrate because (i) it does not require any pre-modification of the antibody backbone *e.g.,* addition of amino acids or deglycosylation and (ii) the robustness of FcBDs allows the application of harsher reaction conditions which could be advantageous for *e.g.,* radiolabeling. Furthermore, their recombinant

expression in *E.coli* is rapid, cost-effective and the domains can be used to form a conjugate with any given antibody of the same isotype. The encouraging results reported by Mazor *et al.*, where they used a non-covalent ZZD-antibody conjugate and successfully delivered toxicity to a tumor site *in vivo*, suggest that the ZZD-IgG interaction is, in contrast to the ZD-IgG interaction, stable in the mouse circulation [131, 132]. However, the results of our *in vitro* studies indicate that the ZZD cannot be used as an adapter molecule on its own. We found clear evidence that the ZZD promoted antibody crosslinking *in vitro* and did not yield defined conjugates but higher molecular weight species. The higher apparent affinity of the ZZD can therefore be attributed to the avidity effect from bivalent binding to the Fc domains of two separate antibodies. This phenomenon has not been described in the literature so far, most likely because the ZZD was either immobilized on a surface or fused to another protein as for example the bulky PE38 protein, thereby preventing the interaction of the second ZD with another IgG by steric hindrance.

On the other hand, incubation of the ZD with antibodies resulted in the formation of defined non-covalent conjugates with a ZD-to-IgG ratio of two, the binding affinity of the antibody to its antigen was not impaired and the conjugate was stable in human plasma for at least 72 h. Nevertheless, we observed rapid accumulation of the radioactivity in the kidneys when injected into tumor-bearing mice, indicating that the activity was no longer attached to the antibody. If the ZD would remain bound to the antibody, we would expect the major fraction to accumulate in the tumor ($\sim$30% IA/g), some activity in the blood pool ($\sim$10% IA/g) but only very low levels of activity in the kidneys ($\sim$3-4% IA/g) [245, 246]. It is unlikely that *in vivo* degradation of the bond between the chelating system and the domain is the reason for this observation since the cysteine-variant of the ZD exhibited the same properties. We would expect a rapid clearance from the body *via* the kidneys if the chelator was separated from the domain, which was not the case. Instead, the biodistribution profile resembles the profile of an affibody, a protein scaffold that was developed based on the ZD [247], where the majority of the injected radiolableled protein is located in the kidneys shortly after injection (>60% IA/g) [244, 248]. Therefore, we hypothesize that the ZD dissociates from the antibody once injected into the mouse circulation and as a consequence, we monitor the *in vivo* behaviour of the domain and not of the conjugate.

Furthermore, comparison between the *in vitro* stability experiments in human, rat and mouse plasma clearly demonstrated that the stability of the ZD-IgG conjugate varies between different species. Whereas it seems to be stable in human and rat plasma, time-dependent disappearance of the radioactive conjugate peak could be observed in mouse plasma. Although the resolution of the SEC column is not sufficient to state whether the observed degradation products correspond to the entire ZD, fragments thereof or a mixture of both, the results support our hypothesis that the affinity of the ZD towards the Fc is not sufficient for *in vivo* studies in mice. However, the concept of having a flexible and robust adaptor molecule that can be employed to readily generate stable non-covalent antibody conjugates with any given antibody of the same subtype for *in vivo* studies remains highly interesting and many disciplines may profit from such a platform. Therefore, the ZD and eventually other FcBDs should be further investigated and evolved to discover novel domains that will exhibit improved properties with respect to *in vivo* stability in mice.

6

Conclusion and Outlook

In this thesis, MTGase-based bioconjugation strategies have been developed and successfully employed to prove their value as tools for site-specific protein modification. We have expanded the range of potential applications and demonstrated that our MTGase-mediated technology could contribute to improve the quality of antibody conjugates such as ADCs. Our novel generic bioconjugation platform allow us to readily modify virtually any given c-myc-tagged protein with various functionalities and is therefore of interest for many scientific disciplines including biotechnology, material sciences and medicine.

In addition, we have investigated the *in vivo* stability of non-covalent ZD-antibody conjugates and could show that they suffer from instability when injected into mice. However, the advantages of using such small domains as flexible adaptor molecules are obvious: (i) The robustness of the domains enables us to apply harsher reaction conditions for modification with different functionalities. This could also open the door to use chemistry that cannot be employed with antibodies. (ii) The domains are easy and cheap to produce. Additionally, functionalized domains could be stored as ready-to-use batches and consequently any given antibody of the same subtype could readily be modified. (iii) Based on the aforementioned aspects and in combination with our c-myc-tag-based conjugation platform, the domains display an adapter molecule with unmatched versatility and flexibility for the generation of antibody conjugates. It is therefore important to further evolve the ZD and investigate other FcBDs in order to find novel domains whose interaction with antibodies exhibit improved *in vivo* stability. Even though the hurdle towards clinical applications of such conjugates might be too high, they would represent a powerful tool for pre-clinical research including *in vivo* evaluation of novel antibodies.

Throughout the entire thesis, we used MTGase to modify glutamine residues on proteins with primary amine-functionalized substrates but it is also possible to target lysine residues on proteins and use MTGase to attach glutamine-mimicking derivatives [182]. However, it is difficult to accomplish high conjugation yields by using this approach because water and alcohols can act as a nucleophile and might compete with the primary amine during the MTGase-catalyzed reaction process, leading to deamidation and esterification of the glutamine residue (Figure 1.8) [158, 175]. Using an excess of amine substrate diminishes these side reactions and eventually leads to quantitative modification of the corresponding glutamine residue

on the protein, as shown in this thesis. On the contrary, it is obvious that the same approach does not apply if the primary amine *i.e.,* lysine residue on the protein is supposed to be modified with a glutamine-derivatized substrate. Mutagenesis of the enzyme to alter its properties might be a valuable strategy to overcome the discussed limitations of MTGase [249–251].

Unlike other protein modification approaches, MTGase-based bioconjugation cannot be used to screen different conjugation sites. Its restriction to specific glutamines prohibits the possibility of genetically incorporating acyl-donors at other positions in the sequence of a given protein. However, it is exactly this feature that makes MTGase such an attractive bioconjugation tool because it enables us to use the enzyme for site-specific modification of proteins. Furthermore, numerous functionalities can be attached to proteins because the enzyme exhibits broad acyl-acceptor substrates specificity. The value of this enzymatic protein modification strategy could be expanded by developing a flow-based approach where MTGase is immobilized on a solid support, similar to the recently presented work of Policarpo *et al.* [214]. Such a system could help to circumvent current shortcomings with regard to acyl-acceptor substrates *i.e.,* low reaction yields and potentially opens the door to a new area of MTGase-suitable functionalities. Besides which, the removal of the enzyme after the reaction would become redundant and thus bioconjugation processes could be simplified and streamlined.

Product homogeneity has become an indispensable prerequisite for therapeutic bioconjugates, in particular for ADCs. While some years ago, chemical conjugation approaches yielded heterogeneous ADCs with respect to both the drug-to-antibody ratio (DAR) and the site of drug attachment, a variety of novel chemical, enzymatic and chemoenzymatic bioconjugation strategies have been developed with the aim to overcome product heterogeneity. We have successfully established a chemoenzymatic MTGase-based approach to generate highly active homogeneous ADCs. In contrast to other site-specific strategies, our method is advantageous since (i) it does not require genetic engineering rearrangement of the antibody sequence, (ii) it does not require reestablishment of expression conditions and (iii) it is highly efficient and requires only a minimal excess of toxin. This means that virtually every IgG1 and IgG4, once deglycosylated, can be directly transformed into a homogeneous ADC by employing our MTGase-based technology.

In collaboration with Innate Pharma, we could demonstrate the impact of product homogeneity on pharmacokinetics, efficiency and safety by directly comparing our homogeneous ADC to Adcetris®, a heterogeneous ADC that is in clinical use (article in press). While we observed equal antitumor efficacy, the maximum tolerated dose in rats was significantly higher for the homogeneous ADC. Our results on this matter are in agreement with published work [18, 45]. The fact that others observed the same trend regarding toxicological properties of ADCs, even though they used a different conjugation approach *i.e.,* attachment of the toxin *via* engineered cysteines or non-canonical amino acids, indicates the general validity of these findings for ADCs. The increasing number of novel approaches that are developed to site-specifically attach toxins to antibodies clearly demonstrates that only homogeneous ADCs will have the potential to become clinically relevant in the future. At the same time, homogeneity is only one piece of the puzzle towards next-generation ADCs. It is as important to review the huge amount of available data from various conjugation strategies and benefit from the findings in order to understand the influence of different parameters on the performance of ADCs *e.g.,* linker properties, toxin characteristics or species in which the ADCs is evaluated. We observed that the same ADC can exhibit varying stability profiles when tested in plasma of different species. Strop et al. reported similar findings indicating that the choice of an appropriate *in vivo* model for pre-clinical evaluation of novel ADCs is crucial [187].

Although nowadays, protein conjugation techniques are directly associated with the term 'site-specificity', it is important to note that not all bioconjugates require site-specific modification. It is, without a doubt, crucial for therapeutic conjugates but chemical conjugation methods that target for example lysines are often sufficient for conjugates that are used on a daily basis in the laboratory. Nevertheless, it can also be beneficial to site-specifically modify these proteins at a location distant from its functional site because the chance that random chemical modification will impair its biological activity increases with decreasing protein size. Another advantage is that site-specifically modified proteins can be, for example, immobilized on surfaces in an oriented manner to increase the sensitivity of biosensors [219, 252].

Our MTGase-based platform targeting the terminal c-myc-tag on proteins is perfectly suited for such applications. This, however, also applies for other site-specific bio-

conjugation approaches *e.g.,* addition of terminal cysteine residues, non-canonical amino acids or other tag-based strategies. The key advantage of our bioconjugation platform is that it targets the c-myc-tag. Lead candidates that derive from antibody discovery platforms *e.g.,* phage display libraries, usually require recloning before their *in vitro* and *in vivo* characteristics can be evaluated. This includes the transformation of the antibody-like protein into another protein scaffold *e.g.,* scFv into Fab-fragment or full length antibody or the introduction of a site for modification *e.g.,* engineered amino acids or tags. The c-myc-tag, however, is a widely used detection tag and thus, often pre-integrated in vector systems of display libraries [217]. This enables us to site-specifically functionalize potential candidates immediately after they have been selected. Potential candidates can be tested and then further selected before they are eventually recloned into their final scaffold. Moreover, the resulting conjugates are, in comparison to random chemical modification, homogeneous with respect to both the site of modification and the payload, which allows a direct comparison of their characteristics.

A

Supporting Information: A Transglutaminase-Based Chemo-Enzymatic Conjugation Approach Yields Homogeneous Antibody-Drug Conjugates

Tab. A.1.: Different reaction conditions and yields for the deacetylation of protected C6-thiol

Stock solution	**NH_2OH/mAb**	**Final pH / temp / inc. time**
0.5 M NH_2OH, 25mM EDTA	10% v/v	7.7 / RT / 2-6h
		8.0 / RT / 2-6h
		8.3 / RT / 2-6h
		7.7 / 37 °C / 2-6h
		7.9 / 37 °C / 2-6h
		8.2 / 37 °C / 2-6h
	20% v/v	8.8 / RT / 2 h
	40% v/v	8.8 / RT / 2 h

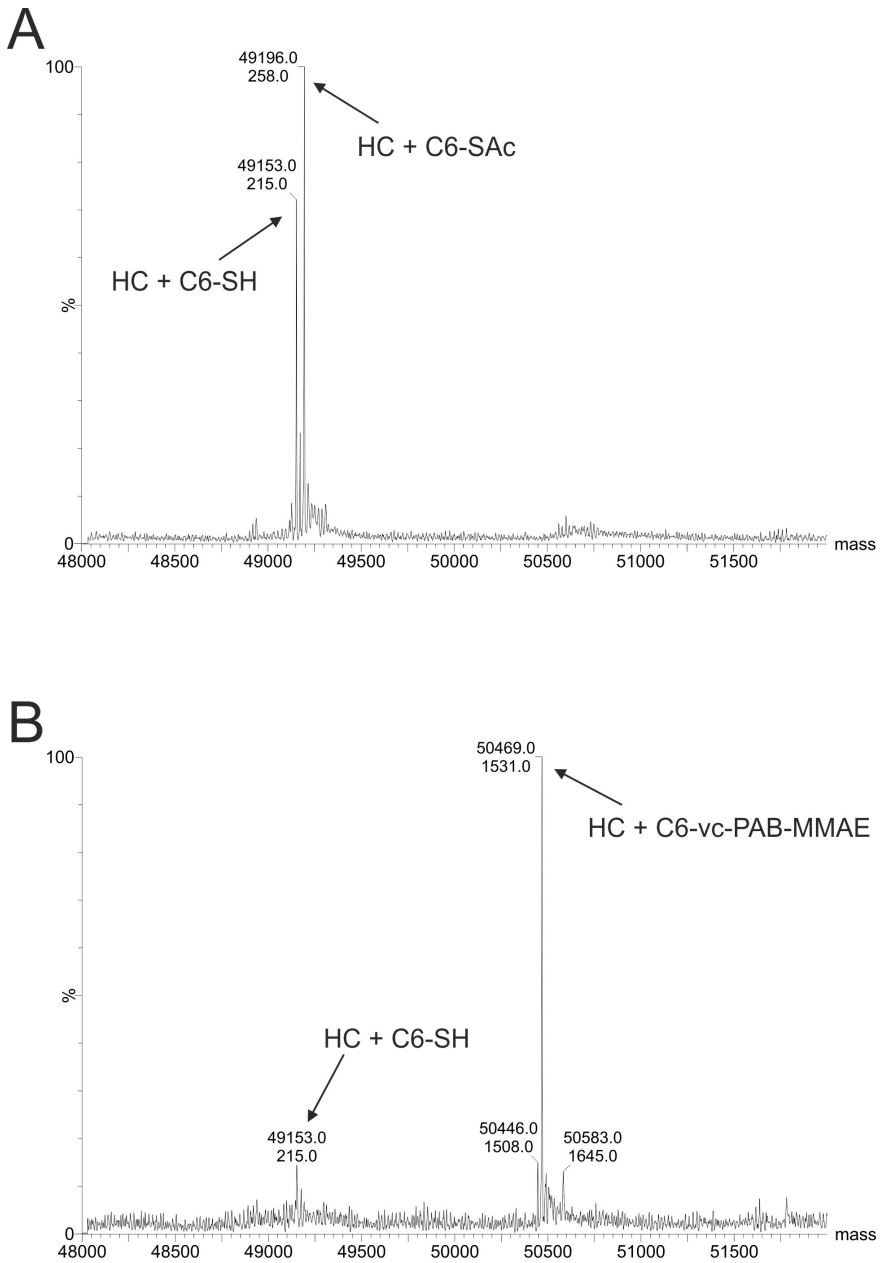

Fig. A.1.: A) Deconvoluted mass spectra of heavy chain (HC) after the enzymatic conjugation of C6-SAc linker by MTGase. Peaks are labelled with the mass (top) and relative mass shift (bottom) to unmodified, deglycosylated HC (48938 Da). Whereas the second mass peak corresponds to the desired intermediate product (mass shift = 258 Da; 274 Da [molecular weight of C6-SAc linker] - 17 Da [ammonia] = 257 Da), the first mass peak corresponds to deprotected HC + deprotected C6-SAc (mass shift = 215 Da; 274 Da [molecular weight of C6-SAc linker] - 17 Da [ammonia] - 42 Da [protection group] = 215 Da). This partial deprotection can be attributed to basic conditions during sample preparation. B) Deconvoluted mass spectra of HC after the chemical reaction of HC + C6-SH with maleimide-vc-PAB-MMAE. Peaks are labelled with the mass (top) and relative mass shift (bottom) to unmodified, deglycosylated HC (48938 Da). The first peak corresponds to unreacted HC + C6-SH (mass shift = 215 Da; 274 Da [molecular weight of C6-SAc linker] - 17 Da [ammonia] - 42 Da [protection group] = 215 Da). The second (major) peak corresponds to the desired product HC + C6-vc- PAB-MMAE (relative mass shift to starting material (HC + C6-SH) = 1316 Da; 1315 Da [molecular weight of maleimide-vc-PAB-MMAE])

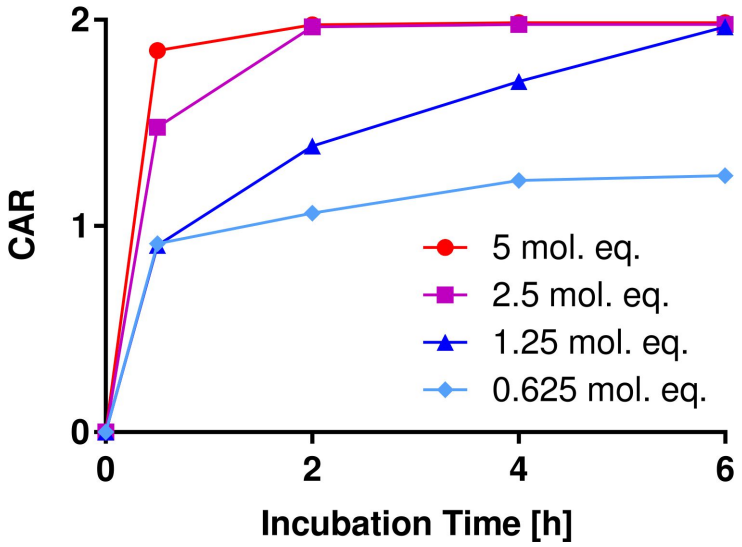

Fig. A.2.: Chemical entity-to-antibody ratios (CAR) of SPAAC with decreasing molar equivalents of DBCO-amine after different incubation intervals. Quantitative yield with a minimum of 1.25 molar equivalents DBCO-amine per azide group could be accomplished after 6 hours incubation time at RT. The reactions with 2.5 and 5 molar equivalents reached the plateau after 2 hours incubation time at RT. The control reaction with a limiting amount of DBCO-amine yielded a CAR of 1.2. This results excludes any technical error.

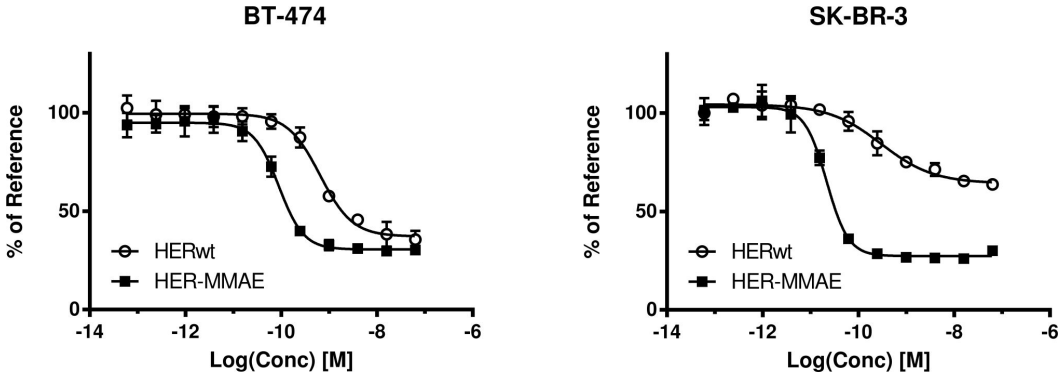

Fig. A.3.: Effect of wild-type trastuzumab (Herceptin®, HERwt) and trastuzumab-MMAE (HER-MMAE) on BT-474 and SK-BR-3 proliferation.

B

Supporting Information: Microbial Transglutaminase and c-myc-Tag: A Strong Couple for the Functionalization of Antibody-Like Protein Scaffolds from Discovery Platforms

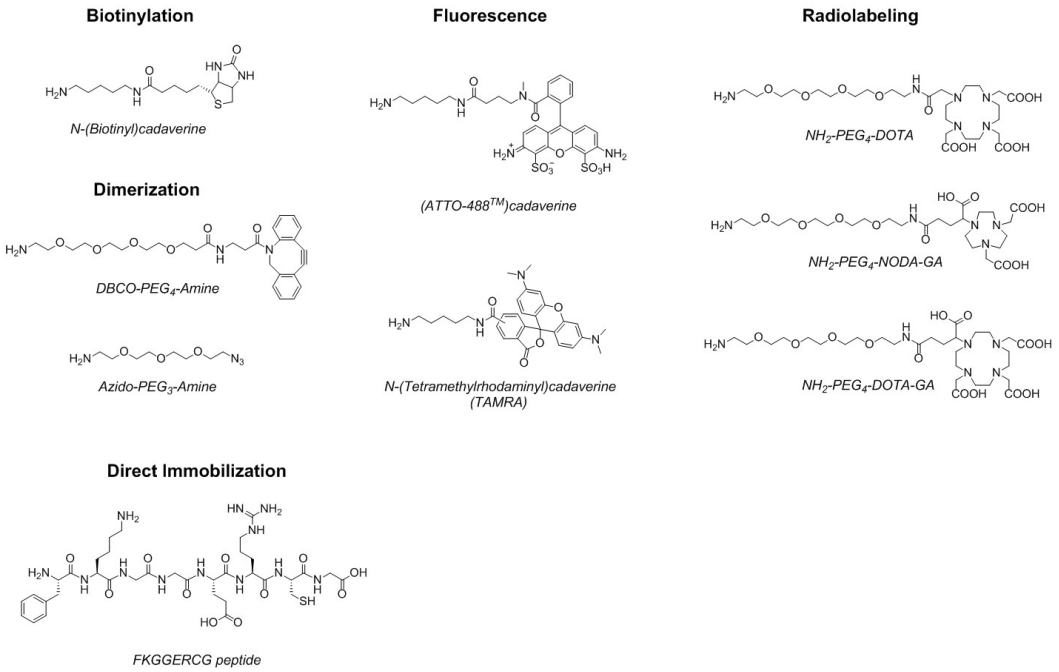

Fig. B.1.: Chemical structures of different functionalities (primary amine donors) that have been used for enzymatic modification of c-myc-tagged proteins.

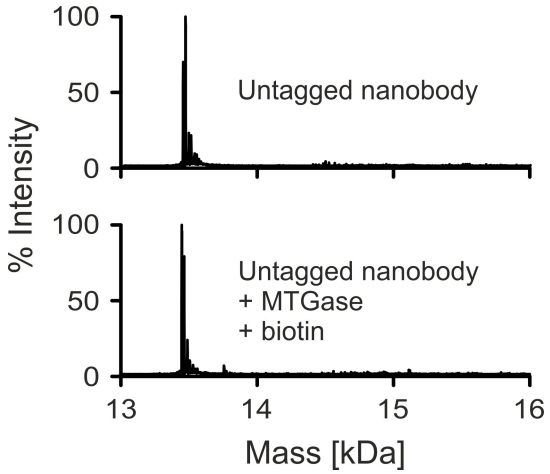

Fig. B.2.: Deconvoluted mass spectra of non-c-myc-tagged (untagged) nanobody before and after MTGase-mediated bioconjutation with biotin. No modification could be observed.

Tab. B.1.: Calculated and observed masses of *N*-(Biotinyl)cadaverine modified peptides that could be identified by peptide mapping. The corresponding donor glutamines (Q) are indicated by asterisks.

Protein	Peptide	Mass (calculated)	Mass (found)
Affibody	TPTGQGTQVTVSSAAAAEQ*K	2171.0891	2171.0613
Nanobody	VDANSEQ*K	1200.5808	1200.5671

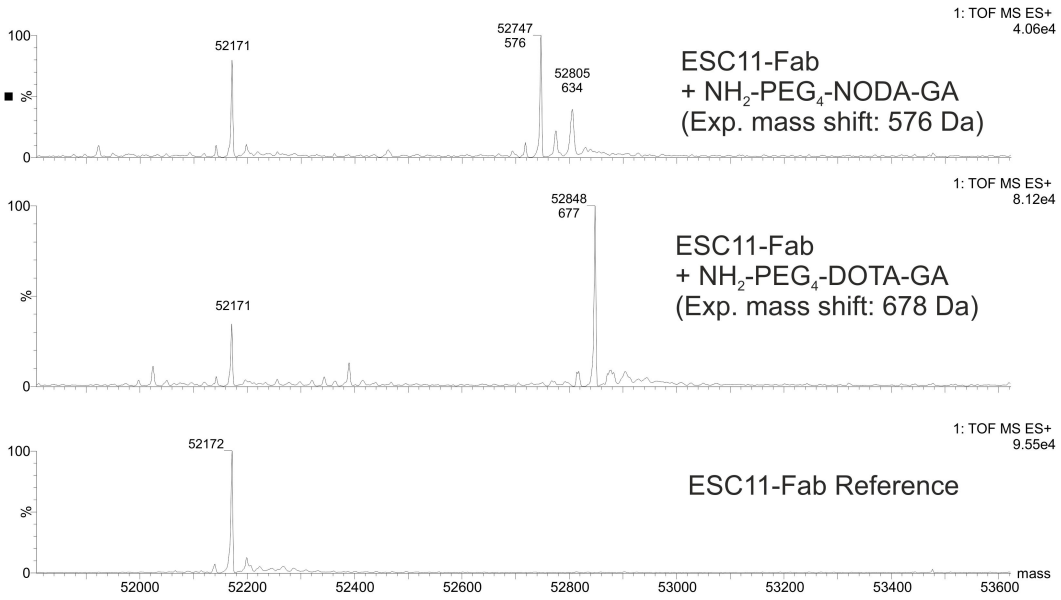

Fig. B.3.: Deconvoluted mass spectra of different chelators conjugated to the ESC11-Fab. Relative mass shifts in relation to the unmodified ESC11-Fab (reference) are indicated below the peak mass.

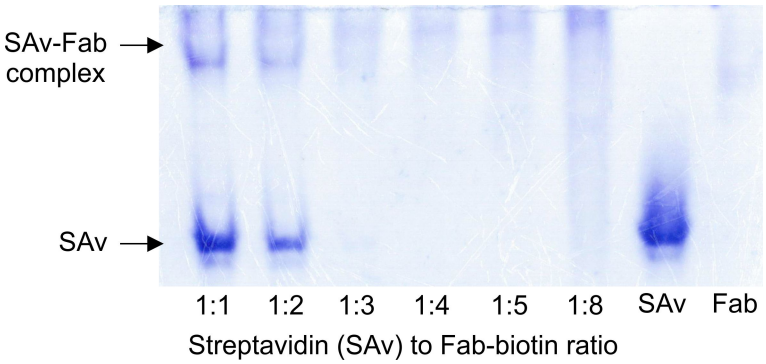

Fig. B.4.: Multimerization of biotinylated ESC11-Fab with recombinant streptavidin (SAv). Different molar ratios of Fab fragment with SAv were incubated to monitor the formation of tetramers by native PAGE. The formation of the tetramer can indirectly be monitored by the disappearance of the SAv. Since the isoelectric point of the Fab is nearly the same as the pH of the gel, it does not migrate into the gel. Therefore, the SAv-Fab complex (top band) disappears with increased Fab-loading.

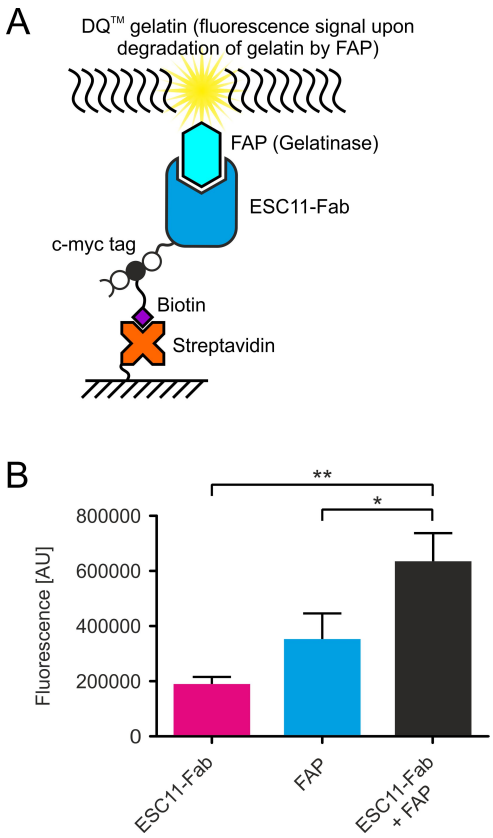

Fig. B.5.: A) Schematic setup of experiments to test the ability of biotinylated immobilized ESC11-Fab to bind to its antigen FAP. B) Functionality test of biotinylated ESC11-Fab (anti-FAP Fab) that is immobilized on a streptavidin coated surface (here 96-well plate).

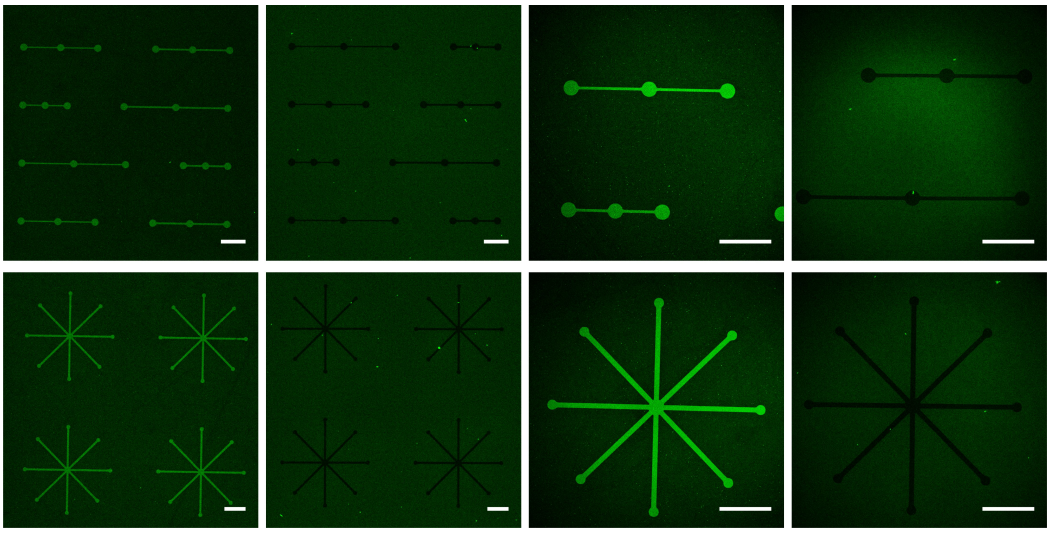

Fig. B.6.: Specific immobilization of Alexa Fluor® 488 labeled ESC11-Fab (green) and Alexa Fluor® 488 labeled, non-biotinylated ESC11-Fab (negative control, black) on avidin-coated micropatterns. Scale bar: 50 µm

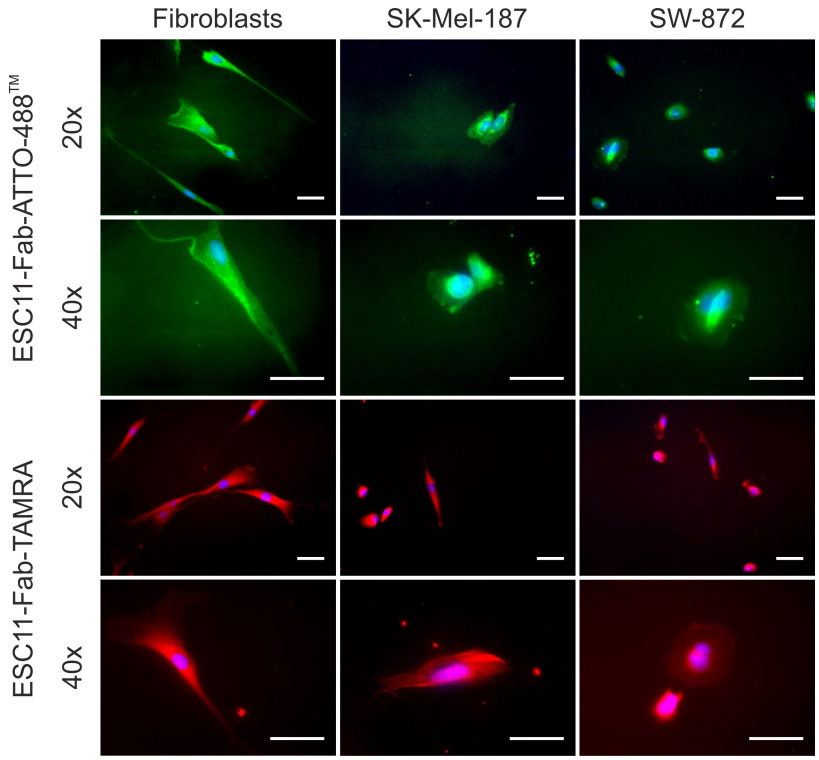

Fig. B.7.: Direct immunofluorescence staining of different FAP+ cells with ESC11-Fab-ATTO-488™ (green), ESC11-Fab-TAMRA (red) and Hoechst 33342 to visualize the cell nucleus (blue). Scale bar: 50 µm

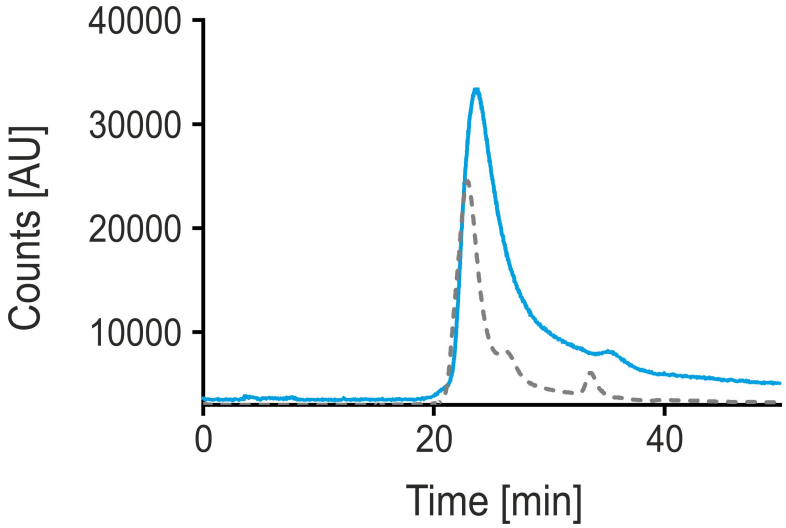

Fig. B.8.: SEC trace (cyan: counts; gray dashed line: UV trace as reference) after radiolabeling ESC11-Fab-DOTA with $^{111}InCl_3$.

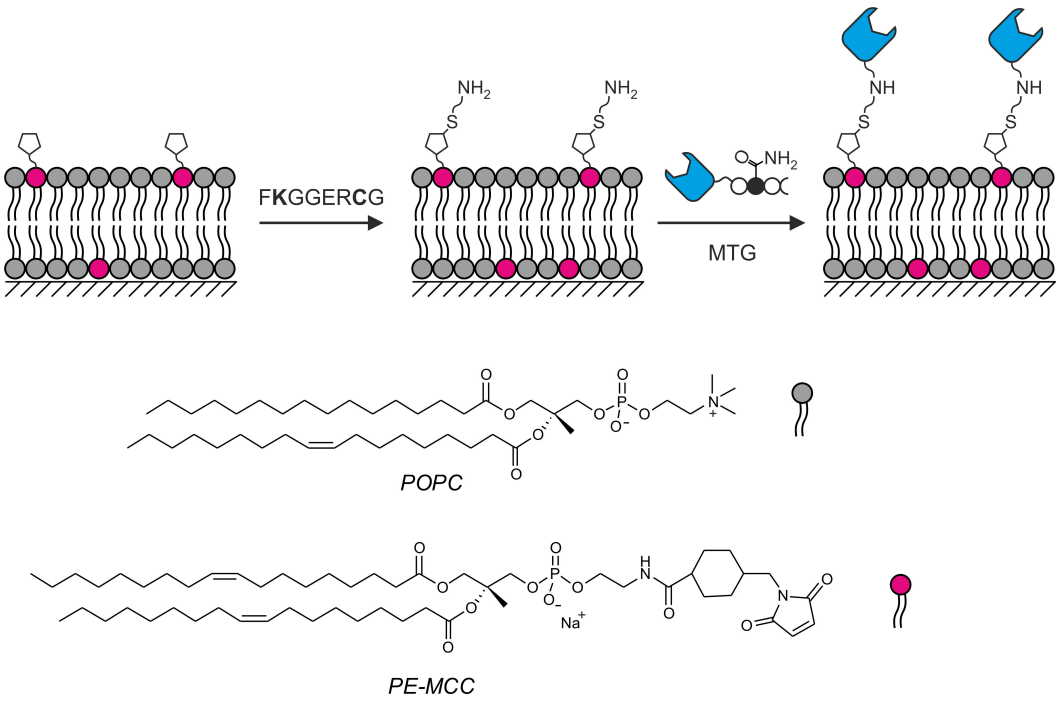

Fig. B.9.: Schematic procedure of the direct immobilization of ESC11-Fab onto supported lipid bilayers (SLBs). Thiol-reactive functionalities have been integrated into the lipid bilayer by using maleimide-functionalized phospholipids (PE-MCC) in combination with phosphocholine lipids (POPC). The octapeptide FKGGERCG (Cysteine reacts with maleimide) has been used to functionalize the surface with lysine residues that act as primary amine donors for the transglutaminase-catalyzed crosslinking reaction of the c-myc-tag and the surface.

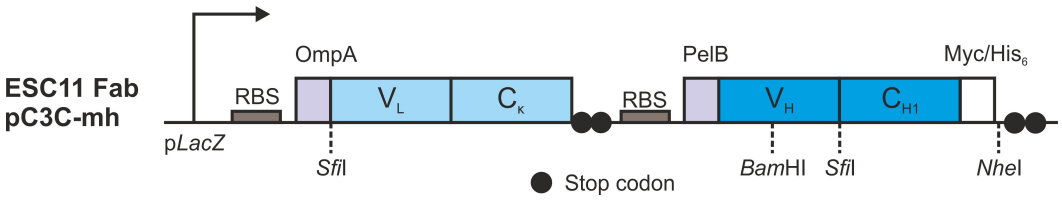

Fig. B.10.: Vector construction for bacterial expression of the c-myc-tagged ESC11-Fab fragment. The c-myc-tagged ESC11-Fab was cloned into a bicistronic vector (pC3C) suitable for bacterial expression.

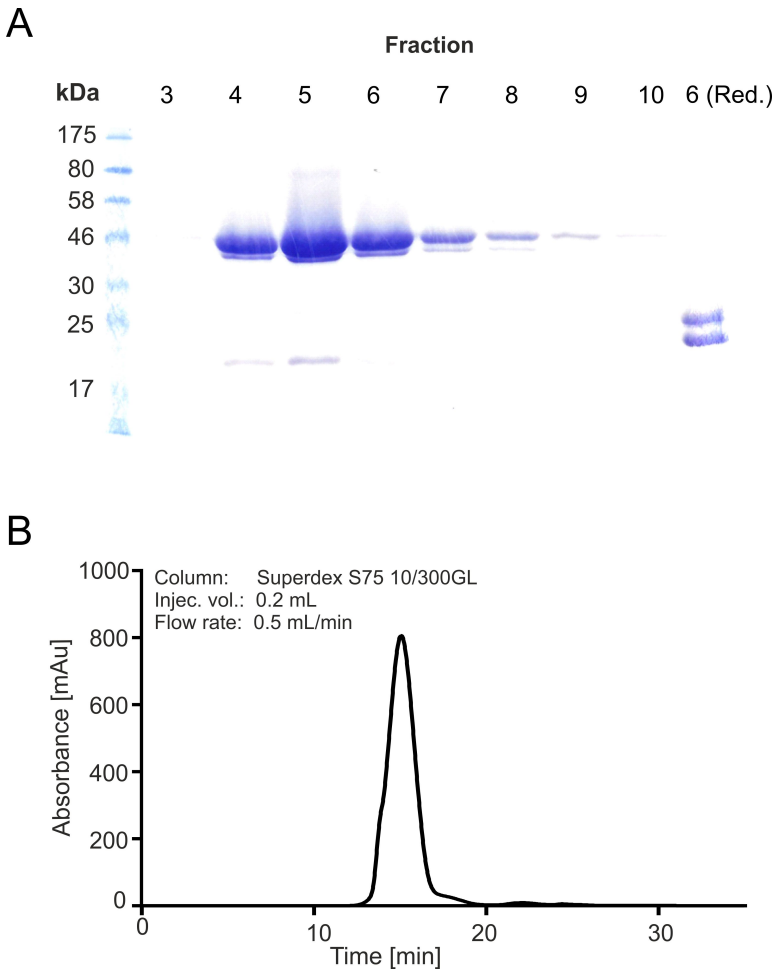

Fig. B.11.: The purification of the ESC11-Fab from the culture media using CaptureSelect™ technology rather than immobilized metal ion affinity chromatography (IMAC) yielded highly pure recombinant protein (∼5 mg/L of culture media). A) SDS-PAGE analysis of eluted fractions after purification of the bacterial media with CaptureSelect™ LC-Kappa. B) UV-trace of SEC purification.

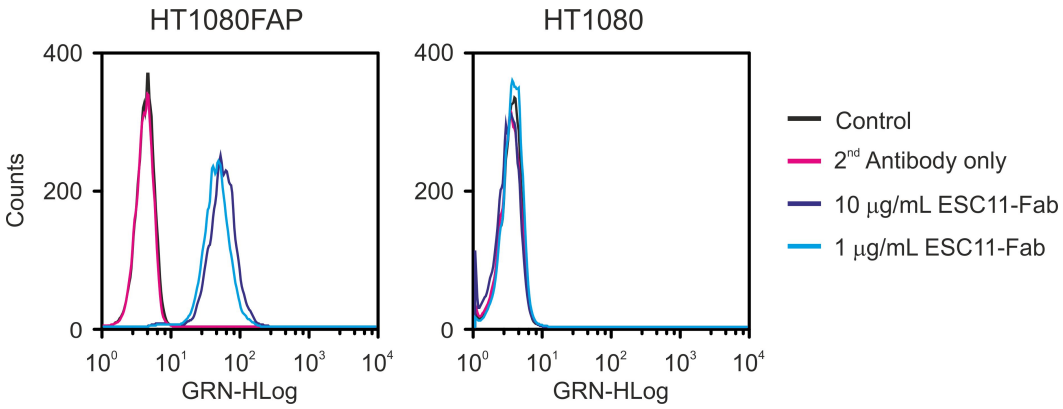

Fig. B.12.: The functional integrity of the ESC11-Fab was tested by fluorescence-activated cell sorting (FACS) and revealed binding to FAP+ cells (HT1080FAP). No unspecific binding was observed on FAP- cells (HT1080).

C

Supporting Information: *In Vitro* and *In Vivo* Characterization of Targeted Non-Covalent Antibody-Z-Domain Conjugates

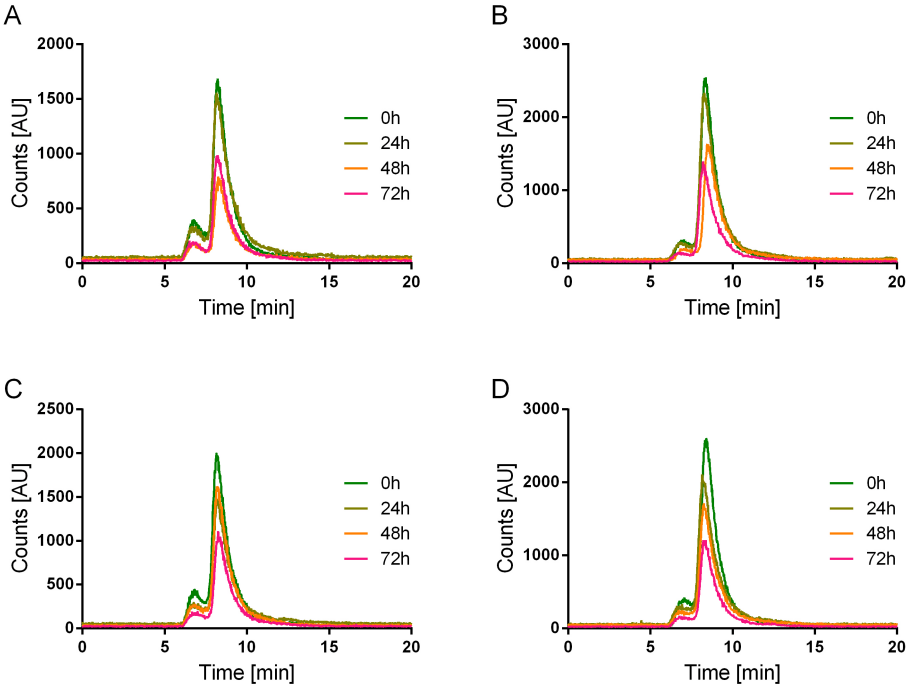

Fig. C.1.: Time dependent stability of (A and B) ZD-chCE7 and (C and D) ZD-control IgG1 in (A and C) non-IgG depleted and (B and D) IgG-depleted human plasma.

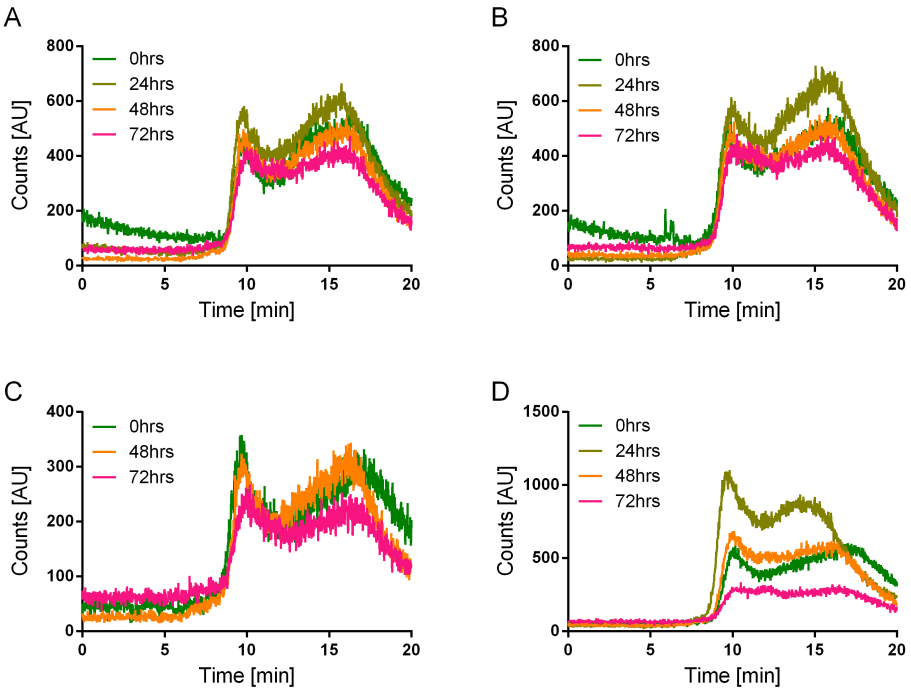

Fig. C.2.: Time dependent stability of (A and B) ZD-chCE7 and (C and D) ZD-control IgG1 in (A and C) non-IgG depleted and (B and D) IgG-depleted rat plasma.

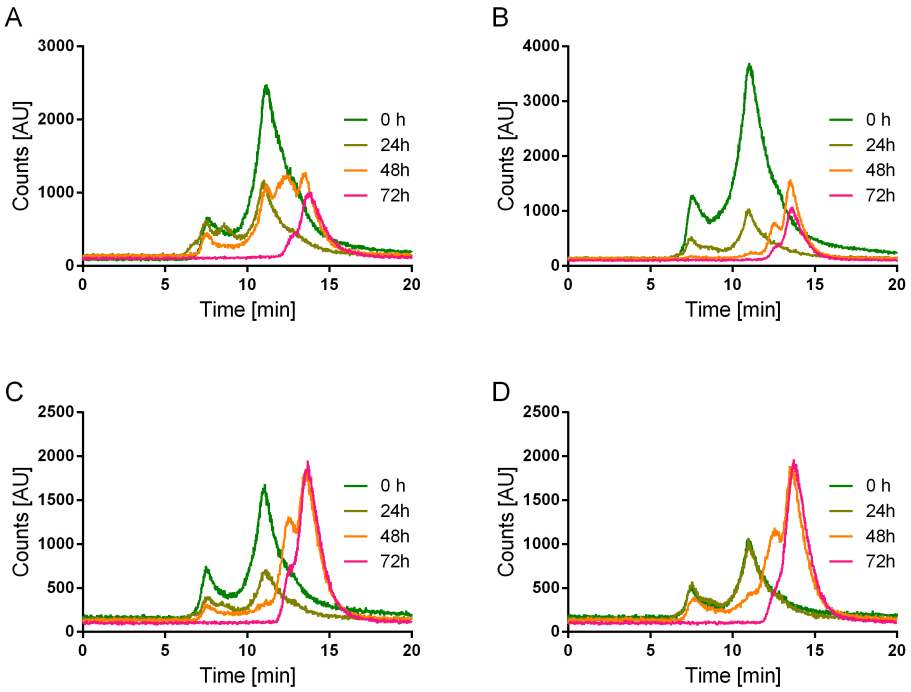

Fig. C.3.: Time dependent stability of (A and B) ZD-chCE7 and (C and D) ZD-control IgG1 in (A and C) non-IgG depleted and (B and D) IgG-depleted mouse plasma.

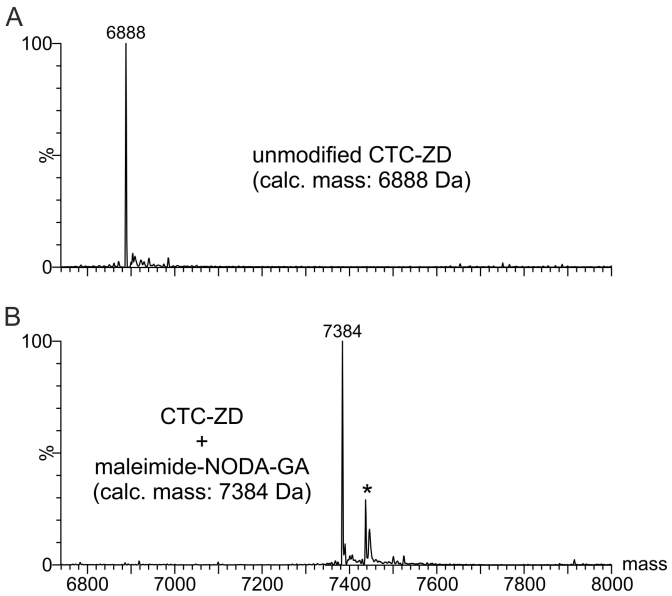

Fig. C.4.: Deconvoluted mass spectra of A) unmodified CTC-ZD and B) CTC-ZD that was modified with maleimide-NODA-GA. Theoretical/calculated masses are indicated. * Copper contaminated CTC-ZD-NODA-GA.

Bibliography

[1] G Köhler and C Milstein. “Continuous cultures of fused cells secreting antibody of predefined specificity”. *Nature* 256.5517 (1975), pp. 495–497.

[2] J M Reichert, C J Rosensweig, L B Faden, and M C Dewitz. “Monoclonal antibody successes in the clinic”. *Nat. Biotechnol.* 23.9 (2005), pp. 1073–1078.

[3] Z An. “Monoclonal antibodies - a proven and rapidly expanding therapeutic modality for human diseases”. *Protein Cell* 1.4 (2010), pp. 319–330.

[4] J M Reichert. “Antibodies to watch in 2010”. *MAbs* 2.1 (2010), pp. 84–100.

[5] E Vacchelli, A Eggermont, J Galon, et al. “Trial watch: Monoclonal antibodies in cancer therapy”. *Oncoimmunology* 2.1 (2013).

[6] J M Reichert. “Which are the antibodies to watch in 2013?” *MAbs* 5.1 (2013), pp. 1–4.

[7] L Ducry and B Stump. “Antibody-drug conjugates: linking cytotoxic payloads to monoclonal antibodies”. *Bioconjugate Chem.* 21.1 (2010), pp. 5–13.

[8] B Hughes. “Antibody-drug conjugates for cancer: poised to deliver?” *Nat. Rev. Drug Discov.* 9.9 (2010), pp. 665–667.

[9] R V Chari. “Targeted cancer therapy: conferring specificity to cytotoxic drugs”. *Acc. Chem. Res.* 41.1 (2008), pp. 98–107.

[10] D M Goldenberg. “Radiolabelled monoclonal antibodies in the treatment of metastatic cancer”. *Curr. Oncol.* 14.1 (2007), pp. 39–42.

[11] A M Wu and P D Senter. “Arming antibodies: prospects and challenges for immunoconjugates”. *Nat. Biotechnol.* 23.9 (2005), pp. 1137–1146.

[12] P Sapra, A T Hooper, C J O’Donnell, and H P Gerber. “Investigational antibody drug conjugates for solid tumors”. *Expert Opin. Invest. Drugs* 20.8 (2011), pp. 1131–1180.

[13] J Flygare, T Pillow, and P Aristoff. “Antibody-drug conjugates for the treatment of cancer”. *Chem. Biol. Drug Des.* 81.1 (2013), pp. 113–121.

[14] R V Chari, M L Miller, and W C Widdison. “Antibody-drug conjugates: an emerging concept in cancer therapy”. *Angew. Chem. Int. Ed.* 53.15 (2014), pp. 3796–3827.

[15] N Stephanopoulos and M B Francis. “Choosing an effective protein bioconjugation strategy”. *Nat. Chem. Biol.* 7.12 (2011), pp. 876–884.

[16] K J Hamblett, P D Senter, D F Chace, et al. “Effects of drug loading on the antitumor activity of a monoclonal antibody drug conjugate”. *Clin. Cancer Res.* 10.20 (2004), pp. 7063–7070.

[17] C A Boswell, E E Mundo, C Zhang, et al. “Impact of drug conjugation on pharmacokinetics and tissue distribution of anti-STEAP1 antibody-drug conjugates in rats”. *Bioconjugate Chem.* 22.10 (2011), pp. 1994–2004.

[18] D Jackson, J Atkinson, C I Guevara, et al. “*In vitro* and *in vivo* evaluation of cysteine and site specific conjugated herceptin antibody-drug conjugates”. *PLoS One* 9.1 (2014).

[19] A N Glazer. “Specific chemical modification of proteins”. *Annu. Rev. Biochem.* 39 (1970), pp. 101–130.

[20] T I Ghose, A H Blair, and P N Kulkarni. “Preparation of antibody-linked cytotoxic agents”. *Methods Enzymol.* 93 (1983), pp. 280–333.

[21] G T Hermanson. *Bioconjugate Techniques*. Ed. by G T Hermanson. New York: Academic Press, 2008, pp. 1041–1132.

[22] M A Gauthier and H A Klok. “Peptide/protein-polymer conjugates: synthetic strategies and design concepts”. *Chem. Commun. (Cambridge, U. K.)* (2008), pp. 2591–2611.

[23] M B Francis. “New methods for protein bioconjugation”. *Chem. Biol.* Wiley-VCH Verlag GmbH, 2008, pp. 593–634.

[24] E M Sletten and C R Bertozzi. “Bioorthogonal chemistry: fishing for selectivity in a sea of functionality”. *Angew. Chem. Int. Ed.* 48.38 (2009), pp. 6974–6998.

[25] B M Mueller, W A Wrasidlo, and R A Reisfeld. “Determination of the number of ϵ-amino groups available for conjugation of effector molecules to monoclonal antibodies”. *Hybridoma* 7.5 (1988), pp. 453–456.

[26] W C Widdison, S D Wilhelm, E E Cavanagh, et al. “Semisynthetic maytansine analogues for the targeted treatment of cancer”. *J. Med. Chem.* 49.14 (2006), pp. 4392–4408.

[27] A A Wakankar, M B Feeney, J Rivera, et al. “Physicochemical stability of the antibody-drug conjugate Trastuzumab-DM1: changes due to modification and conjugation processes”. *Bioconjugate Chem.* 21.9 (2010), pp. 1588–1595.

[28] M M Siegel, K Tabei, A Kunz, et al. “Calicheamicin derivatives conjugated to monoclonal antibodies: determination of loading values and distributions by infrared and UV matrix-assisted laser desorption/ionization mass spectrometry and electrospray ionization mass spectrometry”. *Anal. Chem.* 69.14 (1997), pp. 2716–2726.

[29] M Adamczyk, J Gebler, K Shreder, and J Wu. “Region-selective labeling of antibodies as determined by electrospray ionization-mass spectrometry (ESI-MS)”. *Bioconjugate Chem.* 11.4 (2000), pp. 557–563.

[30] L Wang, G Amphlett, W A Blattler, J M Lambert, and W Zhang. “Structural characterization of the maytansinoid-monoclonal antibody immunoconjugate, huN901-DM1, by mass spectrometry”. *Protein Sci.* 14.9 (2005), pp. 2436–2446.

[31] Y Feng, Z Zhu, W Chen, et al. “Conjugates of small molecule drugs with antibodies and other proteins”. *Biomedicines* 2.1 (2014), pp. 1–13.

[32] C Hess, D Venetz, and D Neri. “Emerging classes of armed antibody therapeutics against cancer”. *Med. Chem. Commun.* 5.4 (2014), pp. 408–431.

[33] S Kalkhof and A Sinz. “Chances and pitfalls of chemical cross-linking with amine-reactive *N*-hydroxysuccinimide esters”. *Anal. Bioanal. Chem.* 392.1-2 (2008), pp. 305–312.

[34] S Madler, C Bich, D Touboul, and R Zenobi. “Chemical cross-linking with NHS esters: a systematic study on amino acid reactivities”. *J. Mass. Spectrom.* 44.5 (2009), pp. 694–706.

[35] H W Chih, B Gikanga, Y Yang, and B Zhang. “Identification of amino acid residues responsible for the release of free drug from an antibody-drug conjugate utilizing lysine-succinimidyl ester chemistry”. *J. Pharm. Sci.* 100.7 (2011), pp. 2518–2525.

[36] Y Goto and K Hamaguchi. “The role of the intrachain disulfide bond in the conformation and stability of the constant fragment of the immunoglobulin light chain”. *J. Biochem.* 86.5 (1979), pp. 1433–1441.

[37] K Proba, A Honegger, and A Pluckthun. “A natural antibody missing a cysteine in VH: consequences for thermodynamic stability and folding”. *J. Mol. Biol.* 265.2 (1997), pp. 161–172.

[38] M J Thies, F Talamo, M Mayer, et al. “Folding and oxidation of the antibody domain CH3”. *J. Mol. Biol.* 319.5 (2002), pp. 1267–1277.

[39] A McAuley, J Jacob, C G Kolvenbach, et al. “Contributions of a disulfide bond to the structure, stability, and dimerization of human IgG1 antibody CH3 domain”. *Protein Sci.* 17.1 (2008), pp. 95–106.

[40] H Liu, C Chumsae, G Gaza-Bulseco, K Hurkmans, and C H Radziejewski. “Ranking the susceptibility of disulfide bonds in human IgG1 antibodies by reduction, differential alkylation, and LC-MS analysis”. *Anal. Chem.* 82.12 (2010), pp. 5219–5226.

[41] M M Sun, K S Beam, C G Cerveny, et al. “Reduction-alkylation strategies for the modification of specific monoclonal antibody disulfides”. *Bioconjugate Chem.* 16.5 (2005), pp. 1282–1290.

[42] C F McDonagh, E Turcott, L Westendorf, et al. “Engineered antibody-drug conjugates with defined sites and stoichiometries of drug attachment”. *Protein Eng. Des. Sel.* 19.7 (2006), pp. 299–307.

[43] S O Doronina, B E Toki, M Y Torgov, et al. “Development of potent monoclonal antibody auristatin conjugates for cancer therapy”. *Nat. Biotechnol.* 21.7 (2003), pp. 778–784.

[44] J B Stimmel, B M Merrill, L F Kuyper, et al. “Site-specific conjugation on serine right-arrow cysteine variant monoclonal antibodies”. *J. Biol. Chem.* 275.39 (2000), pp. 30445–30450.

[45] J R Junutula, H Raab, S Clark, et al. “Site-specific conjugation of a cytotoxic drug to an antibody improves the therapeutic index”. *Nature Biotechnol.* 26.8 (2008), pp. 925–932.

[46] S Bhakta, H Raab, and J R Junutula. “Engineering THIOMABs for site-specific conjugation of thiol-reactive linkers”. eng. *Antibody-Drug Conjugates*. Ed. by Laurent Ducry. Vol. 1045. Humana Press, 2013. Chap. 11, pp. 189–203.

[47] B Q Shen, K Xu, L Liu, et al. “Conjugation site modulates the *in vivo* stability and therapeutic activity of antibody-drug conjugates”. *Nat. Biotechnol.* 30 (2012), pp. 184–189.

[48] G W Seegan, C A Smith, and V N Schumaker. “Changes in quaternary structure of IgG upon reduction of the interheavy-chain disulfide bond”. *Proc. Natl. Acad. Sci. U.S.A.* 76.2 (1979), pp. 907–911.

[49] T E Michaelsen, O H Brekke, A Aase, et al. “One disulfide bond in front of the second heavy chain constant region is necessary and sufficient for effector functions of human IgG3 without a genetic hinge”. *Proc. Natl. Acad. Sci. U.S.A.* 91.20 (1994), pp. 9243–9247.

[50] P C Caron, W Laird, M S Co, et al. “Engineered humanized dimeric forms of IgG are more effective antibodies”. *J. Exp. Med.* 176.4 (1992), pp. 1191–1195.

[51] B Shopes. “A genetically engineered human IgG with limited flexibility fully initiates cytolysis *via* complement”. *Mol. Immunol.* 30.6 (1993), pp. 603–609.

[52] S C Alley, D R Benjamin, S C Jeffrey, et al. “Contribution of linker stability to the activities of anticancer immunoconjugates”. *Bioconjugate Chem.* 19.3 (2008), pp. 759–765.

[53] A D Baldwin and K L Kiick. “Tunable degradation of maleimide-thiol adducts in reducing environments”. *Bioconjugate Chem.* 22.10 (2011), pp. 1946–1953.

[54] J T Patterson, S Asano, X Li, C Rader, and C F Barbas. “Improving the serum stability of site-specific antibody conjugates with sulfone linkers”. *Bioconjugate Chem.* (2014).

[55] G Badescu, P Bryant, M Bird, et al. “Bridging disulfides for stable and defined antibody drug conjugates”. *Bioconjugate Chem.* 25.6 (2014), pp. 1124–1136.

[56] F F Schumacher, J P Nunes, A Maruani, et al. “Next generation maleimides enable the controlled assembly of antibody-drug conjugates *via* native disulfide bond bridging”. *Org Biomol Chem* 12.37 (2014), pp. 7261–7269.

[57] R P Lyon, J R Setter, T D Bovee, et al. “Self-hydrolyzing maleimides improve the stability and pharmacological properties of antibody-drug conjugates”. *Nat. Biotechnol.* 32.10 (2014), pp. 1059–1062.

[58] L N Tumey, M Charati, T He, et al. “Mild method for succinimide hydrolysis on ADCs: impact on ADC potency, stability, exposure, and efficacy”. *Bioconjugate Chem.* 25.10 (2014), pp. 1871–1880.

[59] L Johansson, C Chen, J O Thorell, et al. “Exploiting the 21st amino acid-purifying and labeling proteins by selenolate targeting”. *Nat. Methods* 1.1 (2004), pp. 61–66.

[60] T Hofer, J D Thomas, T R Burke Jr., and C Rader. “An engineered selenocysteine defines a unique class of antibody derivatives”. *Proc. Natl. Acad. Sci. U.S.A.* 105.34 (2008), pp. 12451–12456.

[61] T Hofer, L R Skeffington, C M Chapman, and C Rader. “Molecularly defined antibody conjugation through a selenocysteine interface”. *Biochemistry* 48.50 (2009), pp. 12047–12057.

[62] Xiuling Li, Jiahui Yang, and Christoph Rader. “Antibody conjugation via one and two C-terminal selenocysteines”. *Methods* 65.1 (2014), pp. 133–138.

[63] H Ban, J Gavrilyuk, and C F Barbas. “Tyrosine bioconjugation through aqueous ene-type reactions: a click-like reaction for tyrosine”. *J. Am. Chem. Soc.* 132.5 (2010), pp. 1523–1525.

[64] H Ban, M Nagano, J Gavrilyuk, et al. “Facile and stabile linkages through tyrosine: bioconjugation strategies with the tyrosine-click reaction”. *Bioconjugate Chem.* 24.4 (2013), pp. 520–532.

[65] J Gavrilyuk, H Ban, M Nagano, W Hakamata, and C Barbas. “Formylbenzene diazonium hexafluorophosphate reagent for tyrosine-selective modification of proteins and the introduction of a bioorthogonal aldehyde”. *Bioconjugate Chem.* 23.12 (2012), pp. 2321–2328.

[66] J Gavrilyuk, H Ban, H Uehara, et al. “Antibody conjugation approach enhances breadth and potency of neutralization of anti-HIV-1 antibodies and CD4-IgG”. *J. Virol.* 87.9 (2013), pp. 4985–4993.

[67] T J Hallam and V V Smider. “Unnatural amino acids in novel antibody conjugates”. *Future Med. Chem.* 6.11 (2014), pp. 1309–1324.

[68] Q Wang, A R Parrish, and L Wang. “Expanding the genetic code for biological studies”. *Chem. Biol.* 16.3 (2009), pp. 323–336.

[69] C H Kim, J Y Axup, and P G Schultz. “Protein conjugation with genetically encoded unnatural amino acids”. *Curr. Opin. Chem. Biol.* 17.3 (2013), pp. 412–419.

[70] J Axup, K Bajjuri, M Ritland, et al. “Synthesis of site-specific antibody-drug conjugates using unnatural amino acids”. *Proc. Natl. Acad. Sci. U.S.A.* 109.40 (2012), pp. 16101–16106.

[71] H Xiao, A Chatterjee, S H Choi, et al. “Genetic incorporation of multiple unnatural amino acids into proteins in mammalian cells”. *Angew. Chem. Int. Ed.* 52.52 (2013), pp. 14080–14083.

[72] L V Abaturov, R S Nezlin, T I Vengerova, and J M Varshavsky. “Conformational studies of immunoglobulin G and its subunits by the methods of hydrogen-deuterium exchange and infrared spectroscopy”. *Biochim. Biophys. Acta* 194.2 (1969), pp. 386–396.

[73] P Calmettes, L Cser, and E Rajnavolgyi. “Temperature and pH dependence of immunoglobulin G conformation”. *Arch. Biochem. Biophys.* 291.2 (1991), pp. 277–283.

[74] D Ejima, K Tsumoto, H Fukada, et al. “Effects of acid exposure on the conformation, stability, and aggregation of monoclonal antibodies”. *Proteins* 66.4 (2007), pp. 954–962.

[75] G Yin, E D Garces, J Yang, et al. “Aglycosylated antibodies and antibody fragments produced in a scalable *in vitro* transcription-translation system”. *MAbs* 4.2 (2012), pp. 217–225.

[76] K Ozawa, K V Loscha, K V Kuppan, et al. “High-yield cell-free protein synthesis for site-specific incorporation of unnatural amino acids at two sites”. *Biochem. Biophys. Res. Commun.* 418.4 (2012), pp. 652–656.

[77] F Caschera and V Noireaux. “Synthesis of 2.3 mg/ml of protein with an all *Escherichia coli* cell-free transcription-translation system”. *Biochimie* 99 (2014), pp. 162–168.

[78] S H Hong, Y C C Kwon, and M C Jewett. “Non-standard amino acid incorporation into proteins using *Escherichia coli* cell-free protein synthesis”. *Front. Chem.* 2 (2014), p. 34.

[79] E S Zimmerman, T H Heibeck, A Gill, et al. “Production of site-specific antibody-drug conjugates using optimized non-natural amino acids in a cell-free expression system”. *Bioconjugate Chem.* 25.2 (2014), pp. 351–361.

[80] D J O’Shannessy, M J Dobersen, and R H Quarles. “A novel procedure for labeling immunoglobulins by conjugation to oligosaccharide moieties”. *Immunol. Lett.* 8.5 (1984), pp. 273–277.

[81] J Kralovec, G Spencer, A H Blair, et al. “Synthesis of methotrexate-antibody conjugates by regiospecific coupling and assessment of drug and antitumor activities”. *J. Med. Chem.* 32.11 (1989), pp. 2426–2431.

[82] B C Laguzza, C L Nichols, S L Briggs, et al. “New antitumor monoclonal antibody-vinca conjugates LY203725 and related compounds: design, preparation, and representative *in vivo* activity”. *J. Med. Chem.* 32.3 (1989), pp. 548–555.

[83] D A Johnson, A L Baker, B C Laguzza, D V Fix, and M C Gutowski. “Antitumor activity of L/1C2-4-desacetylvinblastine-3-carboxhydrazide immunoconjugate in xenografts”. *Cancer Res.* 50.6 (1990), pp. 1790–1794.

[84] K Zuberbühler, G Casi, G J Bernardes, and D Neri. “Fucose-specific conjugation of hydrazide derivatives to a vascular-targeting monoclonal antibody in IgG format”. *Chem. Commun.* 48.56 (2012), pp. 7100–7102.

[85] J D Rodwell, V L Alvarez, C Lee, et al. “Site-specific covalent modification of monoclonal antibodies: *in vitro* and *in vivo* evaluations”. *Proc. Natl. Acad. Sci. U.S.A.* 83.8 (1986), pp. 2632–2636.

[86] G N Ranadive, H S Rosenzweig, M W Epperly, T Seskey, and W D Bloomer. “A new method of technetium-99m labeling of monoclonal antibodies through sugar residues. A study with TAG-72 specific CC-49 antibody”. *Nucl. Med. Biol.* 20.6 (1993), pp. 719–726.

[87] M Husain and C Bieniarz. “Fc site-specific labeling of immunoglobulins with calf intestinal alkaline phosphatase”. *Bioconjugate Chem.* 5.5 (1994), pp. 482–490.

[88] J F Liang, Y T Li, M E Connell, and V C Yang. “Synthesis and characterization of positively charged tPA as a prodrug using heparin/protamine-based drug delivery system”. *AAPS Pharm. Sci.* 2.1 (2000), E7.

[89] J F Liang, Y J Park, H Song, Y T Li, and V C Yang. “ATTEMPTS: a heparin/protamine-based prodrug approach for delivery of thrombolytic drugs”. *J. Controlled Release* 72.1-3 (2001), pp. 145–156.

[90] Y J Park, J F Liang, H Song, et al. “ATTEMPTS: a heparin/protamine-based triggered release system for the delivery of enzyme drugs without associated side-effects”. *Adv. Drug Delivery Rev.* 55.2 (2003), pp. 251–265.

[91] R Jefferis. “Glycosylation of recombinant antibody therapeutics”. *Biotechnol. Prog.* 21.1 (2005), pp. 11–16.

[92] T S Raju and R E Jordan. “Galactosylation variations in marketed therapeutic antibodies”. *MAbs* 4.3 (2012).

[93] G Zauner, M H Selman, A Bondt, et al. “Glycoproteomic analysis of antibodies”. *Mol. Cell. Proteomics* 12.4 (2013), pp. 856–865.

[94] R Abraham, D Moller, D Gabel, et al. “The influence of periodate oxidation on monoclonal antibody avidity and immunoreactivity”. *J. Immunol. Methods* 144.1 (1991), pp. 77–86.

[95] C A Wolfe and D S Hage. “Studies on the rate and control of antibody oxidation by periodate”. *Anal. Biochem.* 231.1 (1995), pp. 123–130.

[96] D S Hage, C A Wolfe, and M R Oates. “Development of a kinetic model to describe the effective rate of antibody oxidation by periodate”. *Bioconjugate Chem.* 8.6 (1997), pp. 914–920.

[97] B Solomon, R Koppel, F Schwartz, and G Fleminger. “Enzymic oxidation of monoclonal antibodies by soluble and immobilized bifunctional enzyme complexes”. *J. Chromatogr.* 510 (1990), pp. 321–329.

[98] Q Zhou, J E Stefano, C Manning, et al. “Site-specific antibody-drug conjugation through glycoengineering”. *Bioconjugate Chem.* 25.3 (2014), pp. 510–520.

[99] E Boeggeman, B Ramakrishnan, C Kilgore, et al. “Direct identification of nonreducing GlcNAc residues on N-glycans of glycoproteins using a novel chemoenzymatic method”. *Bioconjug Chem* 18.3 (2007), pp. 806–814.

[100] E Boeggeman, B Ramakrishnan, M Pasek, et al. “Site-specific conjugation of fluoroprobes to the remodeled Fc N-glycans of monoclonal antibodies using mutant glycosyltransferases: application for cell surface antigen detection”. *Bioconjugate Chem.* 20.6 (2009), pp. 1228–1236.

[101] B M Zeglis, C B Davis, R Aggeler, et al. “An enzyme-mediated methodology for the site-specific radiolabeling of antibodies based on catalyst-free click chemistry”. *Bioconjugate Chem.* 24.6 (2013), pp. 1057–1067.

[102] B M Zeglis, C B Davis, D Abdel-Atti, et al. “Chemoenzymatic strategy for the synthesis of site-specifically labeled immunoconjugates for multimodal PET and optical imaging”. *Bioconjugate Chem.* 25.12 (2014), pp. 2123–2128.

[103] Z Zhu, B Ramakrishnan, J Li, et al. “Site-specific antibody-drug conjugation through an engineered glycotransferase and a chemically reactive sugar”. *MAbs* 6.5 (2014), pp. 1190–1200.

[104] N M Okeley, B E Toki, X Zhang, et al. “Metabolic engineering of monoclonal antibody carbohydrates for antibody-drug conjugation”. *Bioconjugate Chem.* 24.10 (2013), pp. 1650–1655.

[105] G Vidarsson, G Dekkers, and T Rispens. “IgG subclasses and allotypes: from structure to effector functions”. *Front. Immunol.* 5.520 (2014).

[106] J N Arnold, M R Wormald, R B Sim, P M Rudd, and R A Dwek. “The impact of glycosylation on the biological function and structure of human immunoglobulins”. *Annu. Rev. Immunol.* 25 (2007), pp. 21–50.

[107] A Bondt, Y Rombouts, M H Selman, et al. “Immunoglobulin G (IgG) Fab glycosylation analysis using a new mass spectrometric high-throughput profiling method reveals pregnancy-associated changes”. *Mol. Cell. Biol.* 13.11 (2014), pp. 3029–3039.

[108] D Rabuka. “Chemoenzymatic methods for site-specific protein modification”. *Curr. Opin. Chem. Biol.* 14.6 (2010), pp. 790–796.

[109] M Rashidian, J Dozier, and M Distefano. “Enzymatic labeling of proteins: techniques and approaches”. *Bioconjugate Chem.* 24.8 (2013), pp. 1277–1294.

[110] I S Carrico, B L Carlson, and C R Bertozzi. “Introducing genetically encoded aldehydes into proteins”. *Nat. Chem. Biol.* 3.6 (2007), pp. 321–322.

[111] P Wu, W Shui, B L Carlson, et al. “Site-specific chemical modification of recombinant proteins produced in mammalian cells by using the genetically encoded aldehyde tag”. *Proc. Natl. Acad. Sci. U. S. A., Early Ed.* 106.9 (2009), pp. 1–6.

[112] J Hudak, R Barfield, G de Hart, et al. “Synthesis of heterobifunctional protein fusions using copper-free click chemistry and the aldehyde tag”. *Angew. Chem. Int. Ed.* 51.17 (2012), pp. 4161–4166.

[113] P Agarwal, J van der Weijden, E M Sletten, D Rabuka, and C R Bertozzi. “A Pictet-Spengler ligation for protein chemical modification”. *Proc. Natl. Acad. Sci. U.S.A.* 110.1 (2013), pp. 46–51.

[114] D Rabuka, J Rush, G DeHart, P Wu, and C R Bertozzi. “Site-specific chemical protein conjugation using genetically encoded aldehyde tags”. *Nat. Protoc.* 7.10 (2012), pp. 1052–1119.

[115] R Parthasarathy, S Subramanian, and E T Boder. “Sortase A as a novel molecular ’stapler’ for sequence-specific protein conjugation”. *Bioconjugate Chem.* 18.2 (2007), pp. 469–476.

[116] M W Popp, J M Antos, G M Grotenbreg, E Spooner, and H L Ploegh. “Sortagging: a versatile method for protein labeling”. *Nat. Chem. Biol.* 3.11 (2007), pp. 707–708.

[117] Markus Ritzefeld. “Sortagging: a robust and efficient chemoenzymatic ligation strategy”. *Chemistry* 20.28 (2014), pp. 8516–8529.

[118] D A Levary, R Parthasarathy, E T Boder, and M E Ackerman. “Protein-protein fusion catalyzed by sortase A”. *PLoS One* 6.4 (2011).

[119] L K Swee, C P Guimaraes, S Sehrawat, et al. “Sortase-mediated modification of αDEC205 affords optimization of antigen presentation and immunization against a set of viral epitopes”. *Proc. Natl. Acad. Sci. U.S.A.* 110.4 (2013), pp. 1428–1433.

[120] K Wagner, M J Kwakkenbos, Y B Claassen, et al. “Bispecific antibody generated with sortase and click chemistry has broad antiinfluenza virus activity”. *Proc. Natl. Acad. Sci. U.S.A.* 111.47 (2014), pp. 16820–16825.

[121] J J Bellucci, J Bhattacharyya, and A Chilkoti. “A noncanonical function of sortase enables site-specific conjugation of small molecules to lysine residues in proteins”. *Angew. Chem. Int. Ed.* (2014).

[122] B Nilsson, T Moks, B Jansson, et al. “A synthetic IgG-binding domain based on staphylococcal protein A”. *Protein Eng.* 1.2 (1987), pp. 107–113.

[123] A Forsgren and J Sjöquist. “Protein A from *S. Aureus*”. *J. Immunol.* 97.6 (1966), pp. 822–827.

[124] J J Iangone. “Protein A of *Staphylococcus aureus* and related immunoglobulin receptors produced by streptococci and pneumonococci”. *Adv. Immunol.* Ed. by J Dixon Frank and G Kunkel Henry. Vol. Volume 32. Academic Press, 1982, pp. 157–252.

[125] N Kurata, T Shishido, M Muraoka, et al. “Specific protein delivery to target cells by antibody-displaying bionanocapsules”. *J. Biochem.* 144.6 (2008), pp. 701–707.

[126] M Iijima, T Matsuzaki, N Yoshimoto, et al. “Fluorophore-labeled nanocapsules displaying IgG Fc-binding domains for the simultaneous detection of multiple antigens”. *Biomaterials* 32.34 (2011), pp. 9011–9031.

[127] M Iijima, H Kadoya, S Hatahira, et al. “Nanocapsules incorporating IgG Fc-binding domain derived from *Staphylococcus aureus* protein A for displaying IgGs on immunosensor chips”. *Biomaterials* 32.6 (2011), pp. 1455–1519.

[128] M Iijima, M Somiya, N Yoshimoto, T Niimi, and S Kuroda. “Nano-visualization of oriented-immobilized IgGs on immunosensors by high-speed atomic force microscopy”. *Sci. Rep.* 2 (2012), p. 790.

[129] Y Tsutsui, K Tomizawa, M Nagita, et al. “Development of bionanocapsules targeting brain tumors”. *J. Controlled Release* 122.2 (2007), pp. 159–164.

[130] Y Mazor, I Barnea, I Keydar, and I Benhar. “Antibody internalization studied using a novel IgG binding toxin fusion”. *J. Immunol. Methods* 321.1-2 (2007), pp. 41–59.

[131] Y Mazor, R Noy, W S Wels, and I Benhar. “chFRP5-ZZ-PE38, a large IgG-toxin immunoconjugate outperforms the corresponding smaller FRP5(Fv)-ETA immunotoxin in eradicating ErbB2-expressing tumor xenografts”. *Cancer Lett.* 257.1 (2007), pp. 124–135.

[132] S Shapira, A Shapira, A Starr, et al. “An immunoconjugate of anti-CD24 and *Pseudomonas* exotoxin selectively kills human colorectal tumors in mice”. *Gastroenterology* 140.3 (2011), pp. 935–946.

[133] I Barnea, R Ben-Yosef, V Karaush, I Benhar, and A Vexler. “Targeting EGFR-positive cancer cells with cetuximab-ZZ-PE38: Results of *in vitro* and *in vivo* studies”. *Head Neck* 35.8 (2013), pp. 1171–1177.

[134] T Sakamoto, S Sawamoto, T Tanaka, H Fukuda, and A Kondo. “Enzyme-mediated site-specific antibody-protein modification using a ZZ domain as a linker”. *Bioconjugate Chem.* 21.12 (2010), pp. 2227–2233.

[135] F Yu, P Järver, and P Nygren. “Tailor-making a protein a-derived domain for efficient site-specific photocoupling to Fc of mouse IgG1”. *PLoS One* 8.2 (2013).

[136] A Konrad, A E Karlstrom, and S Hober. “Covalent immunoglobulin labeling through a photoactivable synthetic Z domain”. *Bioconjugate Chem.* 22.12 (2011), pp. 2395–2403.

[137] A Perols and A E Karlström. “Site-specific photoconjugation of antibodies using chemically synthesized IgG-binding domains”. *Bioconjugate Chem.* 25.3 (2014), pp. 481–488.

[138] J Z Hui and A Tsourkas. “Optimization of photoactive protein Z for fast and efficient site-specific conjugation of native IgG”. *Bioconjugate Chem.* 25.9 (2014), pp. 1709–1719.

[139] Y Jung, J M Lee, J W Kim, et al. “Photoactivable antibody binding protein: site-selective and covalent coupling of antibody”. *Anal. Chem. Chem* 81.3 (2009), pp. 936–942.

[140] K Rajagopalan, G Pavlinkova, S Levy, et al. “Novel unconventional binding site in the variable region of immunoglobulins”. *Proc. Natl. Acad. Sci. U.S.A.* 93.12 (1996), pp. 6019–6024.

[141] G Pavlinkova, K Rajagopalan, S Muller, et al. “Site-specific photobiotinylation of immunoglobulins, fragments and light chain dimers”. *J. Immunol. Methods Methods* 201.1 (1997), pp. 77–88.

[142] G Pavlinkova, D Lou, and H Kohler. “Site-specific photobiotinylation of antibodies, light chains, and immunoglobulin fragments”. *Methods* 22.1 (2000), pp. 44–48.

[143] N J Alves, M M Champion, J F Stefanick, et al. “Selective photocrosslinking of functional ligands to antibodies via the conserved nucleotide binding site”. *Biomaterials* 34.22 (2013), pp. 5700–5710.

[144] N J Alves, N Mustafaoglu, and B Bilgicer. “Conjugation of a reactive thiol at the nucleotide binding site for site-specific antibody functionalization”. *Bioconjugate Chem.* 25.7 (2014), pp. 1198–1202.

[145] J Wagner, R Lerner, and C Barbas. “Efficient aldolase catalytic antibodies that use the enamine mechanism of natural enzymes”. *Science* 270.5243 (1995), pp. 1797–1800.

[146] C Barbas, A Heine, G Zhong, et al. “Immune *versus* natural selection: antibody aldolases with enzymic rates but broader scope”. *Science* 278.5346 (1997), pp. 2085–2092.

[147] F Tanaka, H Almer, R A Lerner, and C F Barbas. “Catalytic single-chain antibodies possessing β-lactamase activity selected from a phage displayed combinatorial library using a mechanism-based inhibitor”. *Tetrahedron Lett.* 40.46 (1999), pp. 8063–8066.

[148] F Tanaka and C F Barbas. “Reactive immunization: a unique approach to catalytic antibodies”. *J. Immunol. Methods* 269.1-2 (2002), pp. 67–79.

[149] A Bhat, O Laurent, and R Lappe. “CovX-Bodies”. *Fusion Protein Technologies for Biopharmaceuticals*. John Wiley & Sons, Inc., 2013, pp. 571–582.

[150] C Rader, S Sinha, M Popkov, R A Lerner, and C F Barbas. “Chemically programmed monoclonal antibodies for cancer therapy: adaptor immunotherapy based on a covalent antibody catalyst”. *Proc. Natl. Acad. Sci. U.S.A.* 100.9 (2003), pp. 5396–5400.

[151] V Doppalapudi, N Tryder, L Li, et al. “Chemically programmed antibodies: endothelin receptor targeting CovX-Bodies”. *Bioorg. Med. Chem. Lett.* 17.2 (2007), pp. 501–506.

[152] V Doppalapudi, J Huang, D Liu, et al. “Chemical generation of bispecific antibodies”. *Proc. Natl. Acad. Sci. U.S.A.* 107.52 (2010), pp. 22611–22616.

[153] L Li, T A Leedom, J Do, et al. “Antitumor efficacy of a thrombospondin 1 mimetic CovX-body”. *Trans. Oncol.* 4.4 (2011), pp. 249–257.

[154] L Roberts, K Brady, A Brown, et al. “Kappa agonist CovX-Bodies”. *Bioorg. Med. Chem. Lett.* 22.12 (2012), pp. 4173–4178.

[155] M S S Palanki, A Bhat, B Bolanos, et al. “Development of a long acting human growth hormone analog suitable for once a week dosing”. *Bioorg. Med. Chem. Lett.* 23.2 (2013), pp. 402–406.

[156] J E Folk and J S Finlayson. “The epsilon-(gamma-glutamyl)lysine crosslink and the catalytic role of transglutaminases”. *Adv. Protein Chem.* 31 (1977), pp. 1–133.

[157] L Lorand and R M Graham. “Transglutaminases: crosslinking enzymes with pleiotropic functions”. *Nat. Rev. Mol. Cell Biol.* 4.2 (2003), pp. 140–156.

[158] K Mehta and R L Eckert. *Transglutaminases: family of enzymes with diverse functions*. Vol. 38. Karger Publishers, 2005.

[159] S E Iismaa, B M Mearns, L Lorand, and R M Graham. “Transglutaminases and disease: lessons from genetically engineered mouse models and inherited disorders”. *Physiol. Rev.* 89.3 (2009), pp. 991–1023.

[160] Z Nemes. “Effects and analysis of transglutamination on protein aggregation and clearance in neurodegenerative diseases”. *Adv. Enzymol. Relat. Areas Mol. Biol.* 78 (2011), pp. 347–383.

[161] C Tabolacci, A Lentini, B Provenzano, and S Beninati. “Evidences for a role of protein cross-links in transglutaminase-related disease”. *Amino Acids* 42.2-3 (2012), pp. 975–986.

[162] A Lentini, A Abbruzzese, B Provenzano, C Tabolacci, and S Beninati. “Transglutaminases: key regulators of cancer metastasis”. *Amino Acids* 44.1 (2013), pp. 25–32.

[163] A Facchiano and F Facchiano. “Transglutaminases and their substrates in biology and human diseases: 50 years of growing”. *Amino Acids* 36.4 (2009), pp. 599–614.

[164] M Kieliszek and A Misiewicz. “Microbial transglutaminase and its application in the food industry. A review”. *Folia Microbiol. (Praha)* 59.3 (2014), pp. 241–250.

[165] A L Gaspar and S P de Góes-Favoni. “Action of microbial transglutaminase (MTGase) in the modification of food proteins: A review”. *Food Chem.* 171 (2015), pp. 315–322.

[166] N M Rachel and J N Pelletier. “Biotechnological applications of transglutaminases”. *Biomolecules* 3.4 (2013), pp. 870–888.

[167] A Fontana, B Spolaore, A Mero, and F M Veronese. “Site-specific modification and PEGylation of pharmaceutical proteins mediated by transglutaminase”. *Adv. Drug Delivery Rev.* 60.1 (2008), pp. 13–28.

[168] K Yokoyama, N Nio, and Y Kikuchi. “Properties and applications of microbial transglutaminase”. *Appl. Microbiol. Biotechnol.* 64.4 (2004), pp. 447–454.

[169] J H Levy and C Greenberg. “Biology of Factor XIII and clinical manifestations of Factor XIII deficiency”. *Transfusion* 53.5 (2013), pp. 1120–1131.

[170] A Tahlan and J Ahluwalia. “Factor XIII: congenital deficiency factor XIII, acquired deficiency, factor XIII A-subunit, and factor XIII B-subunit”. *Arch. Pathol. Lab. Med.* 138.2 (2014), pp. 278–281.

[171] I M Martins, M Matos, R Costa, et al. “Transglutaminases: recent achievements and new sources”. *Appl. Microbiol. Biotechnol.* 98.16 (2014), pp. 6957–6964.

[172] H Ando, M Adachi, K Umeda, et al. “Purification and characteristics of a novel transglutaminase derived from microorganisms”. *Agric. Biol. Chem.* 53.10 (1989), pp. 2613–2617.

[173] Y Zhu and J Tramper. “Novel applications for microbial transglutaminase beyond food processing”. *Trends Biotechnol.* 26.10 (2008), pp. 559–565.

[174] P Strop. “Versatility of microbial transglutaminase”. *Bioconjugate Chem.* 25.5 (2014), pp. 855–862.

[175] T Kashiwagi, K Yokoyama, K Ishikawa, et al. “Crystal structure of microbial transglutaminase from *Streptoverticillium mobaraense*”. *J. Biol. Chem.* 277.46 (2002), pp. 44252–44260.

[176] N Shimba, K Yokoyama, and E Suzuki. “NMR-based screening method for transglutaminases: rapid analysis of their substrate specificities and reaction rates”. *J. Agric. Food Chem.* 50.6 (2002), pp. 1330–1334.

[177] M T Yang, C H Chang, J M Wang, et al. “Crystal structure and inhibition studies of transglutaminase from *Streptomyces mobaraense*”. *J. Biol. Chem.* 286.9 (2011), pp. 7301–7307.

[178] M T Gundersen, J W Keillor, and J N Pelletier. “Microbial transglutaminase displays broad acyl-acceptor substrate specificity”. *Appl. Microbiol. Biotechnol.* 98.1 (2014), pp. 219–230.

[179] T Ohtsuka, M Ota, N Nio, and M Motoki. “Comparison of substrate specificities of transglutaminases using synthetic peptides as acyl donors”. *Biosci. Biotechnol. Biochem.* 64.12 (2000), pp. 2608–2613.

[180] Y Sugimura, K Yokoyama, N Nio, M Maki, and K Hitomi. “Identification of preferred substrate sequences of microbial transglutaminase from *Streptomyces mobaraensis* using a phage-displayed peptide library”. *Arch. Biochem. Biophys.* 477.2 (2008), pp. 379–383.

[181] U Tagami, N Shimba, M Nakamura, et al. “Substrate specificity of microbial transglutaminase as revealed by three-dimensional docking simulation and mutagenesis”. *Protein Eng. Des. Sel.* 22.12 (2009), pp. 747–752.

[182] B Spolaore, N Damiano, S Raboni, and A Fontana. “Site-specific derivatization of avidin using microbial transglutaminase”. *Bioconjugate Chem.* 25.3 (2014), pp. 470–480.

[183] B Spolaore, S Raboni, A Ramos Molina, et al. “Local unfolding is required for the site-specific protein modification by transglutaminase”. *Biochemistry* 51.43 (2012), pp. 8679–8689.

[184] A Josten, L Haalck, F Spener, and M Meusel. “Use of microbial transglutaminase for the enzymatic biotinylation of antibodies”. *J. Immunol. Methods* 240.1 (2000), pp. 47–54.

[185] T L Mindt, V Jungi, S Wyss, et al. “Modification of different IgG1 antibodies *via* glutamine and lysine using bacterial and human tissue transglutaminase”. *Bioconjugate Chem.* 19.1 (2008), pp. 271–278.

[186] S Jeger, K Zimmermann, A Blanc, et al. “Site-specific and stoichiometric modification of antibodies by bacterial transglutaminase”. *Angew. Chem. Int. Ed.* 49.51 (2010), pp. 9995–9997.

[187] P Strop, S H Liu, M Dorywalska, et al. “Location matters: site of conjugation modulates stability and pharmacokinetics of antibody drug conjugates”. *Chem. Biol.* 20.2 (2013), pp. 161–167.

[188] J R Junutula, K M Flagella, R A Graham, et al. “Engineered thio-trastuzumab-DM1 conjugate with an improved therapeutic index to target human epidermal growth factor receptor 2-positive breast cancer”. *Clin. Cancer Res.* 16.19 (2010), pp. 4769–4778.

[189] M Sunbul and J Yin. “Site-specific protein labeling by enzymatic posttranslational modification”. *Org. Biomol. Chem.* 7.17 (2009), pp. 3361–3371.

[190] K Knogler, J Grünberg, I Novak-Hofer, K Zimmermann, and P A Schubiger. “Evaluation of ^{177}Lu-DOTA-labeled aglycosylated monoclonal anti-L1-CAM antibody chCE7: influence of the number of chelators on the *in vitro* and *in vivo* properties”. *Nucl. Med. Biol.* 33.7 (2006), pp. 883–889.

[191] A Mero, M Schiavon, F M Veronese, and G Pasut. “A new method to increase selectivity of transglutaminase mediated PEGylation of salmon calcitonin and human growth hormone”. *J. Controlled Release* 154.1 (2011), pp. 27–34.

[192] F Sievers, A Wilm, D Dineen, et al. “Fast, scalable generation of high-quality protein multiple sequence alignments using Clustal Omega”. *Mol Syst Biol* 7 (2011), p. 539.

[193] E L Sievers and P D Senter. “Antibody-drug conjugates in cancer therapy”. *Annu. Rev. Med.* 64.1 (2013), pp. 15–29.

[194] H P Gerber, F E Koehn, and R T Abraham. “The antibody-drug conjugate: an enabling modality for natural product-based cancer therapeutics”. *Nat. Prod. Rep.* 30.5 (2013), pp. 625–639.

[195] G Casi and D Neri. “Antibody-drug conjugates: basic concepts, examples and future perspectives”. *J. Controlled Release* 161.2 (2012), pp. 422–428.

[196] I Sassoon and V Blanc. “Antibody-drug conjugate (ADC) clinical pipeline: a review”. *Methods Mol. Biol.* 1045 (2013), pp. 1–27.

[197] J Buchardt, H Selvig, P F Nielsen, and N L Johansen. “Transglutaminase-mediated methods for site-selective modification of human growth hormone”. *Biopolymers* 94.2 (2010), pp. 229–235.

[198] P Dennler, R Schibli, and E Fischer. “Enzymatic antibody modification by bacterial transglutaminase”. *Antibody-Drug Conjugates*. Ed. by Laurent Ducry. Vol. 1045. Humana Press, 2013. Chap. 12, pp. 205–215.

[199] J Grünberg, S Jeger, D Sarko, et al. “DOTA-Functionalized Polylysine: A High Number of DOTA Chelates Positively Influences the Biodistribution of Enzymatic Conjugated Anti-Tumor Antibody chCE7agl”. *PLoS One* 8.4 (2013).

[200] M A Cinelli, B Cordero, T S Dexheimer, Y Pommier, and M Cushman. “Synthesis and biological evaluation of 14-(aminoalkyl-aminomethyl)aromathecins as topoisomerase I inhibitors: investigating the hypothesis of shared structure-activity relationships”. *Bioorg. Med. Chem.* 17.20 (2009), pp. 7145–7155.

[201] P J Roth and P Theato. “Versatile synthesis of functional gold nanoparticles: grafting polymers from and onto”. *Chem. Mater.* 20.4 (2008), pp. 1614–1621.

[202] K Zheng, C Bantog, and R Bayer. “The impact of glycosylation on monoclonal antibody conformation and stability”. *MAbs* 3.6 (2011), pp. 568–576.

[203] D Hristodorov, R Fischer, and L Linden. “With or without sugar? (A)glycosylation of therapeutic antibodies”. *Mol. Biotechnol.* 54.3 (2013), pp. 1056–1068.

[204] B Gorovits and C Krinos-Fiorotti. “Proposed mechanism of off-target toxicity for antibody-drug conjugates driven by mannose receptor uptake”. *Cancer Immunol. Immunother.* 62.2 (2013), pp. 217–223.

[205] C F McDonagh, K M Kim, E Turcott, et al. “Engineered anti-CD70 antibody-drug conjugate with increased therapeutic index”. *Mol. Cancer Ther.* 7.9 (2008), pp. 2913–2923.

[206] L G Perez, S Zolla-Pazner, and D C Montefiori. “Antibody-dependent, FcgammaRI-mediated neutralization of HIV-1 in TZM-bl cells occurs independently of phagocytosis”. *J. Virol.* 87.9 (2013), pp. 5287–5290.

[207] C E Chan, A P Lim, P A MacAry, and B J Hanson. “The role of phage display in therapeutic antibody discovery”. *Int. Immunol.* 26.12 (2014), pp. 649–657.

[208] U H Weidle, J Auer, U Brinkmann, G Georges, and G Tiefenthaler. “The emerging role of new protein scaffold-based agents for treatment of cancer”. *Cancer Genomics Proteomics* 10.4 (2013), pp. 155–168.

[209] B M Hutchins, S A Kazane, K Staflin, et al. “Site-specific coupling and sterically controlled formation of multimeric antibody Fab fragments using unnatural amino acids”. *J. Mol. Biol.* 406.4 (2011), pp. 595–603.

[210] G Papalia and D Myszka. “Exploring minimal biotinylation conditions for biosensor analysis using capture chips”. *Anal. Biochem.* 403.1-2 (2010), pp. 30–35.

[211] E Frampas, C Rousseau, C Bodet-Milin, et al. “Improvement of radioimmunotherapy using pretargeting”. *Front. Oncol.* 3 (2013), p. 159.

[212] P C Weber, D H Ohlendorf, J J Wendoloski, and F R Salemme. “Structural origins of high-affinity biotin binding to streptavidin”. *Science* 243.4887 (1989), pp. 85–88.

[213] H Mao, S A Hart, A Schink, and B A Pollok. “Sortase-mediated protein ligation: a new method for protein engineering”. *J. Am. Chem. Soc.* 126.9 (2004), pp. 2670–2671.

[214] R Policarpo, H Kang, X Liao, et al. “Flow-based enzymatic ligation by sortase A”. *Angew. Chem. Int. Ed.* 53.35 (2014), pp. 9203–9208.

[215] T Tanaka, N Kamiya, and T Nagamune. “Peptidyl linkers for protein heterodimerization catalyzed by microbial transglutaminase”. *Bioconjugate Chem.* 15.3 (2004), pp. 491–497.

[216] K Moriyama, K Sung, M Goto, and N Kamiya. “Immobilization of alkaline phosphatase on magnetic particles by site-specific and covalent cross-linking catalyzed by microbial transglutaminase”. *J. Biosci. Bioeng.* 111.6 (2011), pp. 650–653.

[217] M Weber, E Bujak, A Putelli, et al. “A highly functional synthetic phage display library containing over 40 billion human antibody clones”. *PLoS One* 9.6 (2014).

[218] E Fischer, K Chaitanya, T Wuest, et al. “Radioimmunotherapy of fibroblast activation protein positive tumors by rapidly internalizing antibodies”. *Clin. Cancer Res.* 18.22 (2012), pp. 6208–6218.

[219] A Trilling, M Harmsen, V Ruigrok, H Zuilhof, and J Beekwilder. “The effect of uniform capture molecule orientation on biosensor sensitivity: dependence on analyte properties”. *Biosens. Bioelectron.* 40.1 (2013), pp. 219–226.

[220] Y Li and R Sousa. “Expression and purification of *E. coli* BirA biotin ligase for *in vitro* biotinylation”. *Protein Expression Purif.* 82.1 (2012), pp. 162–167.

[221] R Lameris, R C de Bruin, F L Schneiders, et al. “Bispecific antibody platforms for cancer immunotherapy”. *Crit. Rev. Oncol. Hematol.* 92.3 (2014), pp. 153–165.

[222] M Hutt, A Farber-Schwarz, F Unverdorben, F Richter, and R E Kontermann. “Plasma half-life extension of small recombinant antibodies by fusion to immunoglobulin-binding domains”. *J. Biol. Chem.* 287.7 (2012), pp. 4462–4469.

[223] R M Sharkey, C H Chang, E A Rossi, W J McBride, and D M Goldenberg. “Pretargeting: taking an alternate route for localizing radionuclides”. *Tumour Biol.* 33.3 (2012), pp. 591–600.

[224] P Dennler, A Chiotellis, E Fischer, et al. “A Transglutaminase-based chemoenzymatic conjugation approach yields homogeneous antibody-drug conjugates”. *Bioconjugate Chemistry* 25.3 (2014), pp. 569–578.

[225] E Reimhult, M K Baumann, S Kaufmann, K Kumar, and P R Spycher. “Advances in nanopatterned and nanostructured supported lipid membranes and their applications”. *Biotechnol. Genet. Eng. Rev.* 27.1 (2010), pp. 185–216.

[226] T Hofer, W Tangkeangsirisin, M G Kennedy, et al. “Chimeric rabbit/human Fab and IgG specific for members of the Nogo-66 receptor family selected for species cross-reactivity with an improved phage display vector”. *J. Immunol. Methods* 318.1–2 (2007), pp. 75 –87.

[227] H Xie, A Chakraborty, J Ahn, et al. “Rapid comparison of a candidate biosimilar to an innovator monoclonal antibody with advanced liquid chromatography and mass spectrometry technologies”. *MAbs* 2.4 (2010).

[228] R P Spycher, H Hall, V Vogel, and E Reimhult. “Patterning of supported lipid bilayers and proteins using material selective nitrodopamine-mPEG”. *Biomater. Sci.* 3 (2015), pp. 94–102.

[229] L Jendeberg, B Persson, R Andersson, et al. “Kinetic analysis of the interaction between protein A domain variants and human Fc using plasmon resonance detection”. *J. Mol. Recognit.* 8.4 (1995), pp. 270–278.

[230] M Tashiro, R Tejero, D E Zimmerman, et al. “High-resolution solution NMR structure of the Z domain of staphylococcal protein A”. *J. Mol. Biol.* 272.4 (1997), pp. 573–590.

[231] J Deisenhofer. “Crystallographic refinement and atomic models of a human Fc fragment and its complex with fragment B of protein A from *Staphylococcus aureus* at 2.9- and 2.8-Åresolution”. *Biochemistry* 20.9 (1981), pp. 2361–2370.

[232] L Cedergren, R Andersson, B Jansson, M Uhlen, and B Nilsson. “Mutational analysis of the interaction between staphylococcal protein A and human IgG1”. *Protein Eng.* 6.4 (1993), pp. 441–448.

[233] J A Brockelbank, V Peters, and B H Rehm. “Recombinant *Escherichia coli* strain produces a ZZ domain displaying biopolyester granules suitable for immunoglobulin G purification”. *Appl. Environ. Microbiol.* 72.11 (2006), pp. 7394–7397.

[234] J Nilvebrant, T Alm, and S Hober. “Orthogonal protein purification facilitated by a small bispecific affinity tag”. *J. Vis. Exp.* 59 (2012).

[235] S Gulich, M Uhlen, and S Hober. “Protein engineering of an IgG-binding domain allows milder elution conditions during affinity chromatography”. *J. Biotechnol.* 76.2-3 (2000), pp. 233–244.

[236] Q L Huang, C Chen, Y Z Chen, et al. “Application to immunoassays of the fusion protein between protein ZZ and enhanced green fluorescent protein”. *J. Immunol. Methods* 309.1-2 (2006), pp. 130–138.

[237] Q L Huang, C Chen, Y Z Chen, et al. “Fusion protein between protein ZZ and red fluorescent protein DsRed and its application to immunoassays”. *Biotechnol. Appl. Biochem.* 43.2 (2006), pp. 121–127.

[238] C Huang and K Jacobson. “Detection of protein-protein interactions using nonimmune IgG and BirA-mediated biotinylation”. *Biotechniques* 49.6 (2010), pp. 881–886.

[239] M Iijima, N Yoshimoto, T Niimi, A Maturana, and S Kuroda. “Nanocapsule-based probe for evaluating the orientation of antibodies immobilized on a solid phase”. *The Analyst* 138.12 (2013), pp. 3470–3477.

[240] F Unverdorben, A Farber-Schwarz, F Richter, M Hutt, and R E Kontermann. “Half-life extension of a single-chain diabody by fusion to domain B of staphylococcal protein A”. *Protein Eng. Des. Sel.* 25.2 (2012), pp. 81–88.

[241] J Sockolosky, S Kivimäe, and F Szoka. “Fusion of a short peptide that binds immunoglobulin G to a recombinant protein substantially increases its plasma half-life in mice”. *PLoS One* 9.7 (2014).

[242] B Feng, K Tomizawa, H Michiue, et al. “Delivery of sodium borocaptate to glioma cells using immunoliposome conjugated with anti-EGFR antibodies by ZZ-His”. *Biomaterials* 30.9 (2009), pp. 1746–1755.

[243] H Schägger. “Tricine-SDS-PAGE”. *Nat. Protoc.* 1.1 (2006), pp. 16–22.

[244] M Altai, A Perols, A Karlström, et al. “Preclinical evaluation of anti-HER2 Affibody molecules site-specifically labeled with ^{111}In using a maleimido derivative of NODAGA”. *Nucl. Med. Biol.* 39.4 (2012), pp. 518–529.

[245] E Fischer, J Grünberg, S Cohrs, et al. “L1-CAM-targeted antibody therapy and ^{177}Lu-radioimmunotherapy of disseminated ovarian cancer”. *Int. J. Cancer* 130.11 (2012), pp. 2715–2721.

[246] J Grünberg, D Lindenblatt, H Dorrer, et al. “Anti-L1CAM radioimmunotherapy is more effective with the radiolanthanide terbium-161 compared to lutetium-177 in an ovarian cancer model”. *Eur. J. Nucl. Med. Mol. Imaging* 41.10 (2014), pp. 1907–1915.

[247] J Löfblom, J Feldwisch, V Tolmachev, et al. “Affibody molecules: engineered proteins for therapeutic, diagnostic and biotechnological applications”. *FEBS Lett.* 584.12 (2010), pp. 2670–2680.

[248] H Honarvar, J Strand, A Perols, et al. “Position for site-specific attachment of a DOTA chelator to synthetic affibody molecules has a different influence on the targeting properties of ^{68}Ga- compared to ^{111}In-labeled conjugates”. *Mol. Imaging* 13 (2014).

[249] C K Marx, T C Hertel, and M Pietzsch. “Random mutagenesis of a recombinant microbial transglutaminase for the generation of thermostable and heat-sensitive variants”. *J. Biotechnol.* 136.3 (2008), pp. 156–162.

[250] K Yokoyama, H Utsumi, T Nakamura, et al. “Screening for improved activity of a transglutaminase from *Streptomyces mobaraensis* created by a novel rational mutagenesis and random mutagenesis”. *Appl. Microbiol. Biotechnol.* 87.6 (2010), pp. 2087–2096.

[251] K Chen, S Liu, J Ma, et al. “Deletion combined with saturation mutagenesis of N-terminal residues in transglutaminase from *Streptomyces hygroscopicus* results in enhanced activity and thermostability”. *Process Biochem.* 47.12 (2012), pp. 2329–2334.

[252] A K Trilling, T Hesselink, A van Houwelingen, et al. “Orientation of llama antibodies strongly increases sensitivity of biosensors”. *Biosens. Bioelectron.* 60 (2014), pp. 130–136.

Colophon

This thesis was typeset with LaTeX 2$_\varepsilon$. It uses the *Clean Thesis* style developed by Ricardo Langner. The design of the *Clean Thesis* style is inspired by user guide documents from Apple Inc.